Probing the early Universe
through observations of the
Cosmic Microwave Background

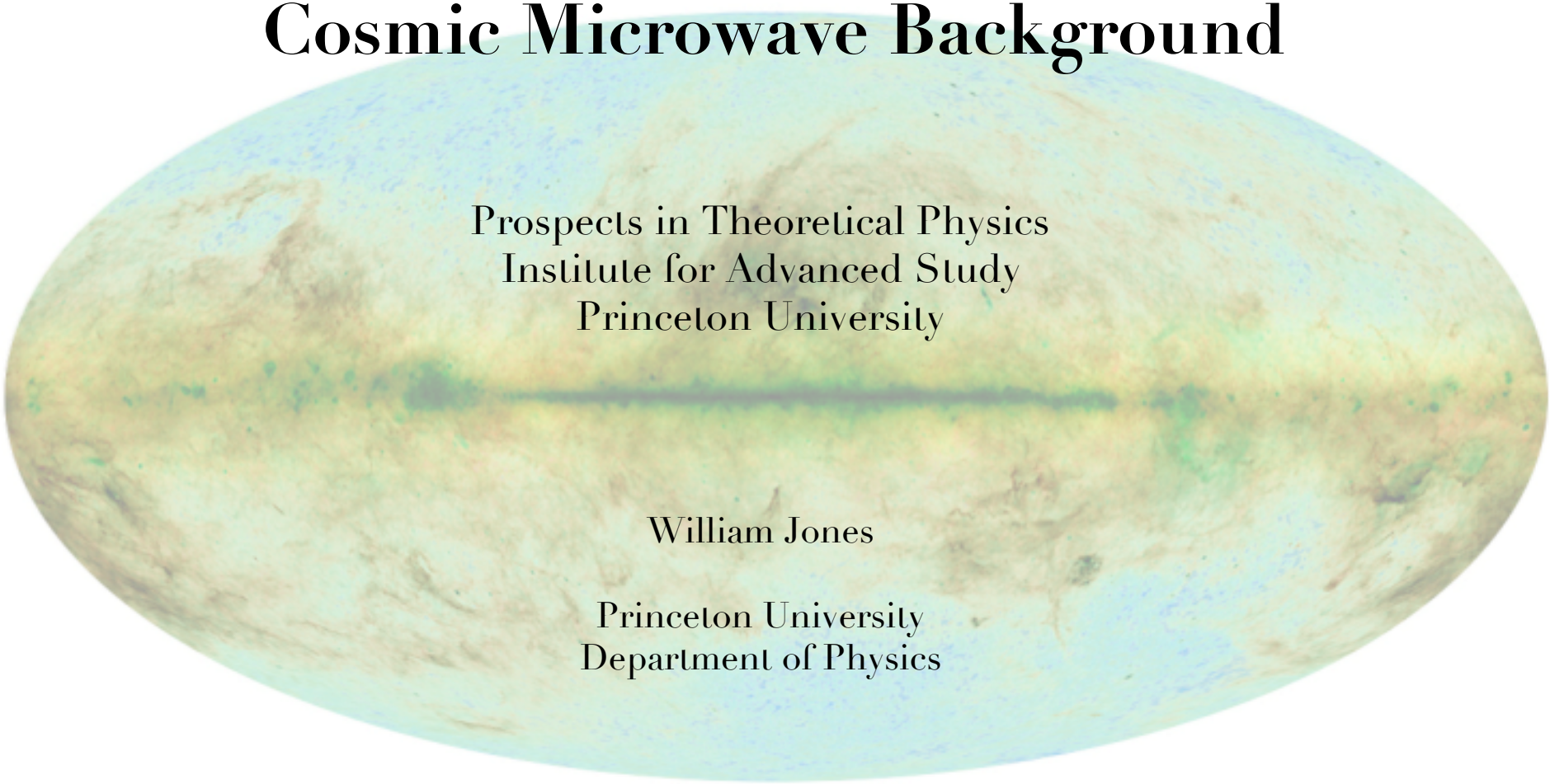

Prospects in Theoretical Physics
Institute for Advanced Study
Princeton University

William Jones

Princeton University
Department of Physics

Probing the early Universe
through observations of the
Cosmic Microwave Background

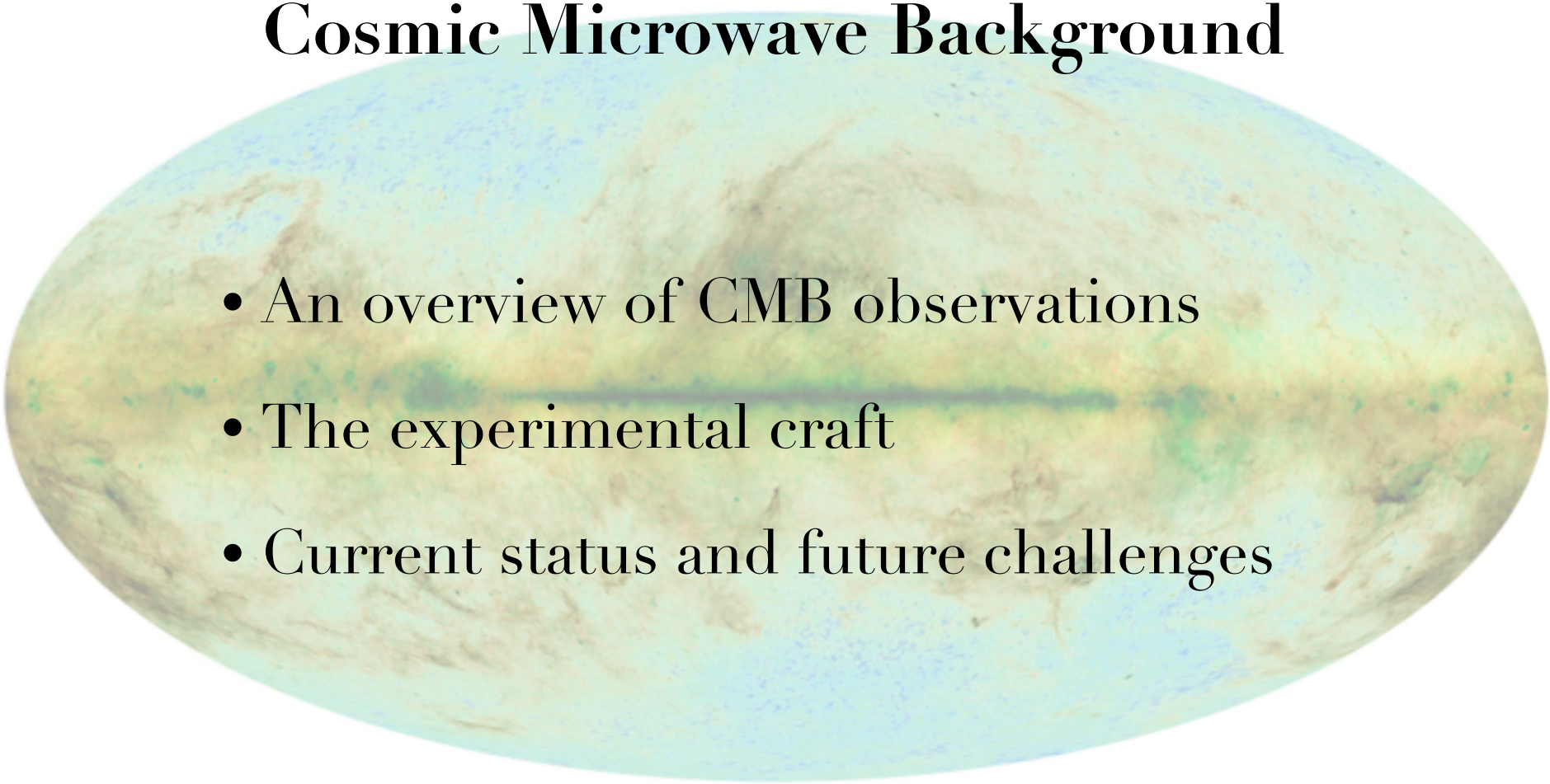

- An overview of CMB observations
- The experimental craft
- Current status and future challenges

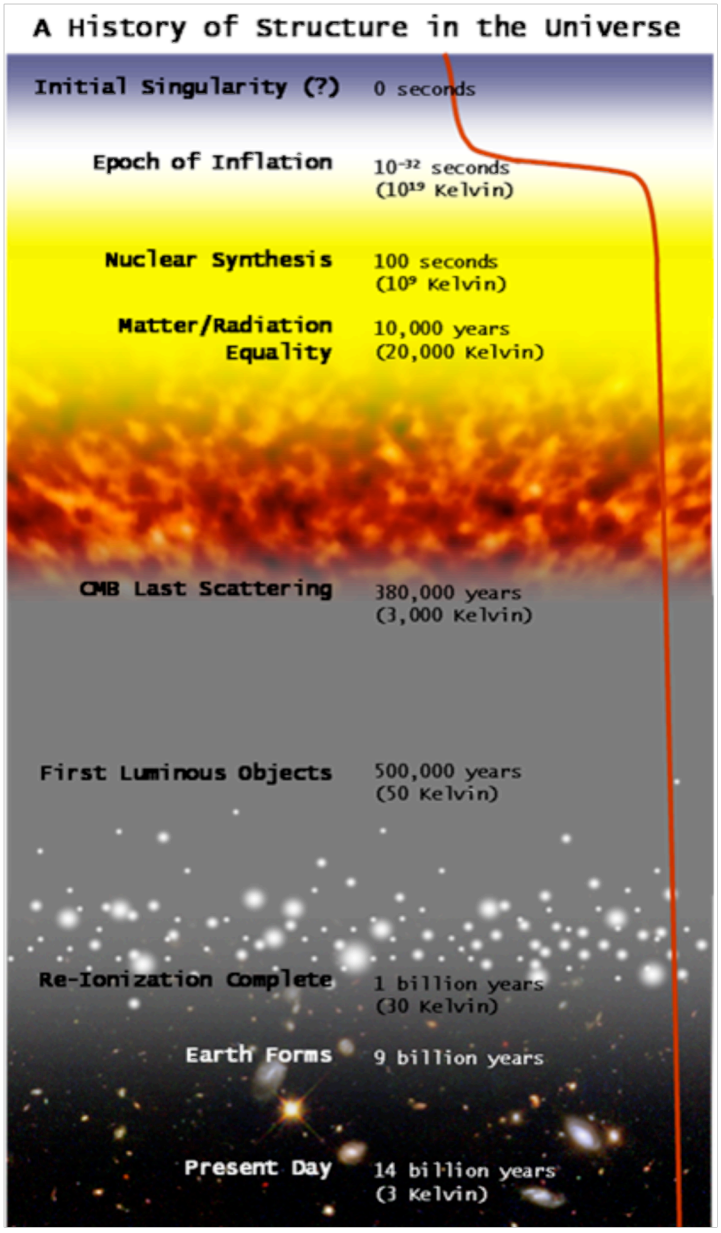

Cosmic Evolution

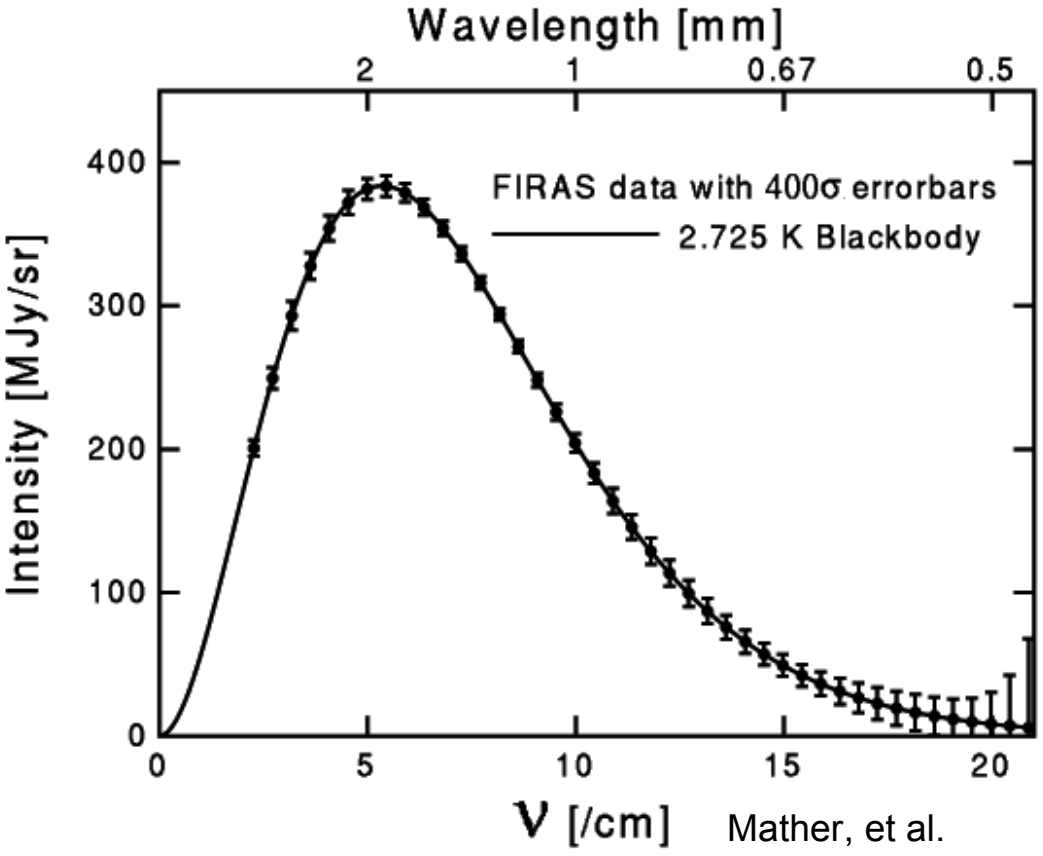

Mather, et al.

Coherent (phase sensitive) amplification

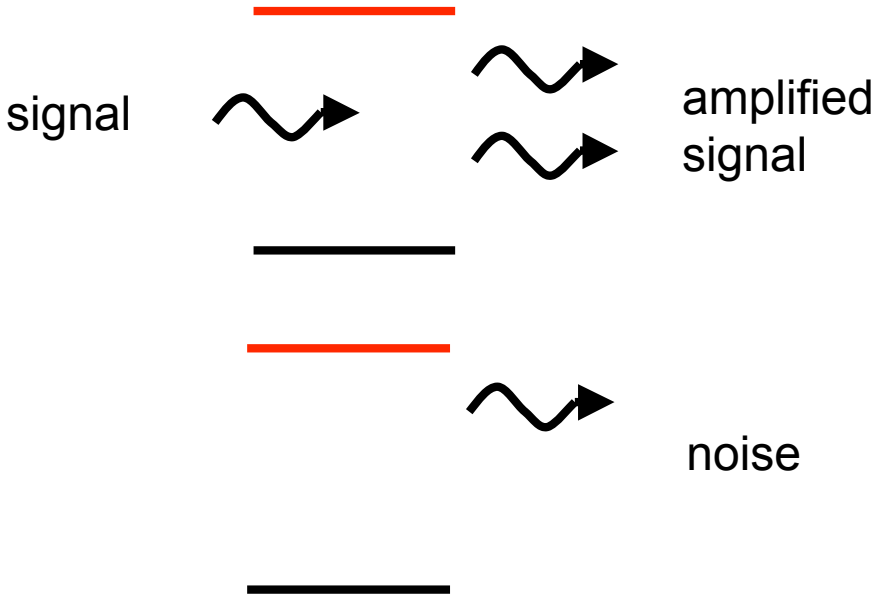

Incoherent (phase insensitive) detection

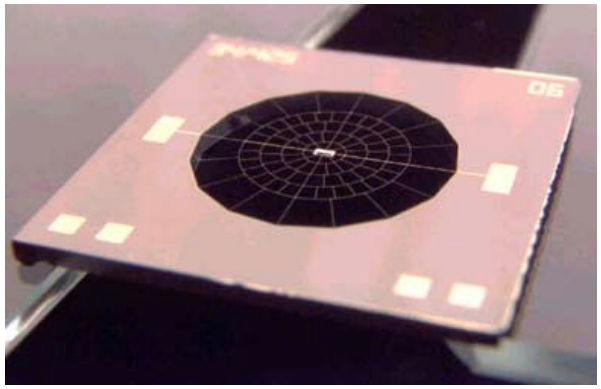

$$\sigma_{11} = h\nu\sqrt{\frac{\Delta\nu}{\tau}}(n+1).$$

$$\sigma_{ii}^2 = (h\nu)^2\frac{\Delta\nu}{\tau}\left[\,(\gamma^2+\delta^2)^2\,n^2+(\gamma^2+\delta^2)\,n\,\right]$$

T_{sys} ~ 4.8 K (ν/100 GHz)

$$\mathrm{NEP}^2_{photon} \simeq 2h\nu\;Q\;\left(1+\eta\;n(T_{RJ})\right).$$

DETECTOR SENSITIVITY

Frequency [GHz]	FROM GROUND (2005) Bolometer [μK s$^{1/2}$]	FROM GROUND (2005) HEMT/$\sqrt{2}$ [μK s$^{1/2}$]	FROM SPACE (~2010) Bolometer [μK s$^{1/2}$]	FROM SPACE (~2010) HEMT/$\sqrt{2}$ [μK s$^{1/2}$]
30	...	93	57	48
40	...	115	51	51
60	...	175	44	60
90	250	224	40	75
120	250	...	40	93
150	250	...	43	...
220	250	...	64	...

[a] Bolometer values from A. Lange and J. Bock; HEMT values from T. Gaier.

[b] The $\sqrt{2}$ in the HEMT values comes from the fact that Q and U can be measured simultaneously behind one feed.

[c] The convention for polarization sensitivity used here is $(T_x - T_y)/2$.

C. Lawrence, 1996

Interferometer Arrays

Very Large Array (VLA)

Cosmic Background Imager (CBI)

Degree Angular Scale Interferometer (DASI)

… and of course many others
(VSA, BIMA, ALMA, CARA, etc)

COBE Differential Microwave Radiometer

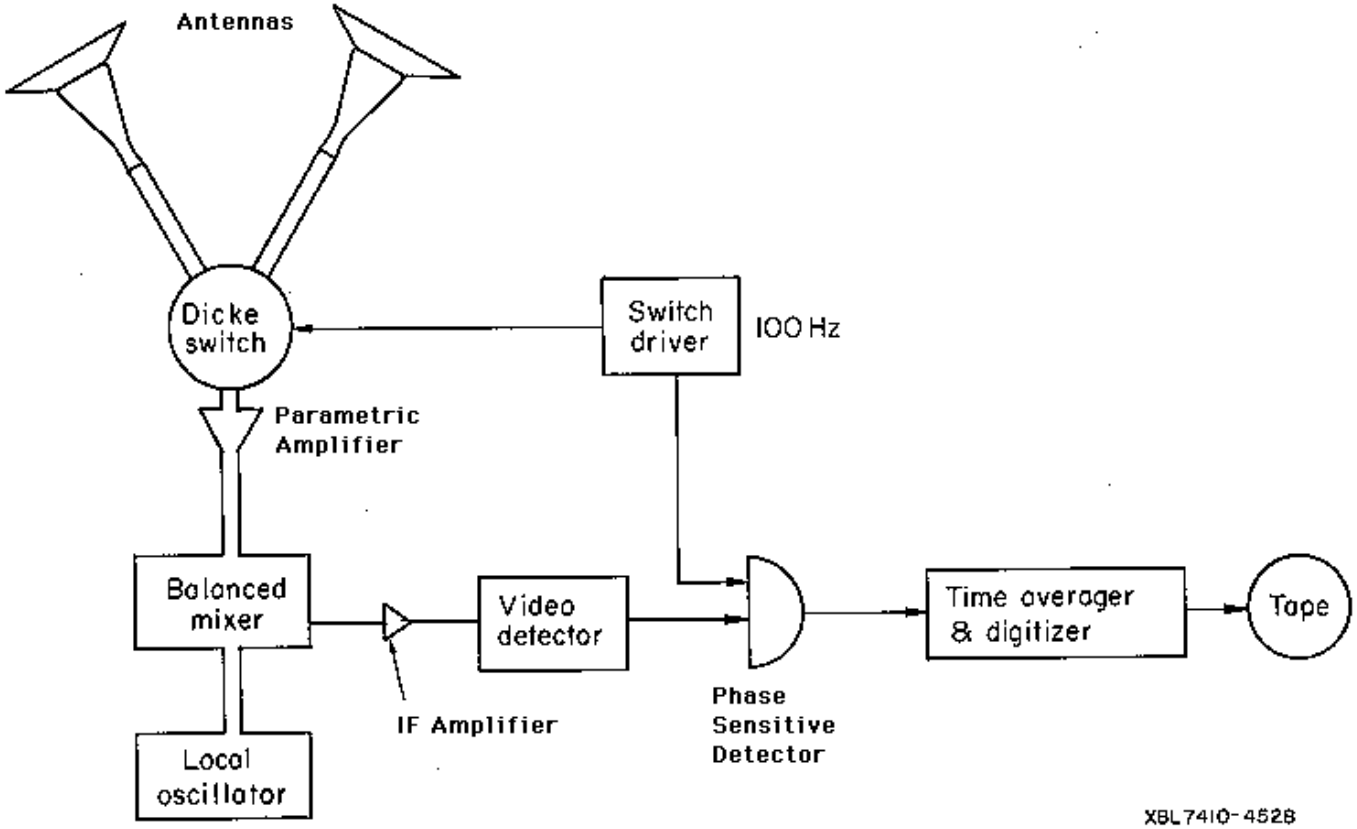

DJ COBE

COBE DMR

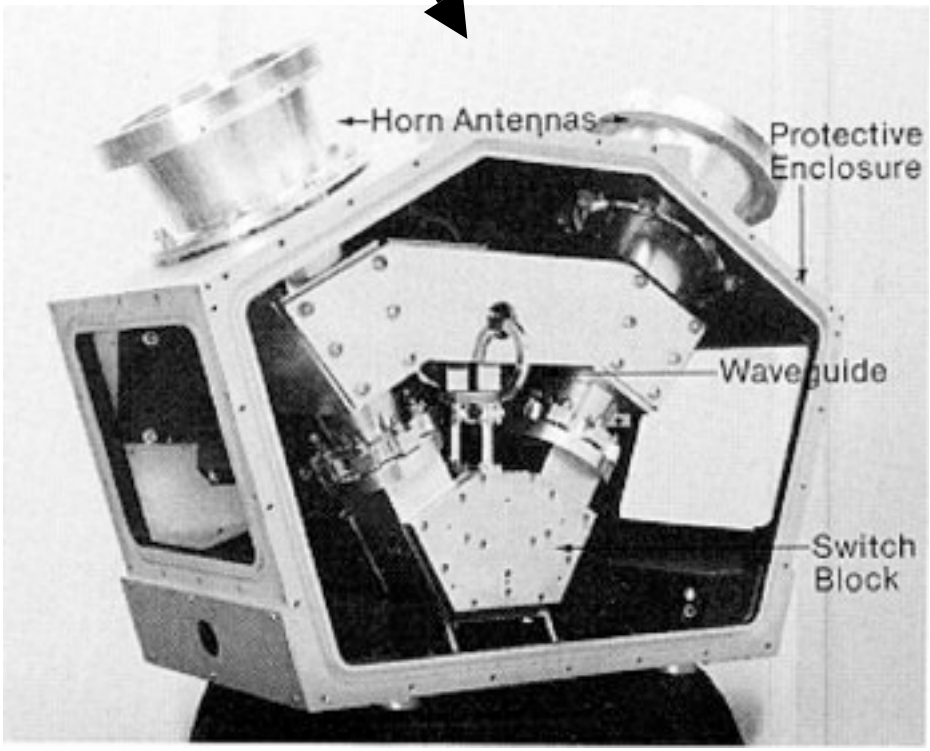

COBE Science Team

COBE DMR

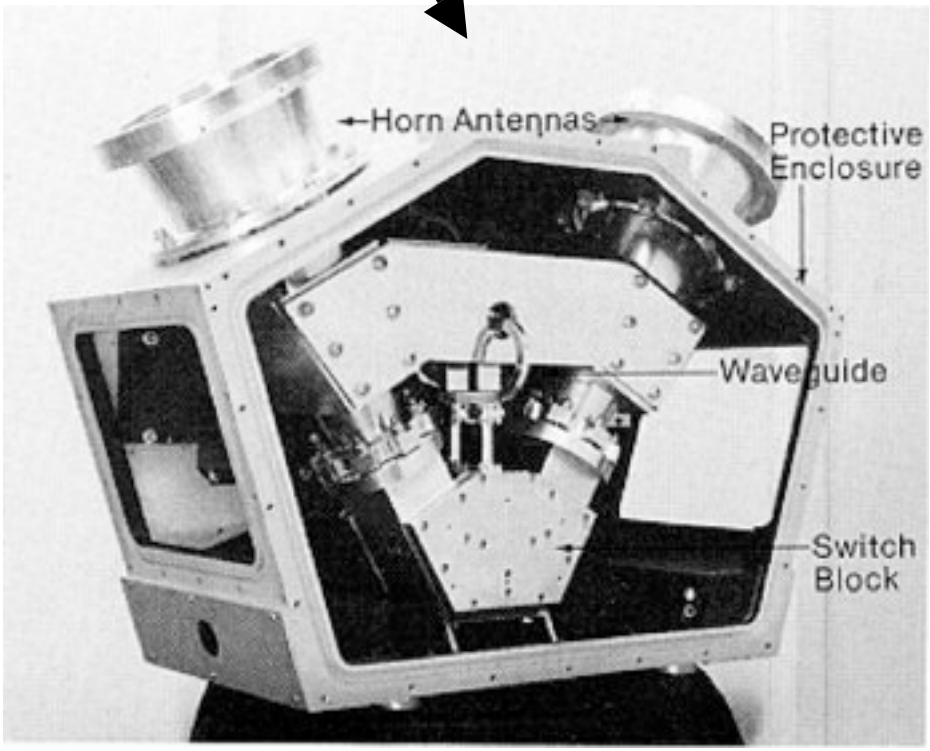

1994

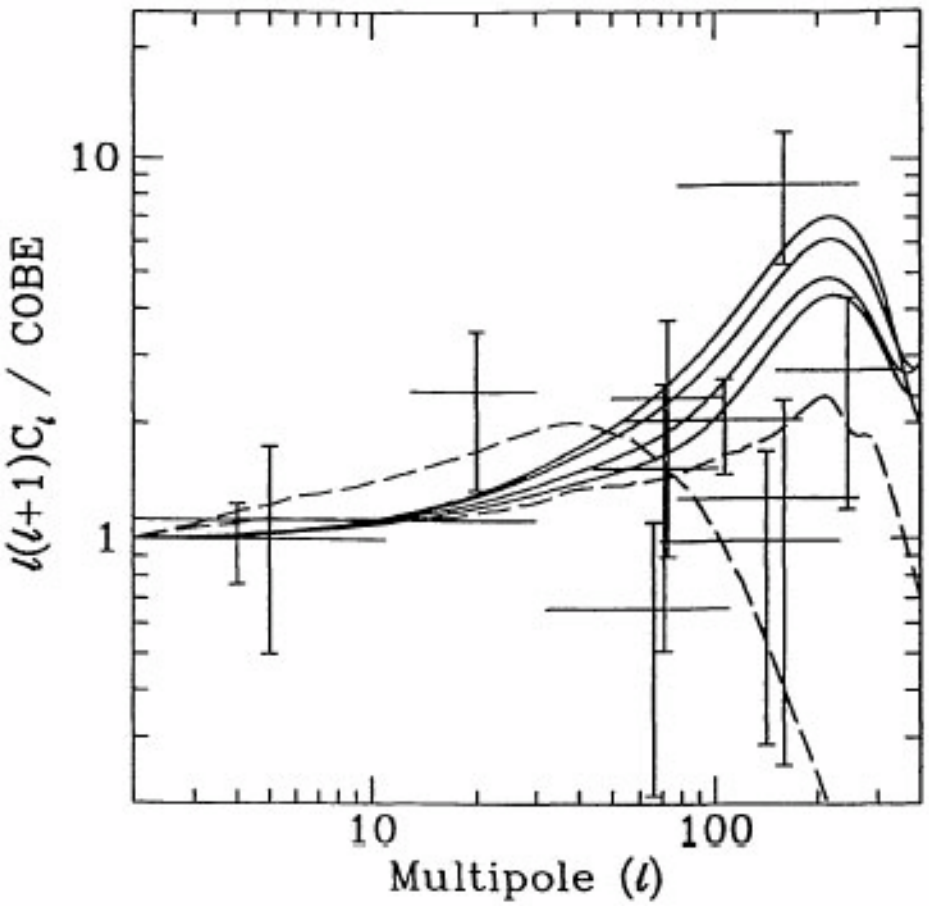

COBE, FIRS, Tenerife, SP91, Saskatoon, Python, ARGO, MSAM, MAX
M. White, Ann. Rev. Astron. & Astrophys., 1994

1999

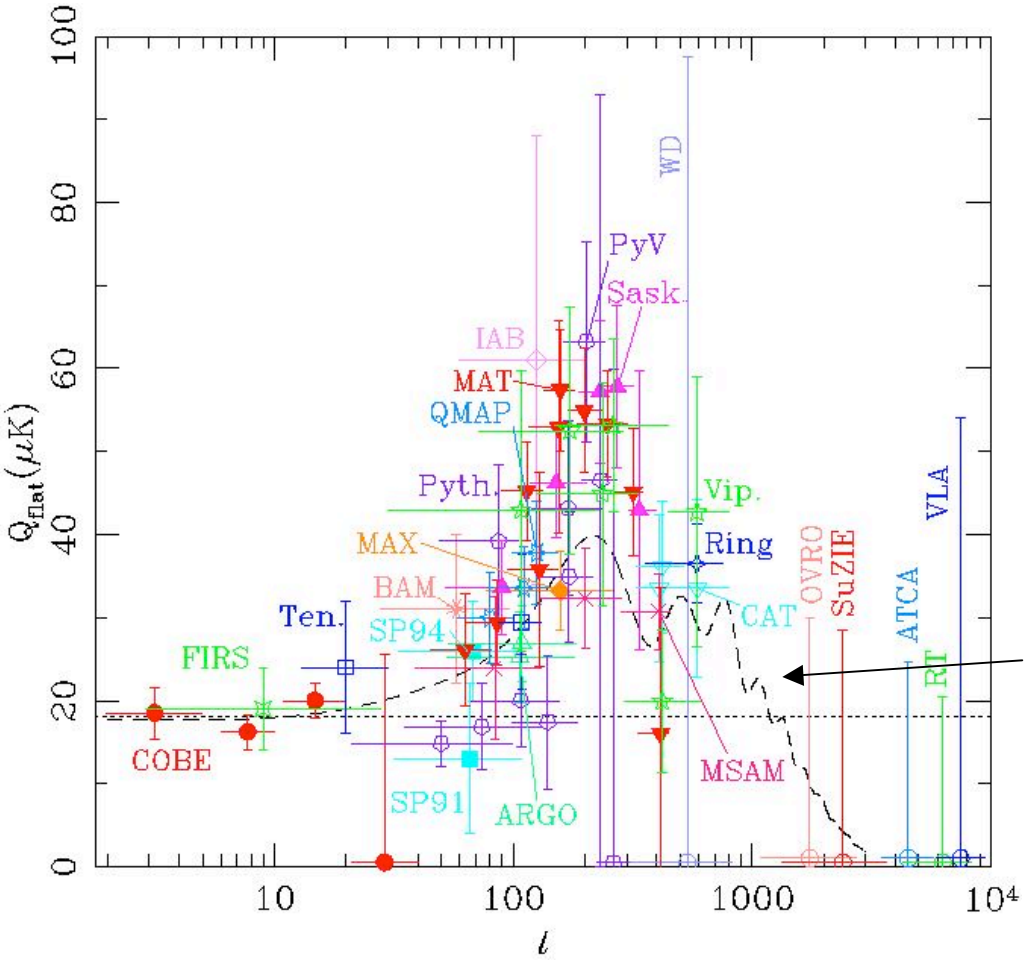

sCDM

COBE, FIRS, Tenerife, SP91/94, Saskatoon, Python, ARGO, MSAM, MAX, OVRO, QMAP, MAT/TOCO, CAT, Viper, SuZIE
Douglas Scott, *New Physics from the Microwave Background*, 1999.

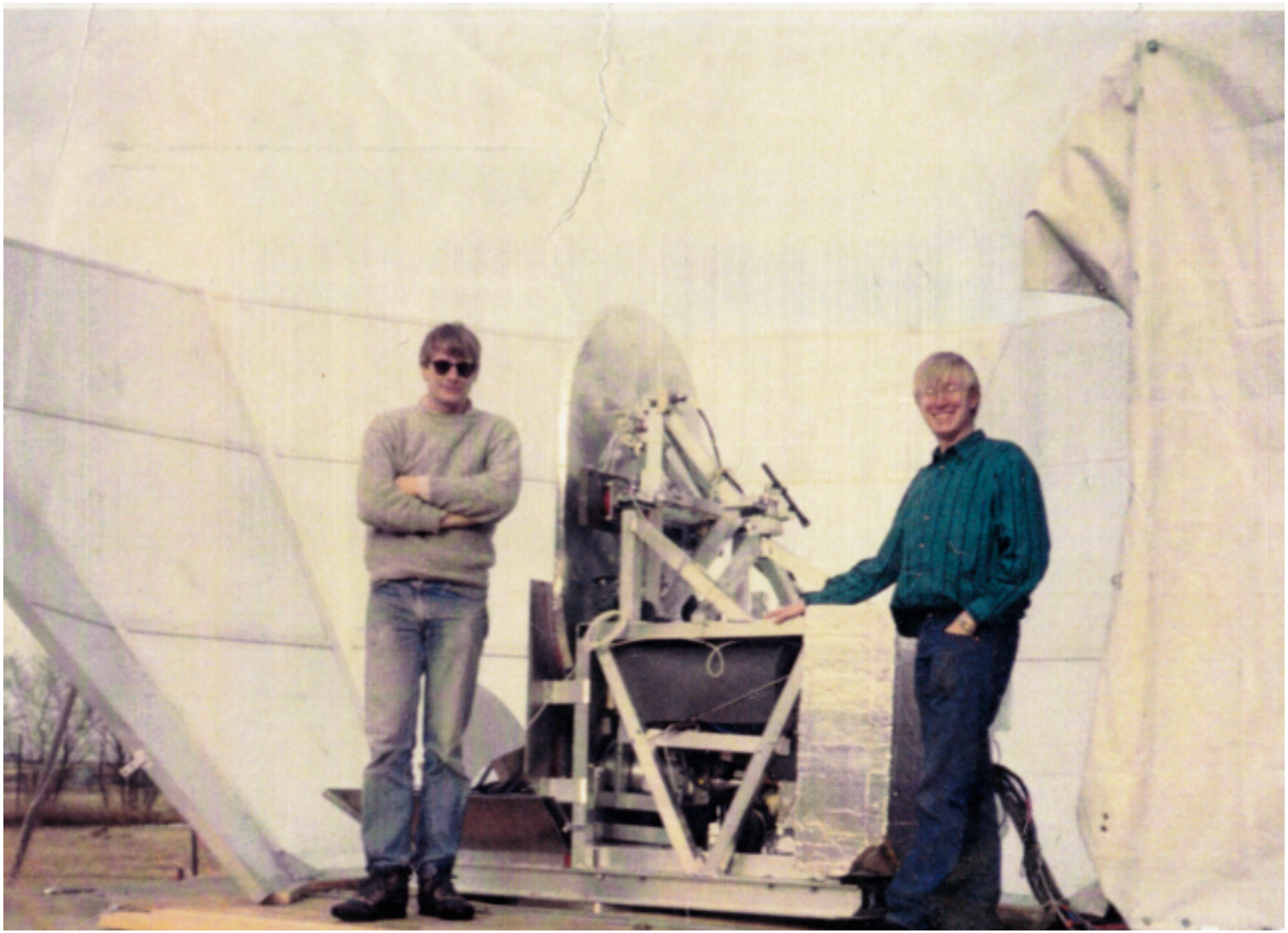

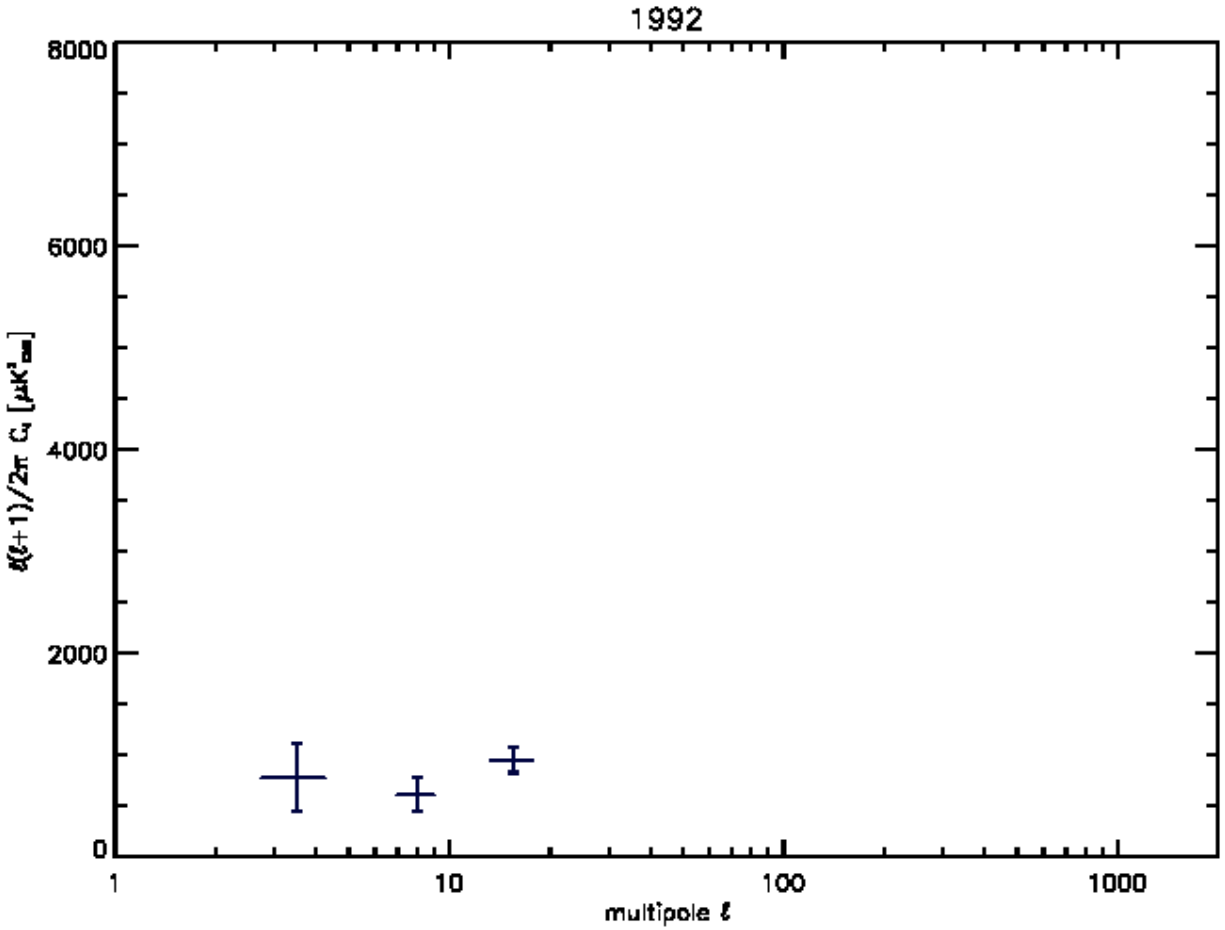

COBE DMR

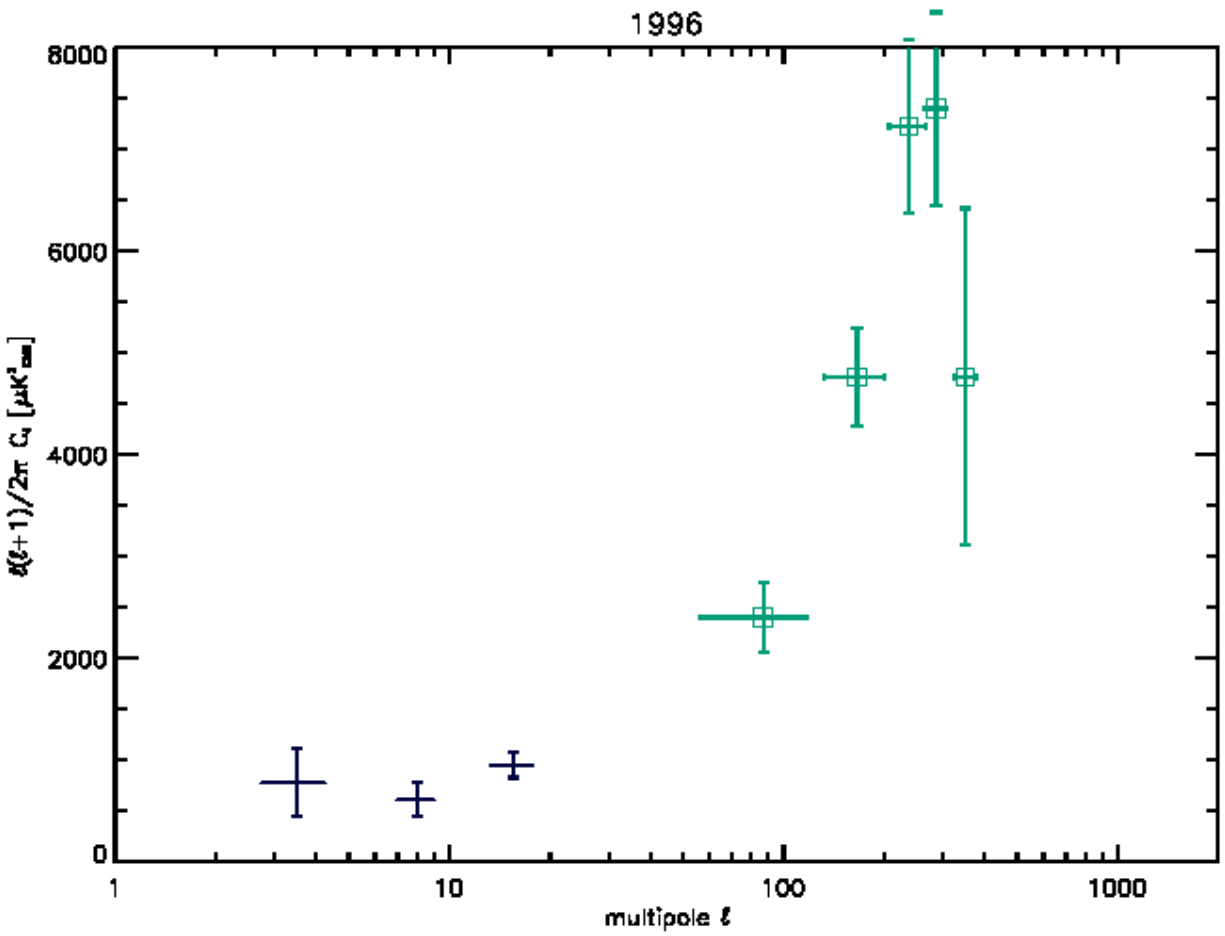

COBE DMR

Saskatoon

1997

2000

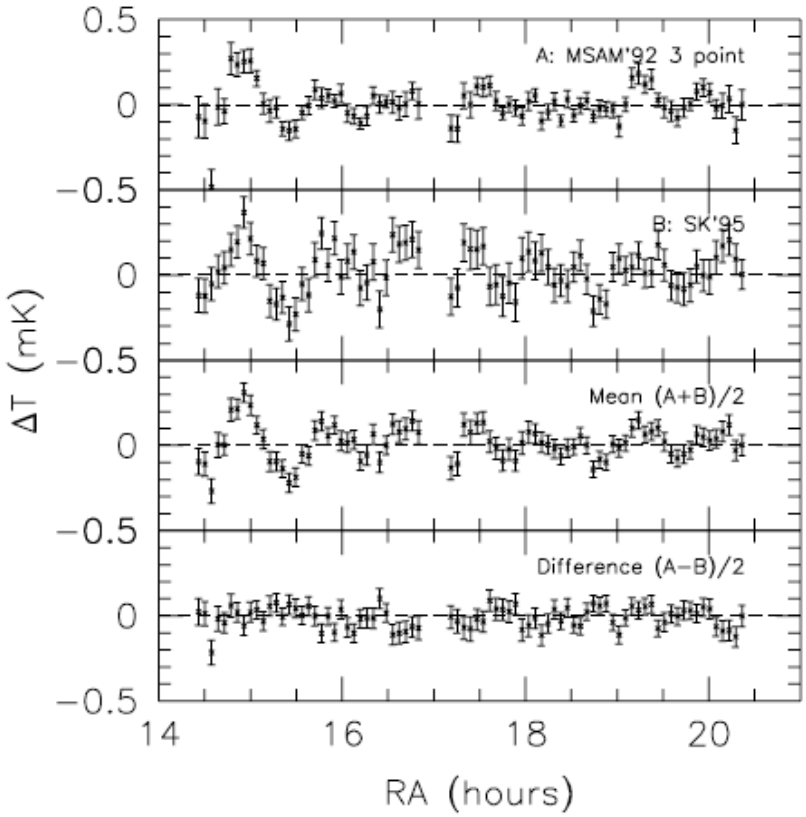

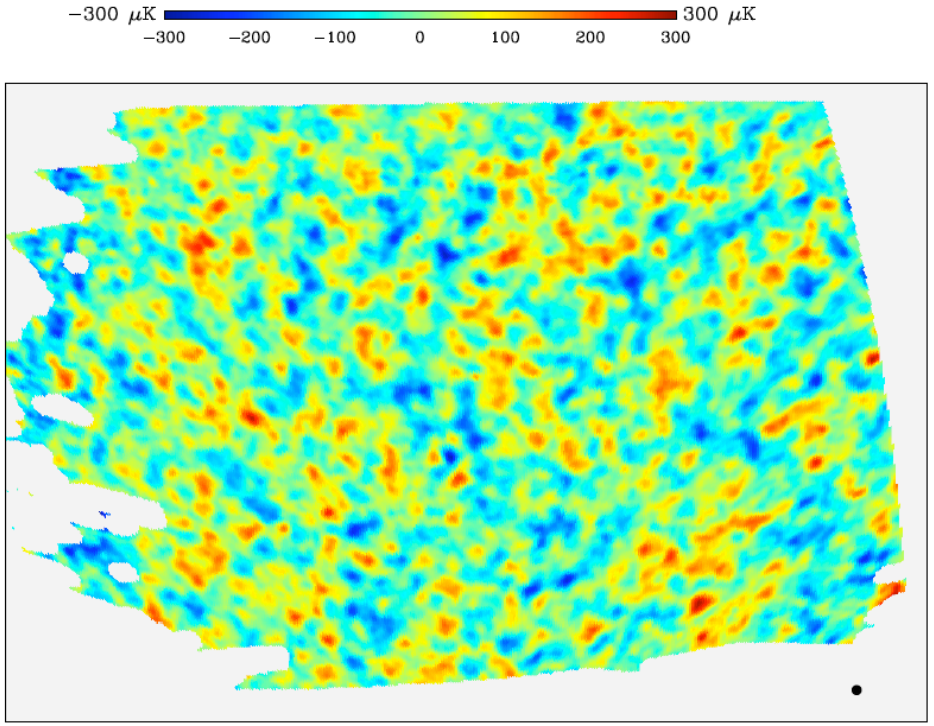

Netterfield et al, MSAM/SK

Boomerang

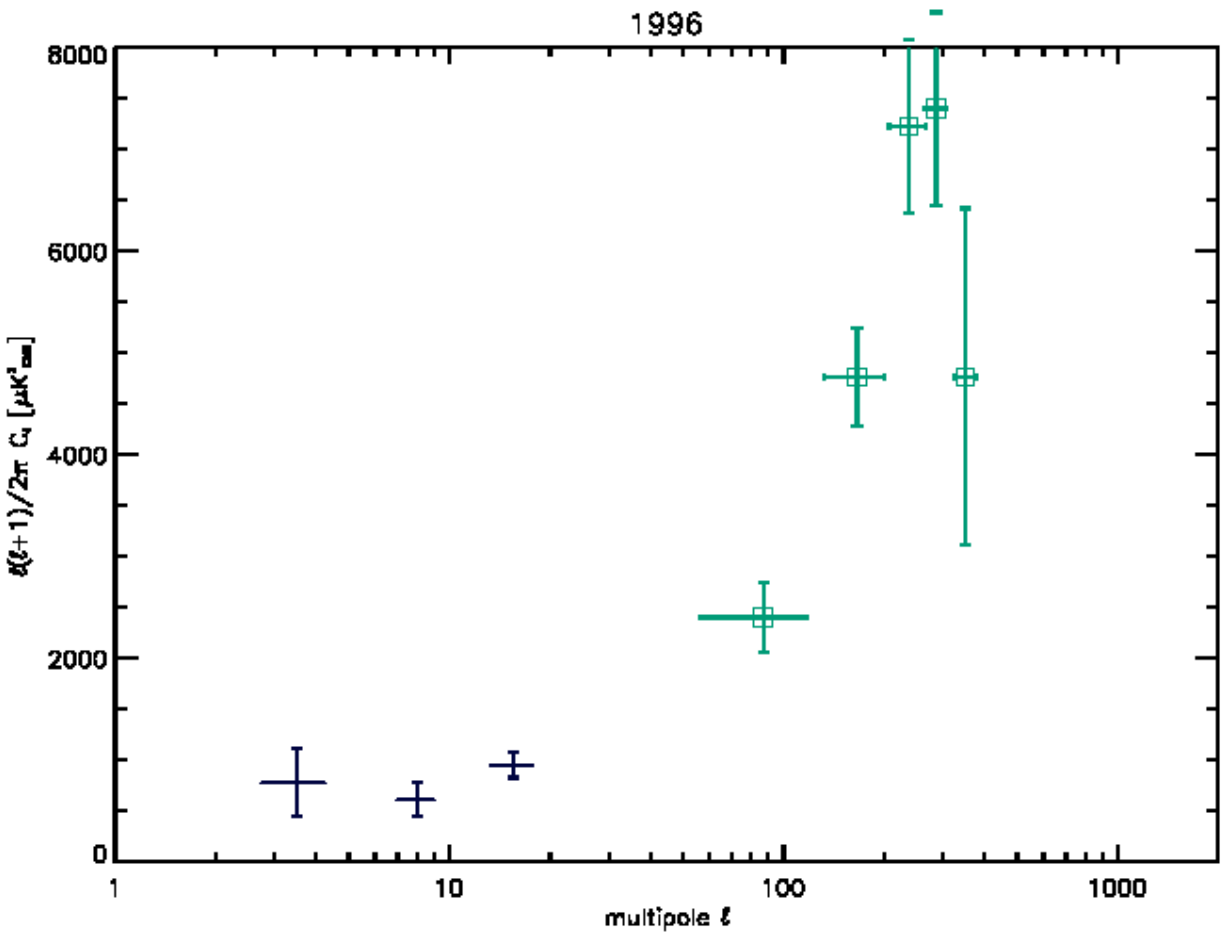

COBE DMR

Saskatoon

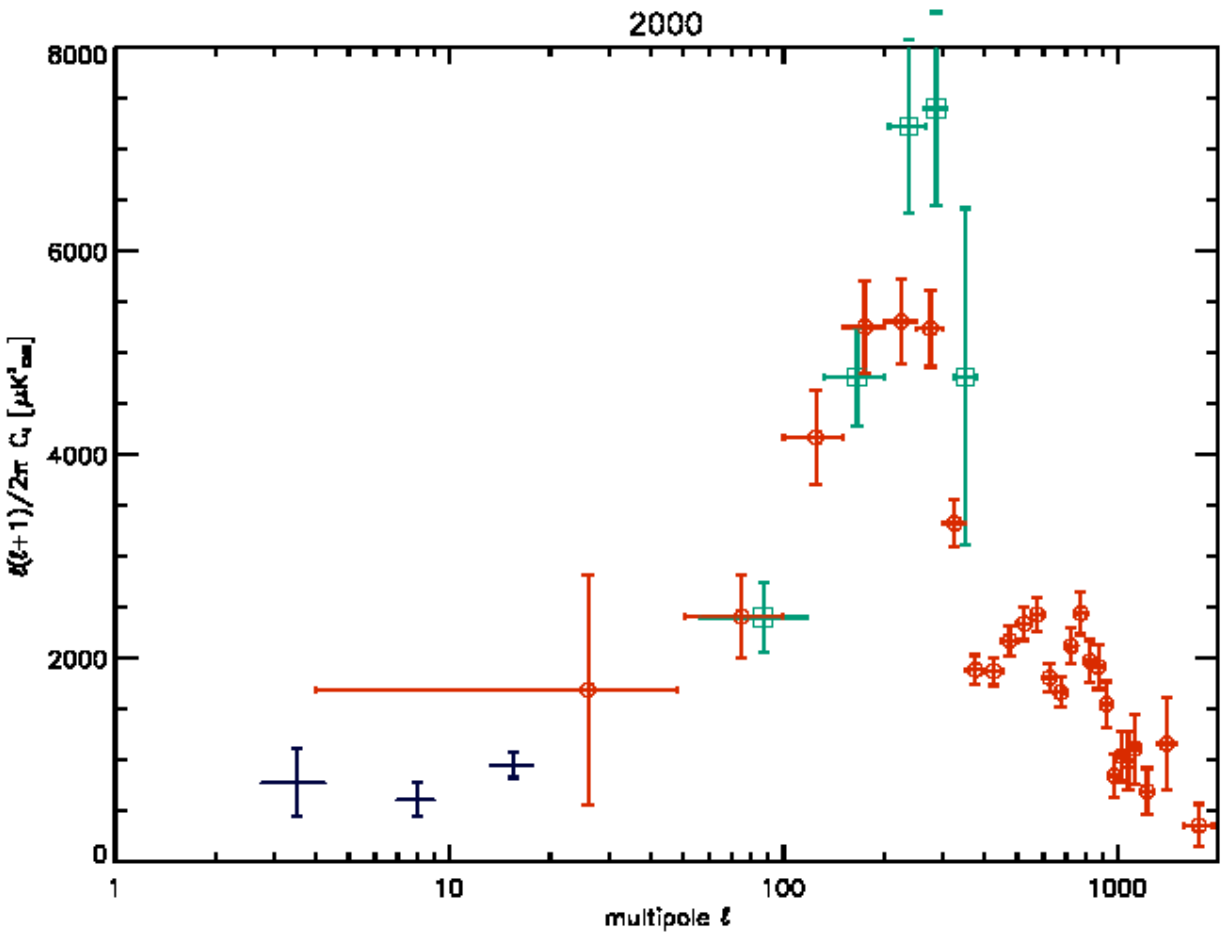

COBE DMR

Saskatoon

Boomerang

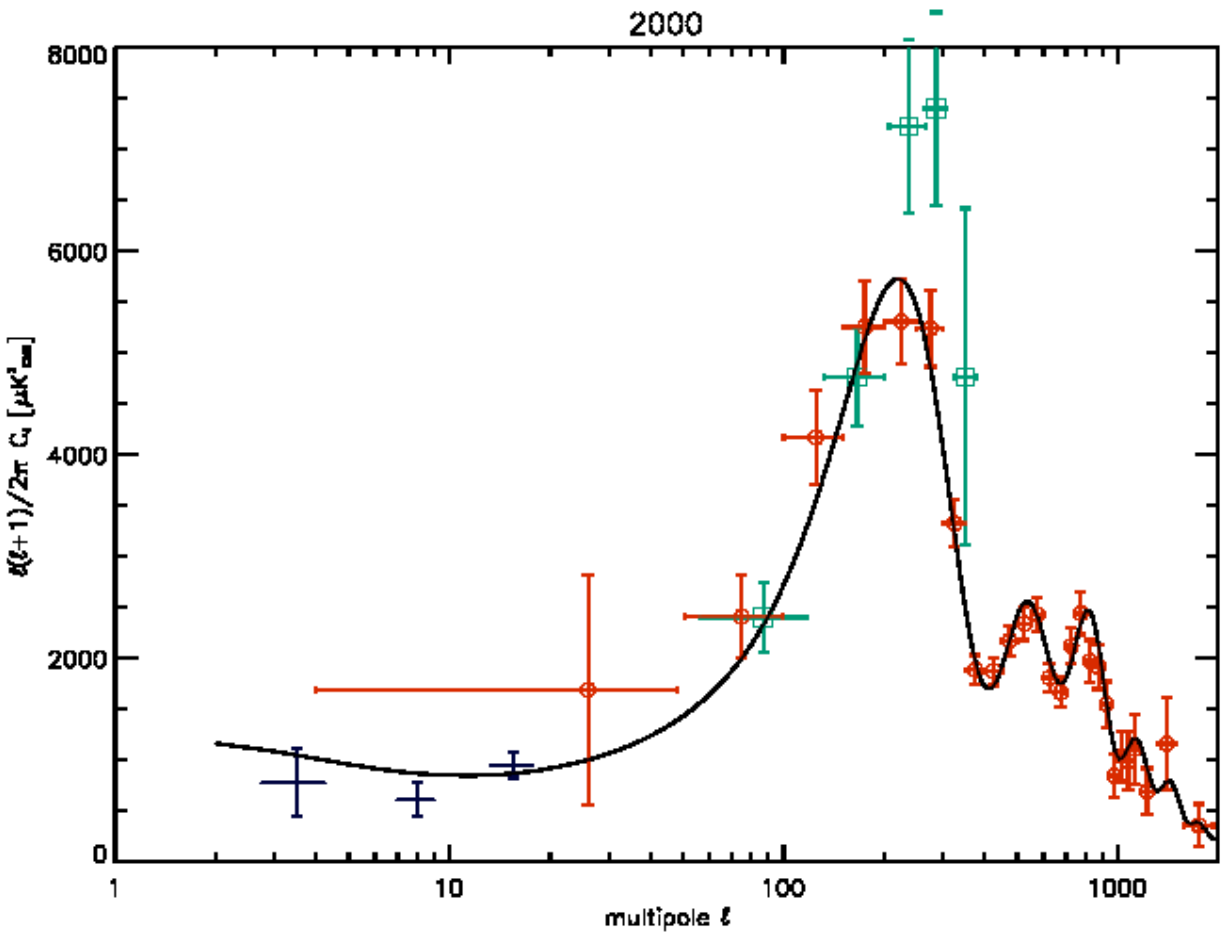

COBE DMR

Saskatoon

Boomerang

CMB Temperature Power Spectrum

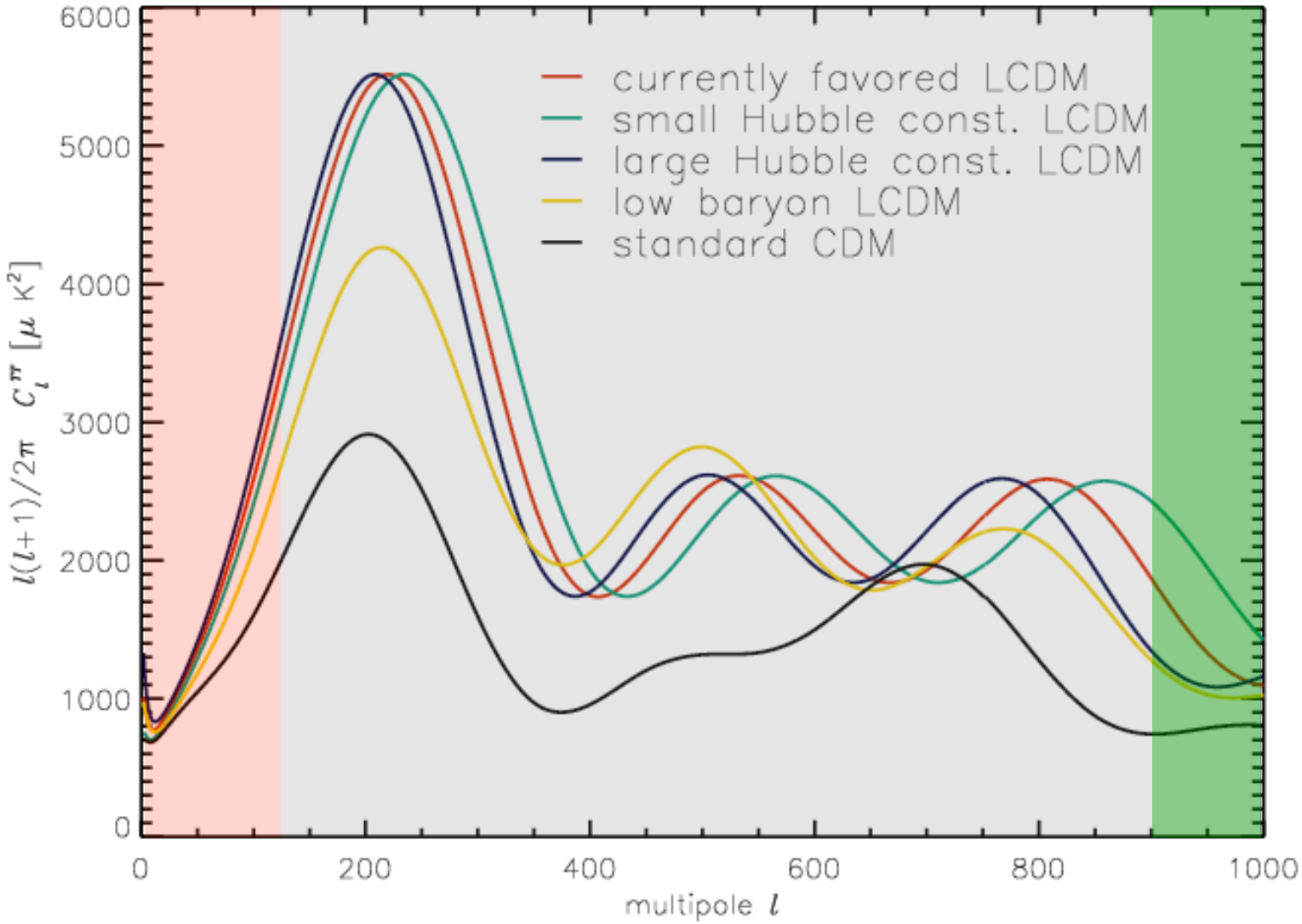

$$d_i \simeq \frac{s}{2} \int d\nu\, \lambda^2\, F_\nu \iint d\Omega\, [I + \gamma \mathcal{P}\,(Q \cos 2\psi_i + U \sin 2\psi_i)]$$

$$\widetilde{\mathbf{m}} = \left(\mathbf{A}^T \mathbf{N}^{-1} \mathbf{A}\right)^{-1} \mathbf{A}^T \mathbf{N}^{-1} \mathbf{d}.$$

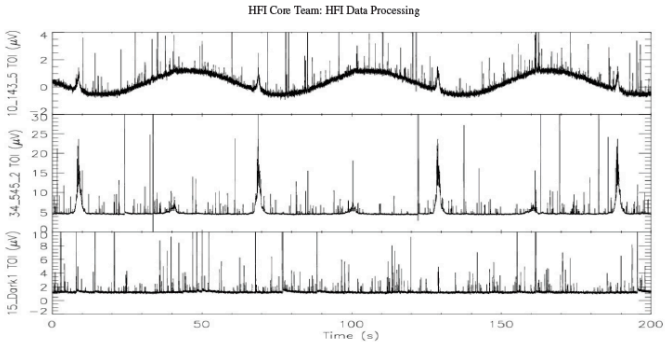

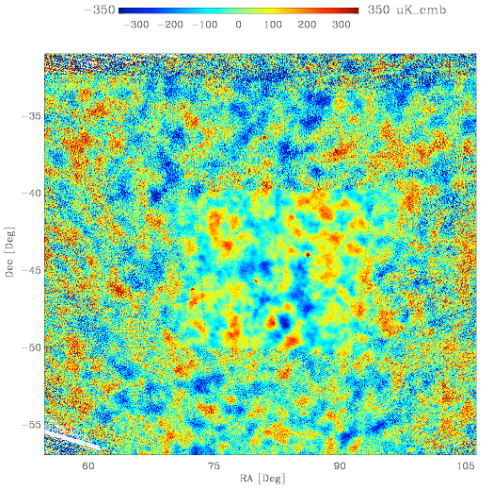

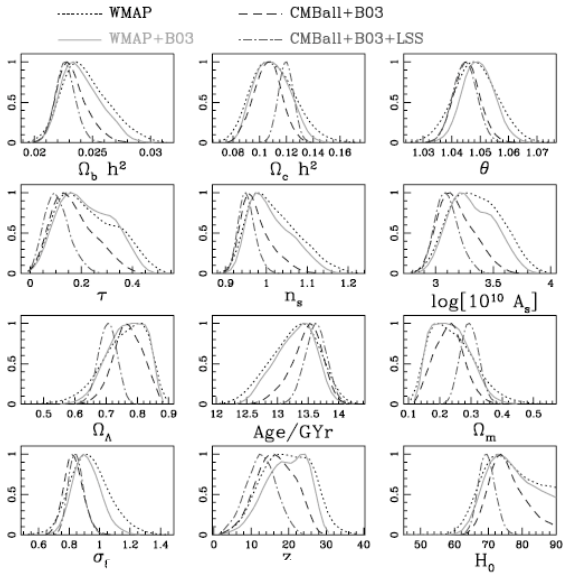

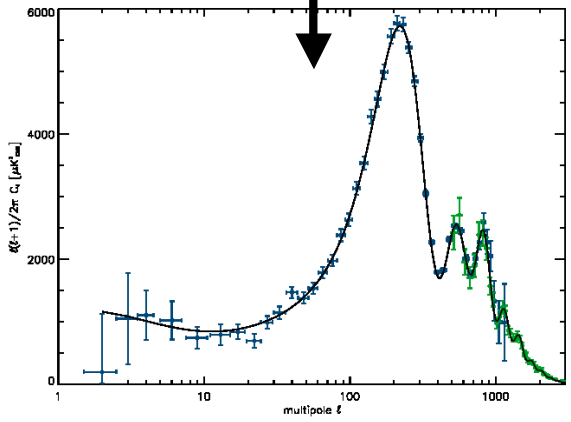

$$P(\mathbf{y}|\mathbf{z}) \propto P(\mathbf{y}) P(\mathbf{z}|\mathbf{y}),$$

$$\tilde{C}_l^{TT} = \sum_{l'} K_{ll'} B_{l'}^2 F_{l'} C_{l'}^{TT} + \tilde{N}_l.$$

Power Spectrum Estimation: Pseudo-C_l's

- Solve for an unbiased estimator of the (binned) underlying power spectrum
  - Correct for bias of scan strategy/time domain filtering with signal only Monte Carlos
  - Correct for noise bias with noise only Monte Carlos
  - Obtain covariance of the power spectrum with signal+noise MC's *or* with a Fisher matrix approach like FASTER
- Achieves sub-optimal errors due to a degradation of signal/noise arising from naïve mapmaking ***and*** heuristic weighting
- Also relies on knowledge of the noise

$$\left\langle \tilde{C}_\ell \right\rangle = \sum_{\ell'} M_{\ell\ell'} F_{\ell'} B_{\ell'}^2 \left\langle C_{\ell'} \right\rangle + \left\langle \tilde{N}_\ell \right\rangle$$

$$C_{\ell\ell'} = \left\langle \left(\hat{C}_\ell - \left\langle C_\ell \right\rangle_{MC} \right) \left(\hat{C}_{\ell'} - \left\langle C_{\ell'} \right\rangle_{MC} \right)^* \right\rangle_{MC}$$

Peebles, Netterfield, Hivon, etc.

HFI Core Team: HFI Data Processing

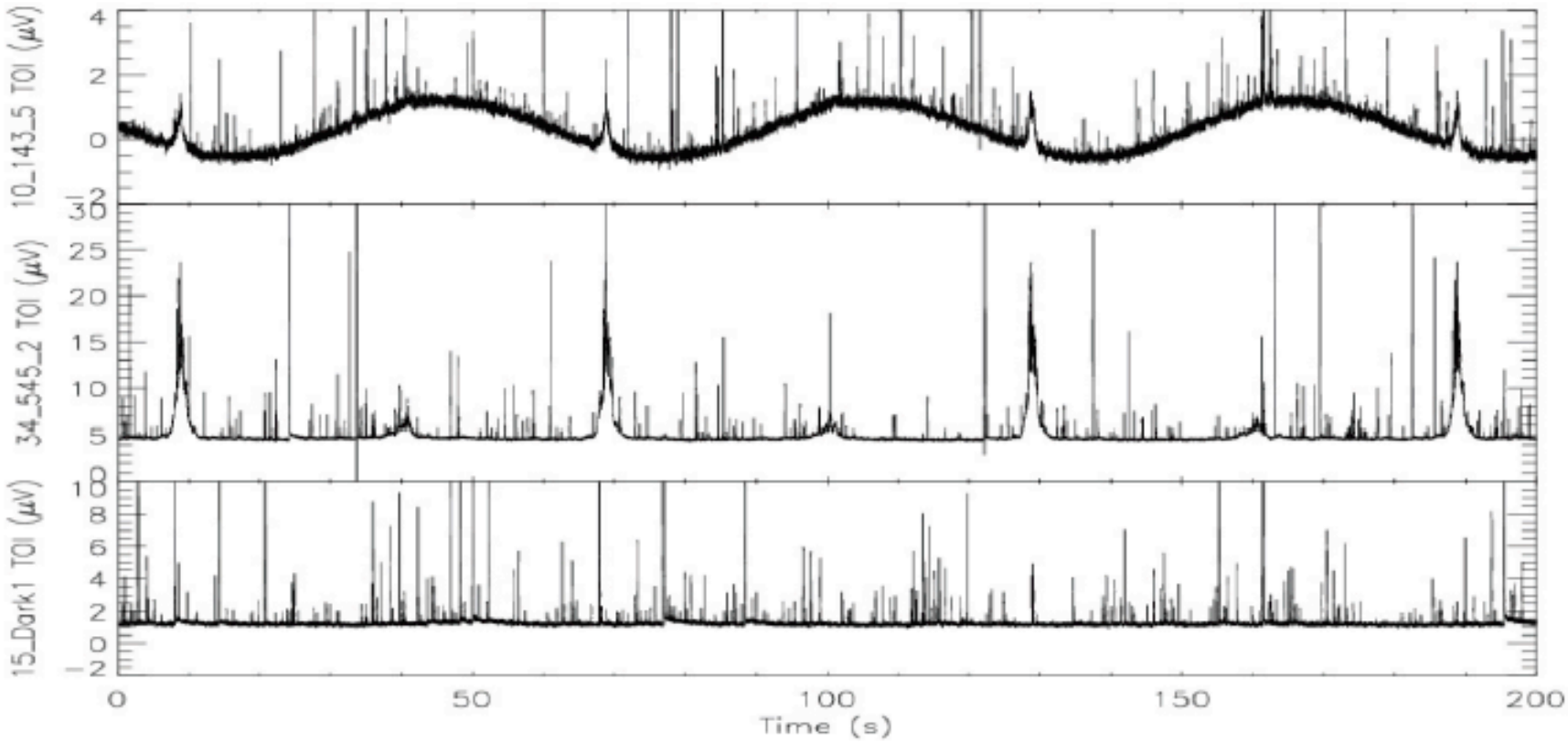

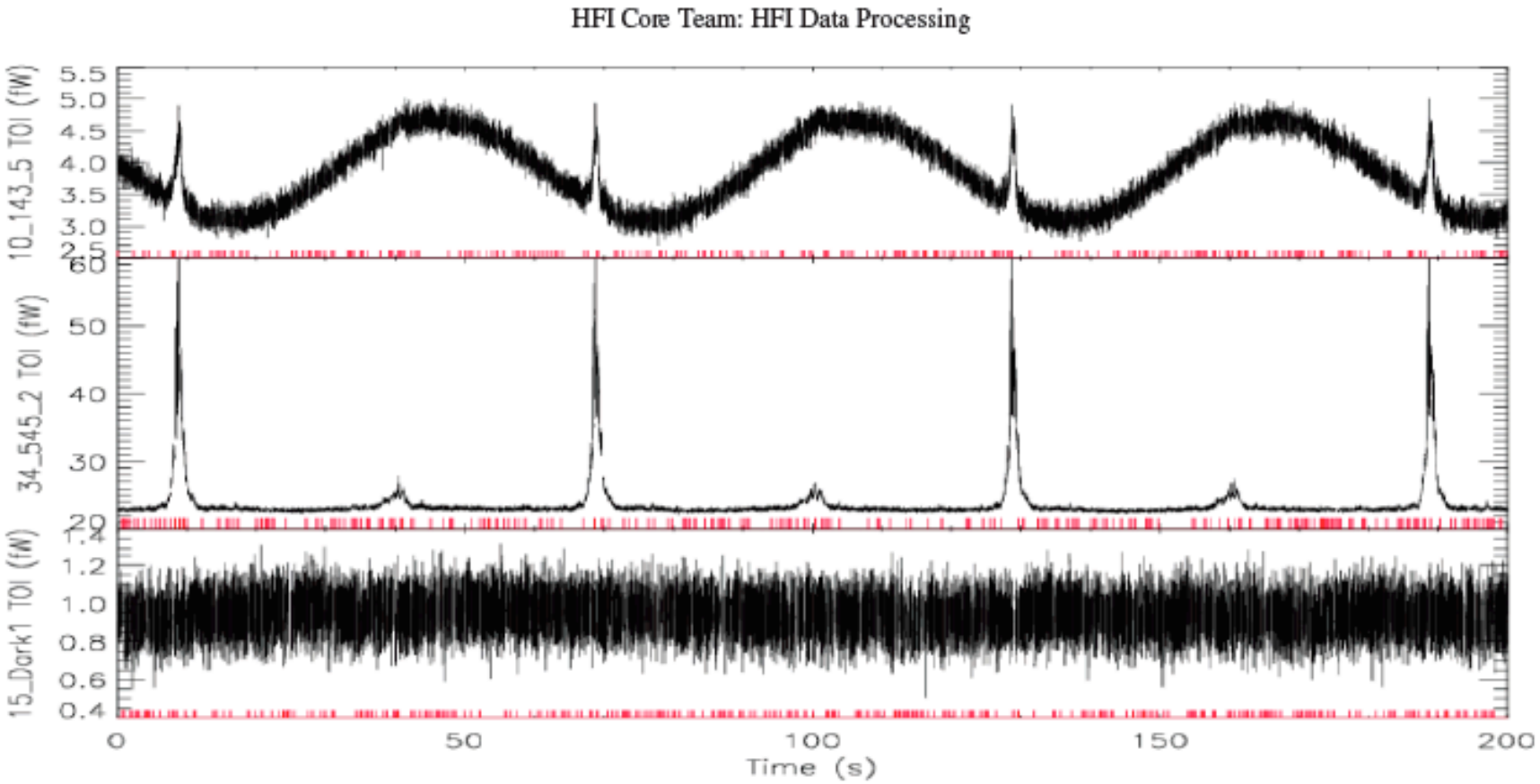
HFI Core Team: HFI Data Processing
10_143_5 TOI (fW)
34_545_2 TOI (fW)
15_Dark1 TOI (fW)
Time (s)

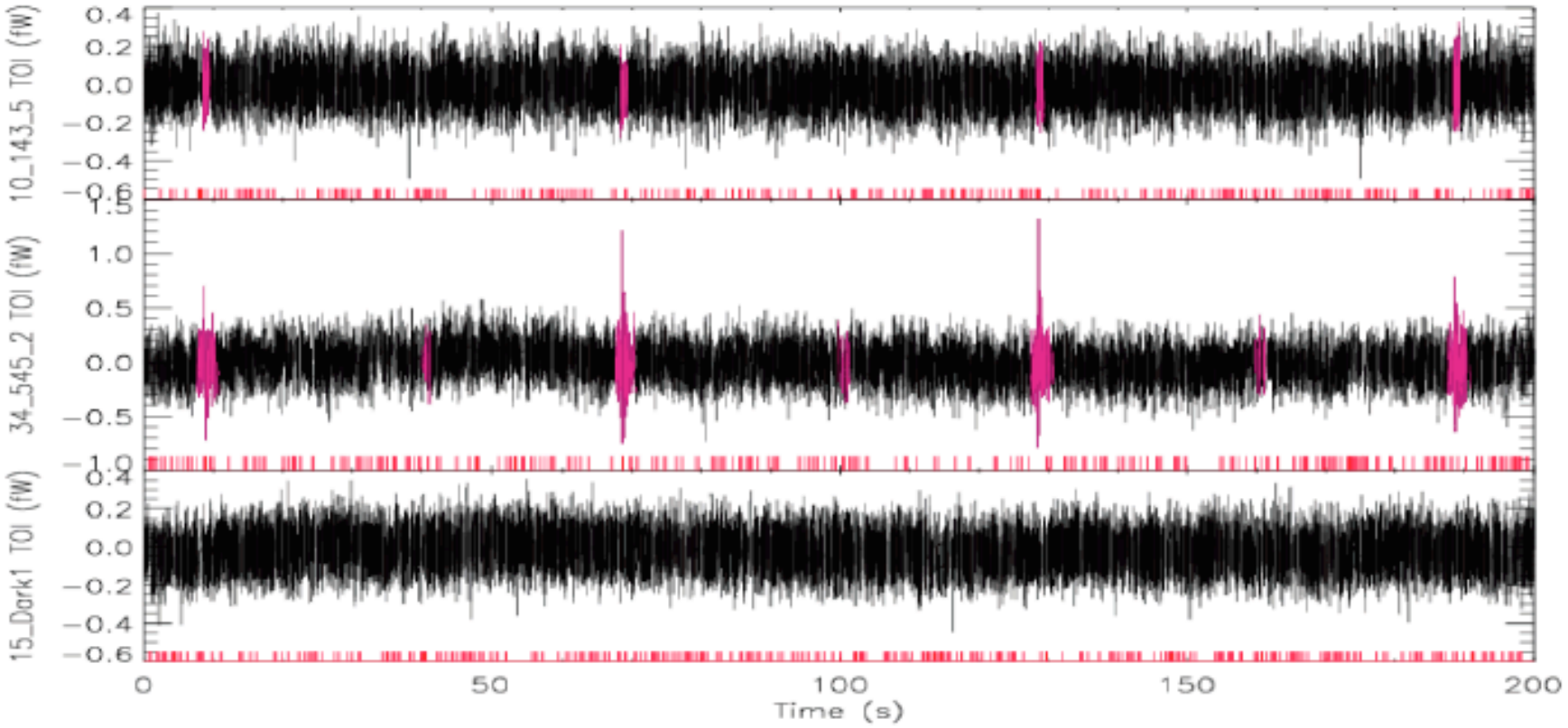

	100	143	217	353	545	857	Dark
N_b	8	11	12	12	3	3	2
%	13.4	15.4	15.8	15.8	9.4	9.2	14.7

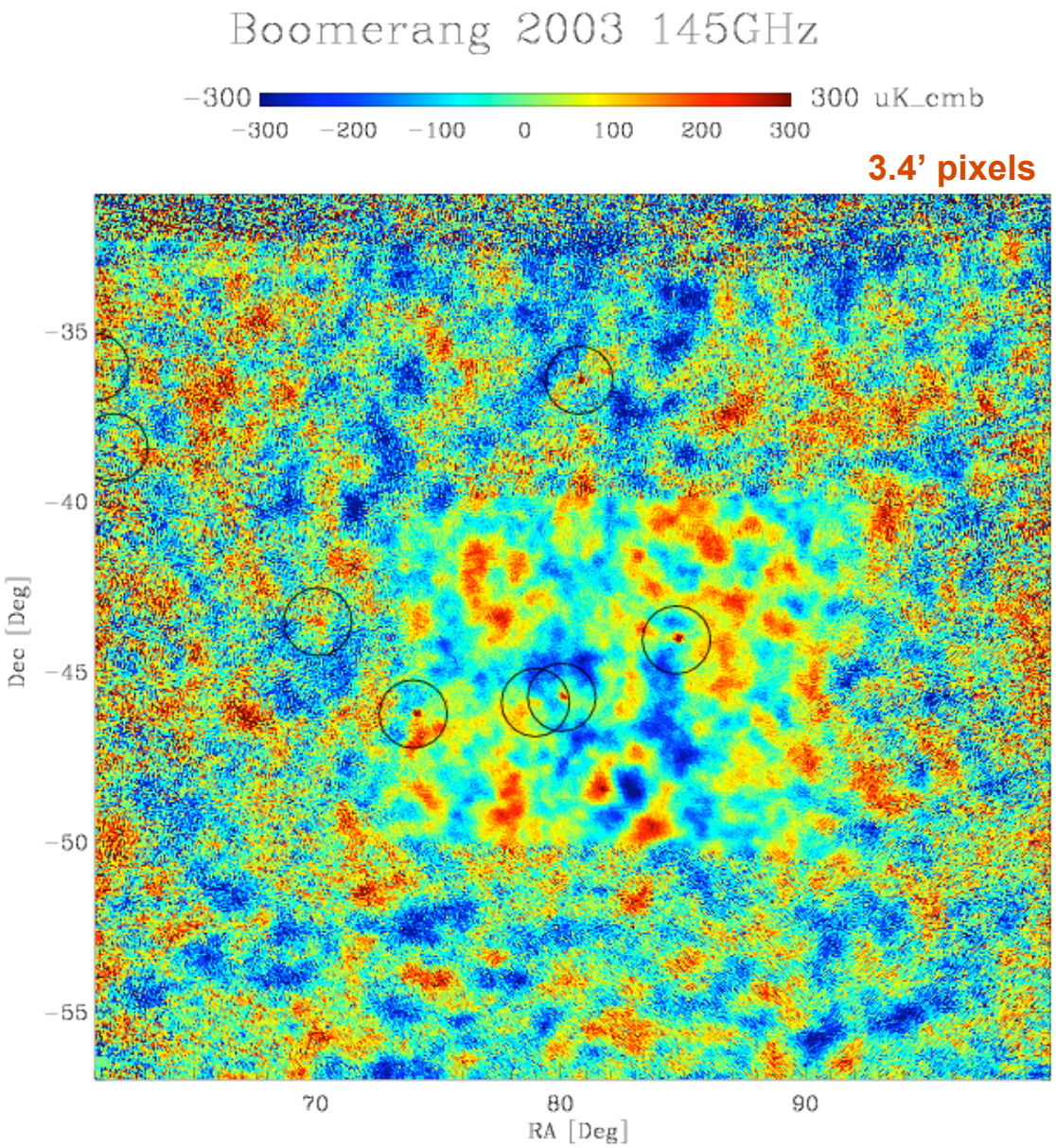

Sum and difference histograms

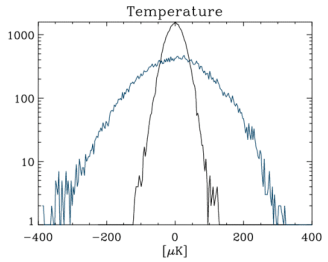

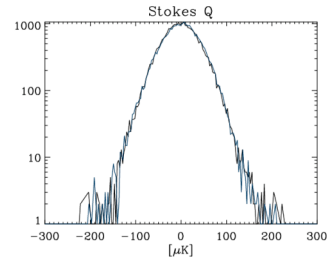

Power Spectrum Estimation

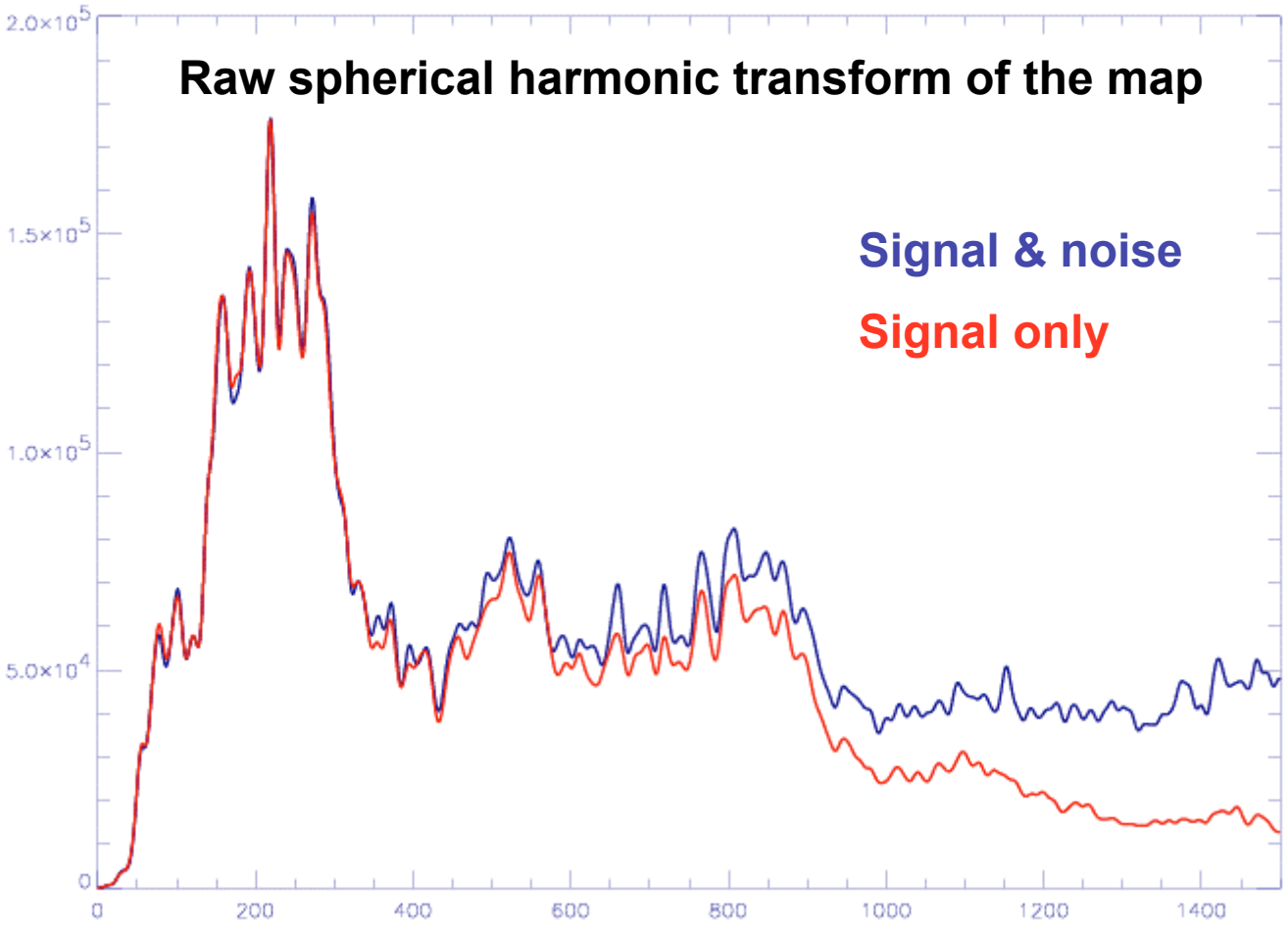

$$\left\langle \tilde{C}_\ell \right\rangle = \sum_{\ell'} M_{\ell\ell'} F_{\ell'} B_{\ell'}^2 \left\langle C_{\ell'} \right\rangle + \left\langle \tilde{N}_\ell \right\rangle$$

Boomerang 2003: Features in the Power Spectrum

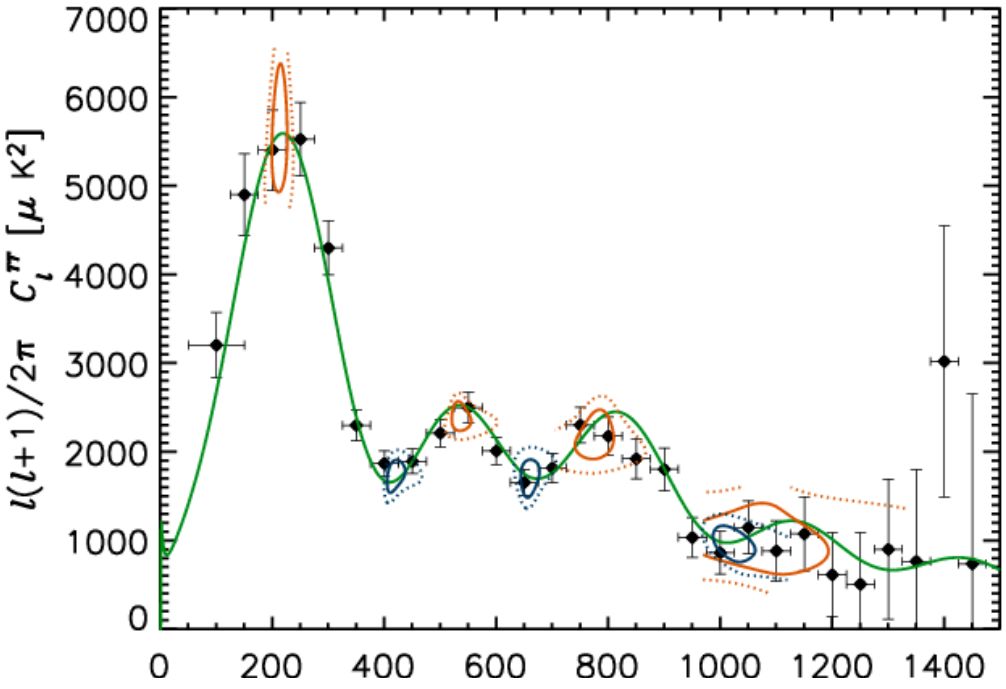

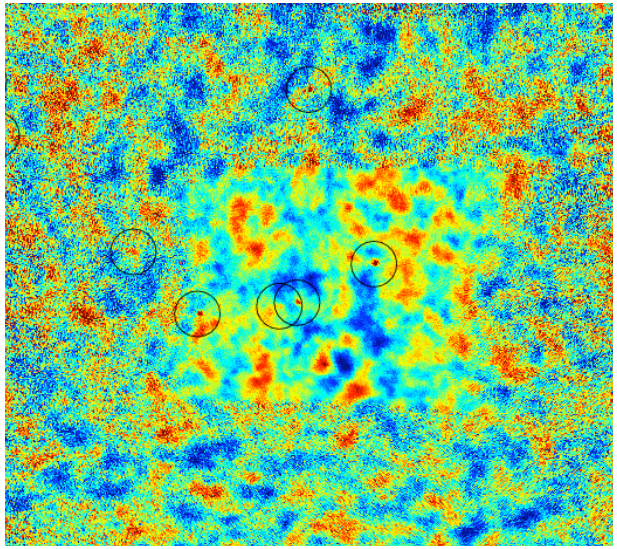

Table 3. Features in the Temperature Power Spectrum

feature	ℓ_{B03}	ΔT^2_{B03}	ℓ_{B98}	ΔT^2_{B98}	ℓ_{WMAP}	ΔT^2_{WMAP}
Peak 1	$214\ ^{+9}_{-12}$	$5614\ ^{+450}_{-443}$	$217\ ^{+10}_{-10}$	$5551\ ^{+477}_{-443}$	$222\ ^{+3}_{-2}$	$5385\ ^{+147}_{-157}$
Valley 1	$413\ ^{+10}_{-5}$	$1717\ ^{+133}_{-70}$	$411\ ^{+9}_{-7}$	$1870\ ^{+136}_{-120}$	$418\ ^{+5}_{-4}$	$1660\ ^{+62}_{-62}$
Peak 2	$529\ ^{+14}_{-6}$	$2419\ ^{+125}_{-128}$	$526\ ^{+17}_{-14}$	$2316\ ^{+119}_{-121}$	$530\ ^{+15}_{-8}$	$2404\ ^{+89}_{-64}$
Valley 2	$659\ ^{+12}_{-11}$	$1780\ ^{+131}_{-165}$	$(677)\ ^{+65}_{-29}$	$(1958)\ ^{+200}_{-170}$	—	—
Peak 3	$781\ ^{+15}_{-22}$	$2166\ ^{+208}_{-216}$	$(766)\ ^{+42}_{-43}$	$(2080)\ ^{+261}_{-227}$	—	—
Valley 3	$1015\ ^{+26}_{-23}$	$991\ ^{+137}_{-192}$	—	—	—	—
Peak 4	$(1055)\ ^{+58}_{-56}$	$(1024)\ ^{+254}_{-271}$	—	—	—	—

8. *WMAP* Power Spectrum Peak and Trough Data

Quantity	l	ΔT_l^2 (μK^2)
First peak	220.7 ± 0.7	5619 ± 30
First trough	412.8 ± 1.9	1704 ± 27
Second peak	531.3 ± 3.5	2476 ± 40
Second trough	674.6 ± 12.1	1668 ± 85
Third Peak	1143 ± 167	2442 ± 355

Hinshaw, WMAP 3yr

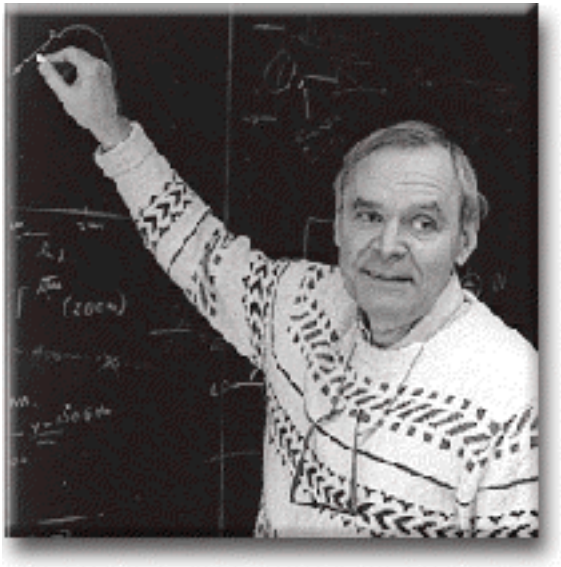

Dave Wilkinson

WMAP

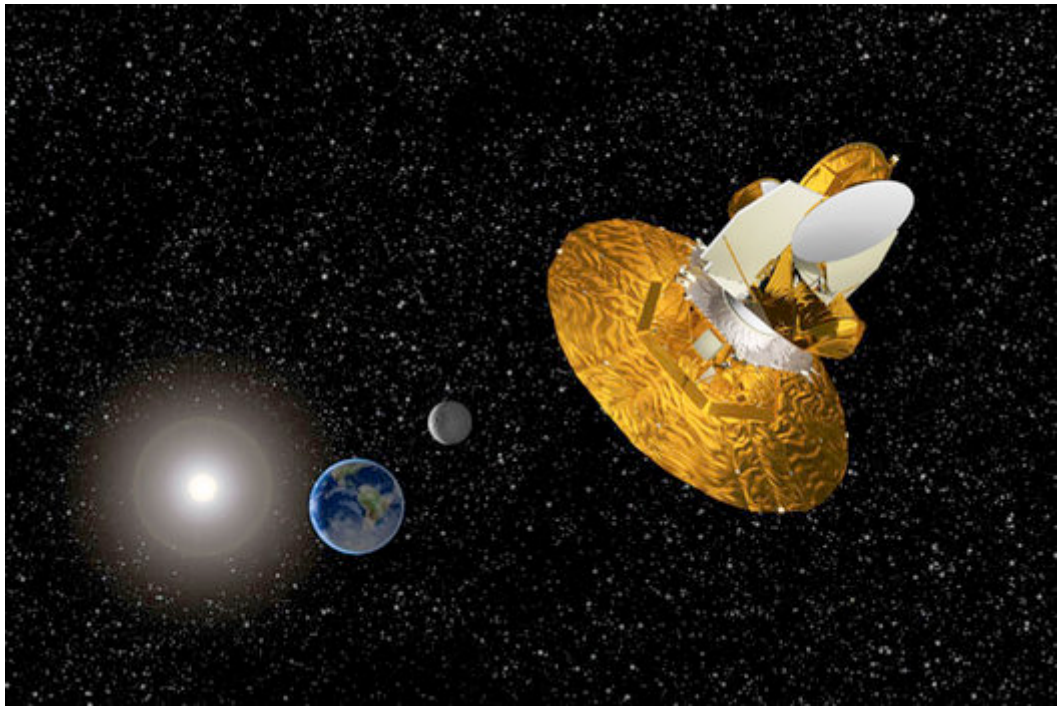

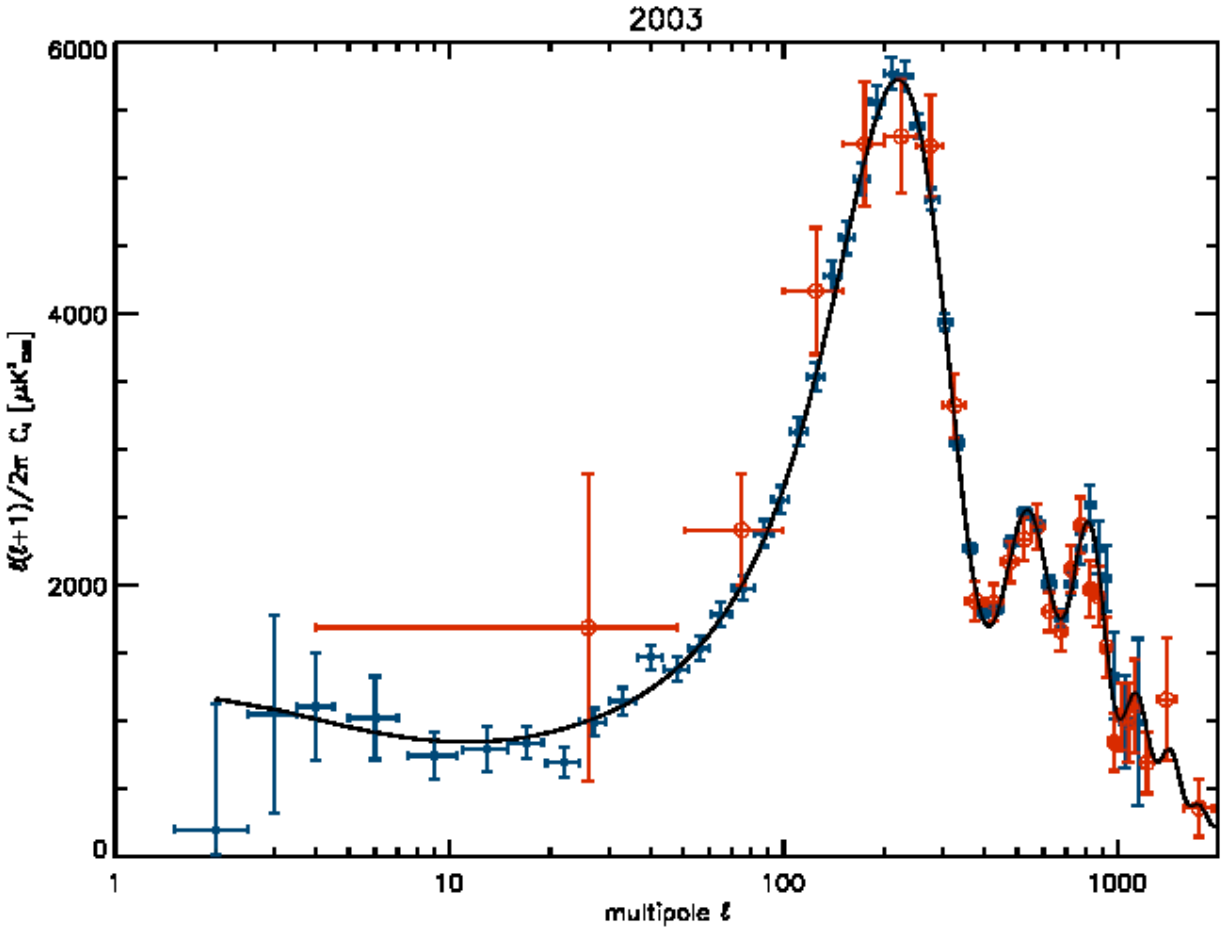

WMAP

Boomerang

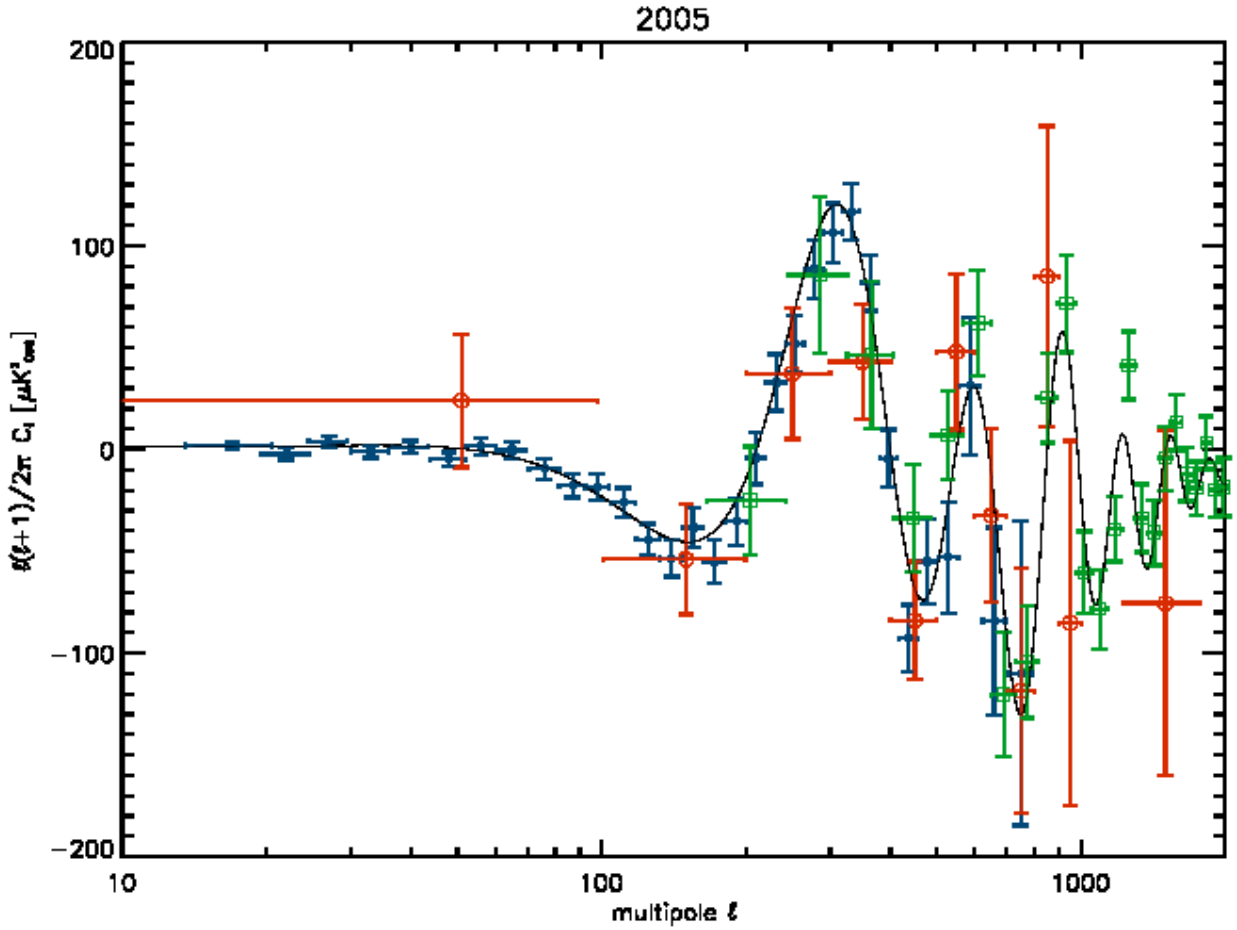

WMAP

Boomerang

QUaD

The near and intermediate future of CMB observations

- Extracting the remaining information from primary anisotropies

  (sample variance limited observations of all available sky)
- Model testing/probes of Inflation

  (polarization on large scales)
- Secondary anisotropies - SZ, lensing and far-IR background

  (smaller angular scales, wide frequency coverage and polarization)

Completing the primary anisotropies

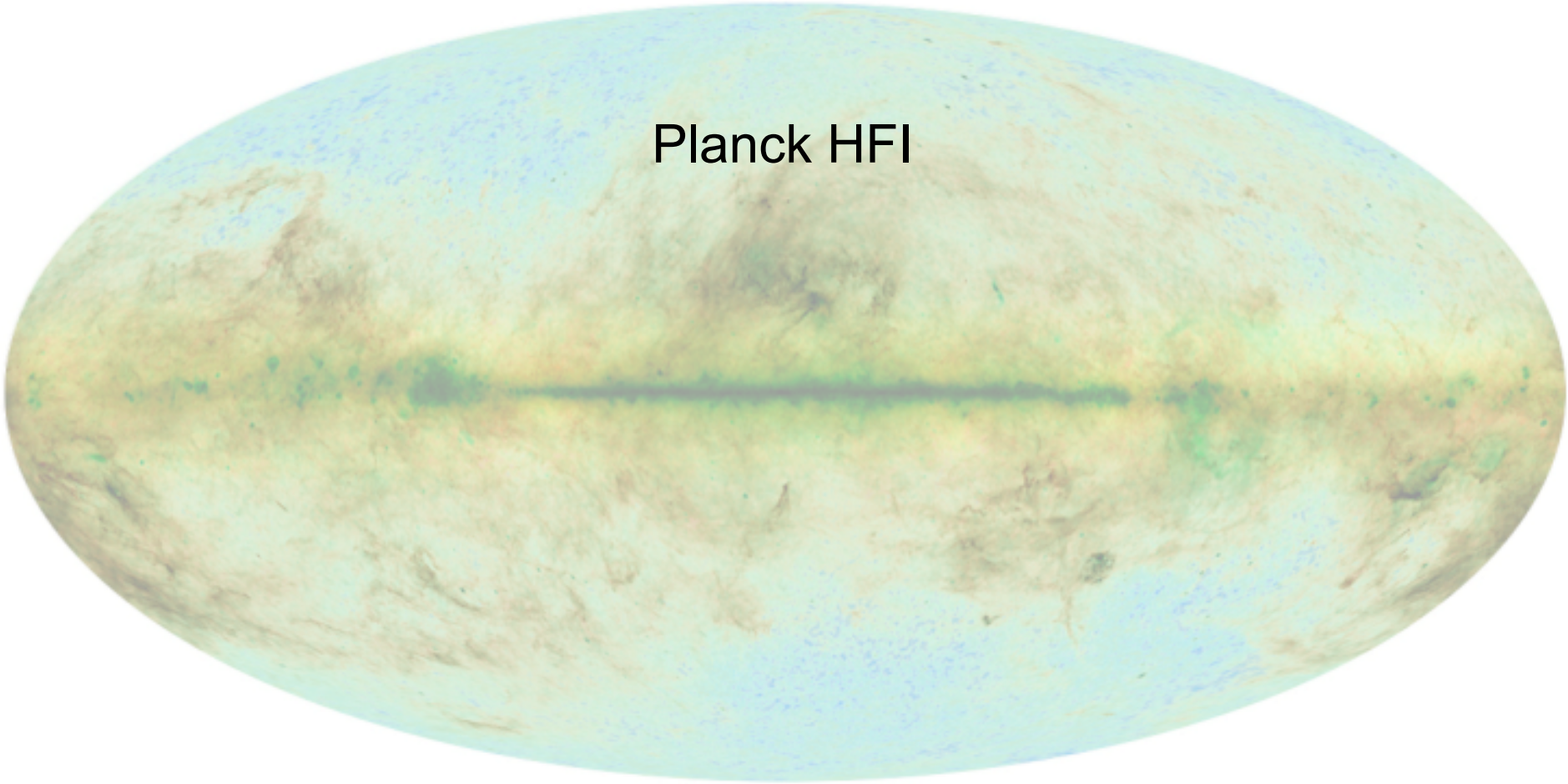

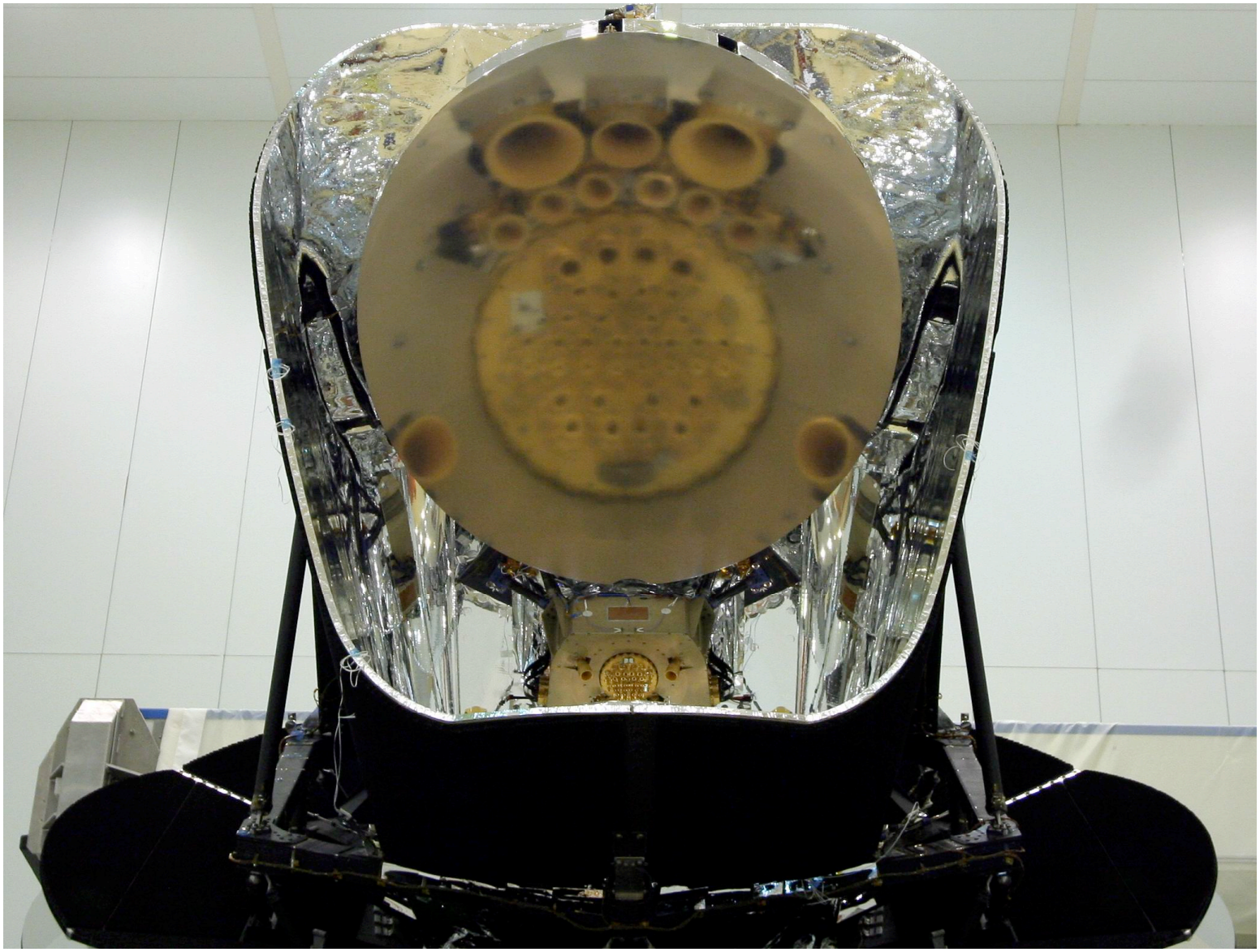

- 14 May, 2009: Launch
- 4 July: HFI sees the dipole
- 13 August: Beginning of first scientific survey
- January 2010 First data release
- February 2012 Expected HFI end of life
- November 2012 First cosmological data release

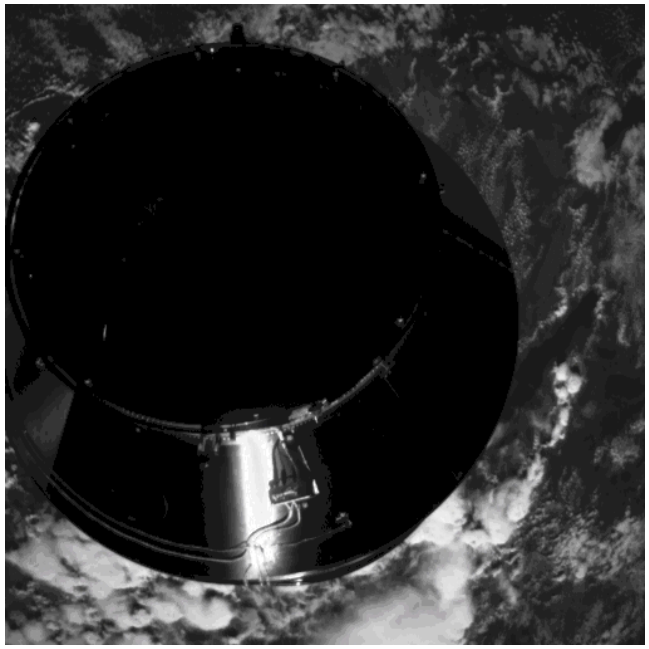

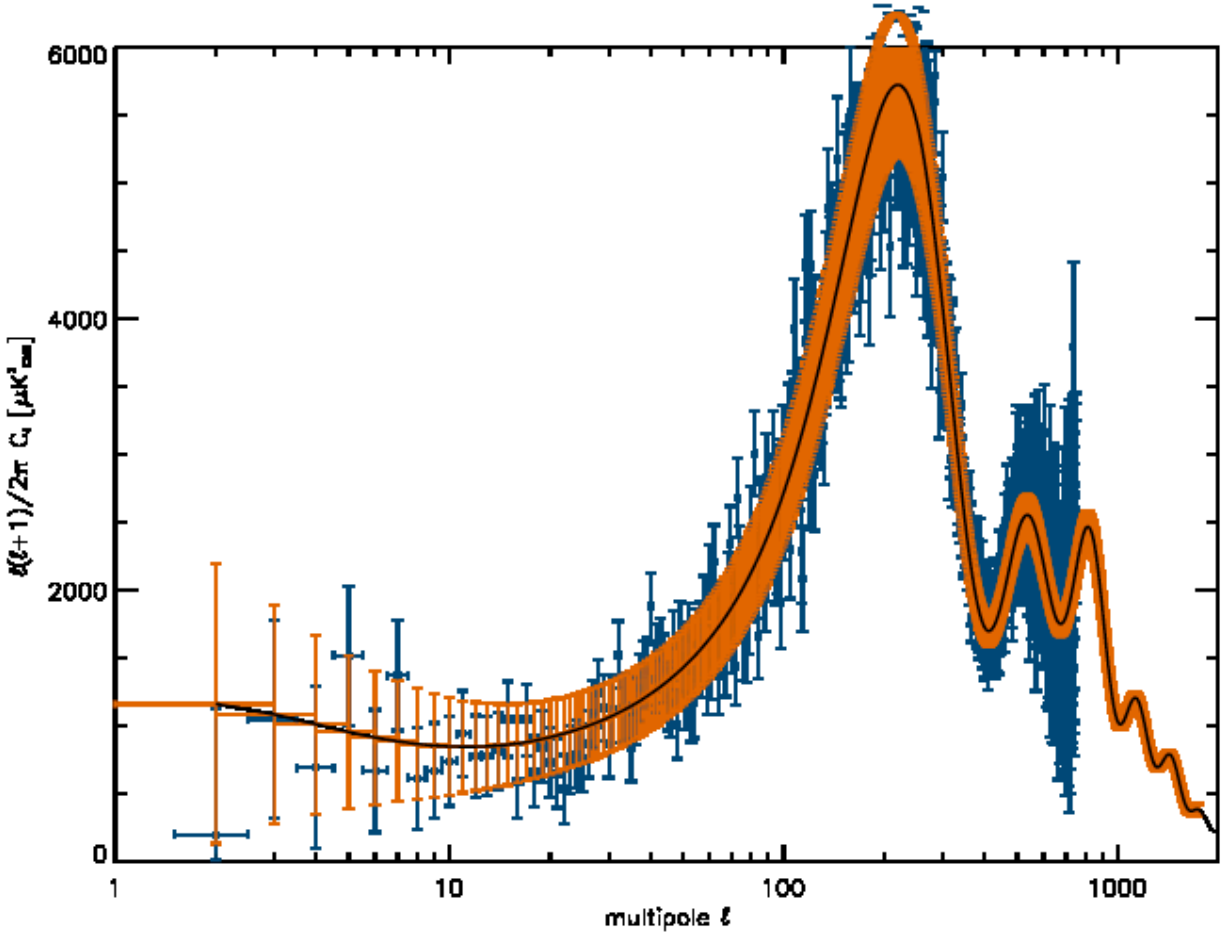

WMAP

Planck HFI

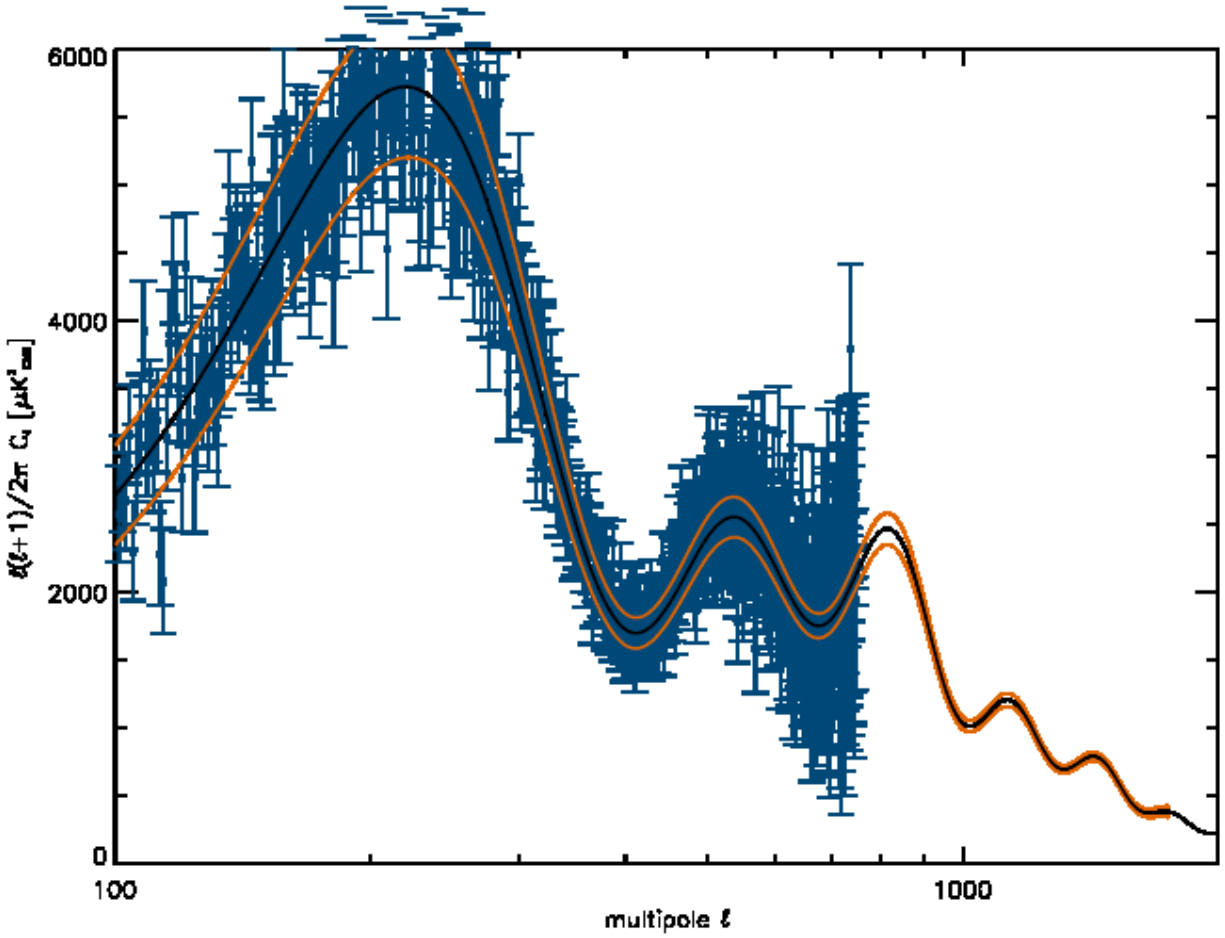

WMAP

Planck HFI

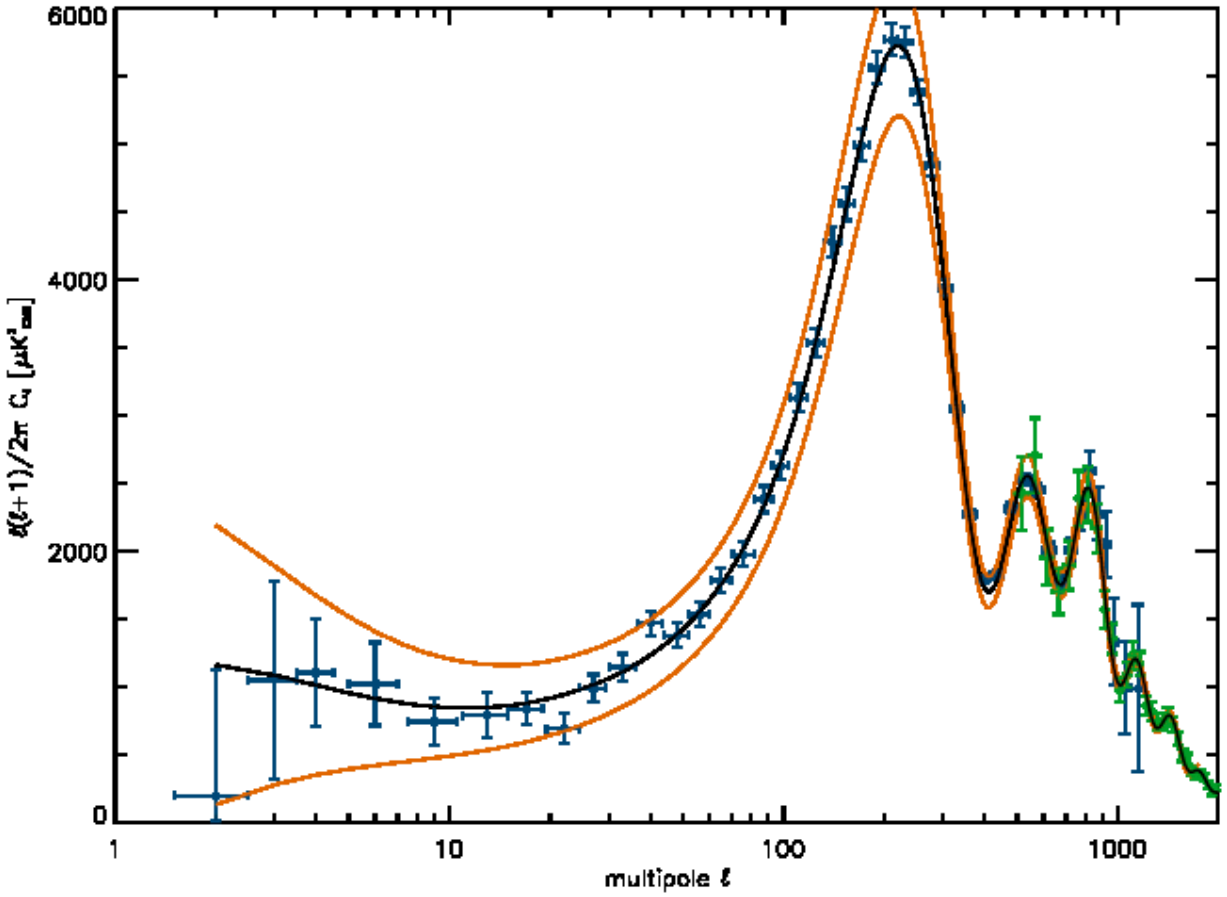

WMAP

Planck HFI

ACT

Small scale anisotropies

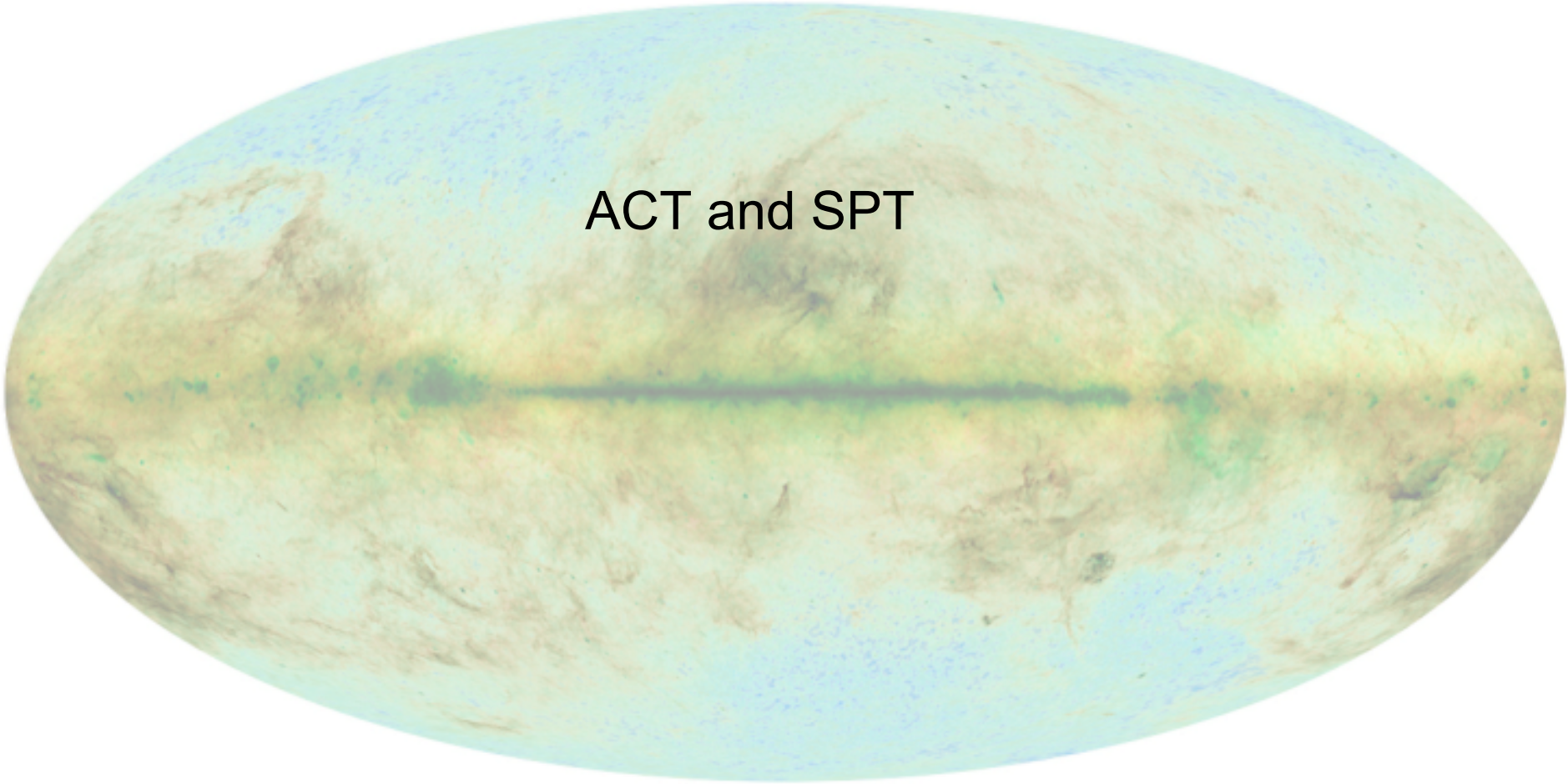

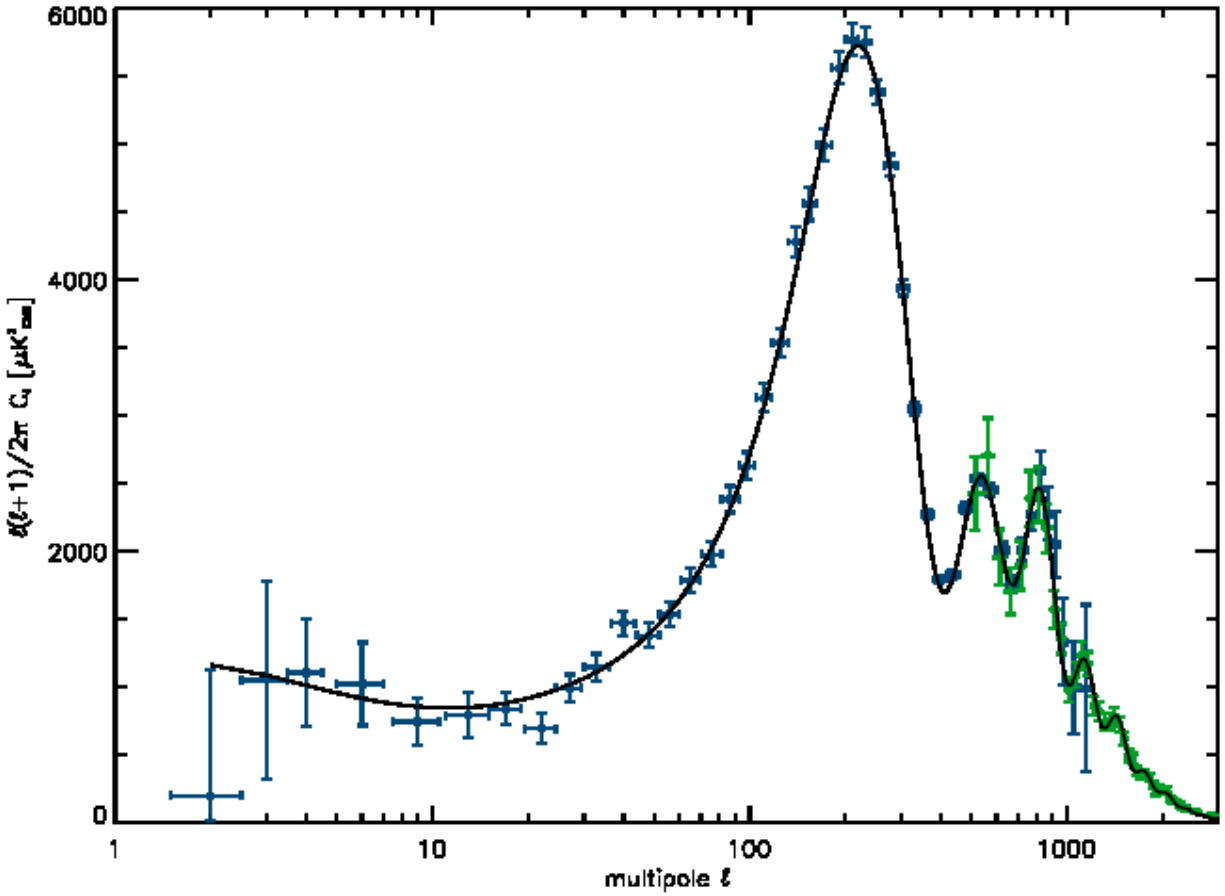
6000
4000
2000
0
1
10
100
1000
multipole ℓ
ℓ(ℓ+1)/2π C_ℓ [μK²]

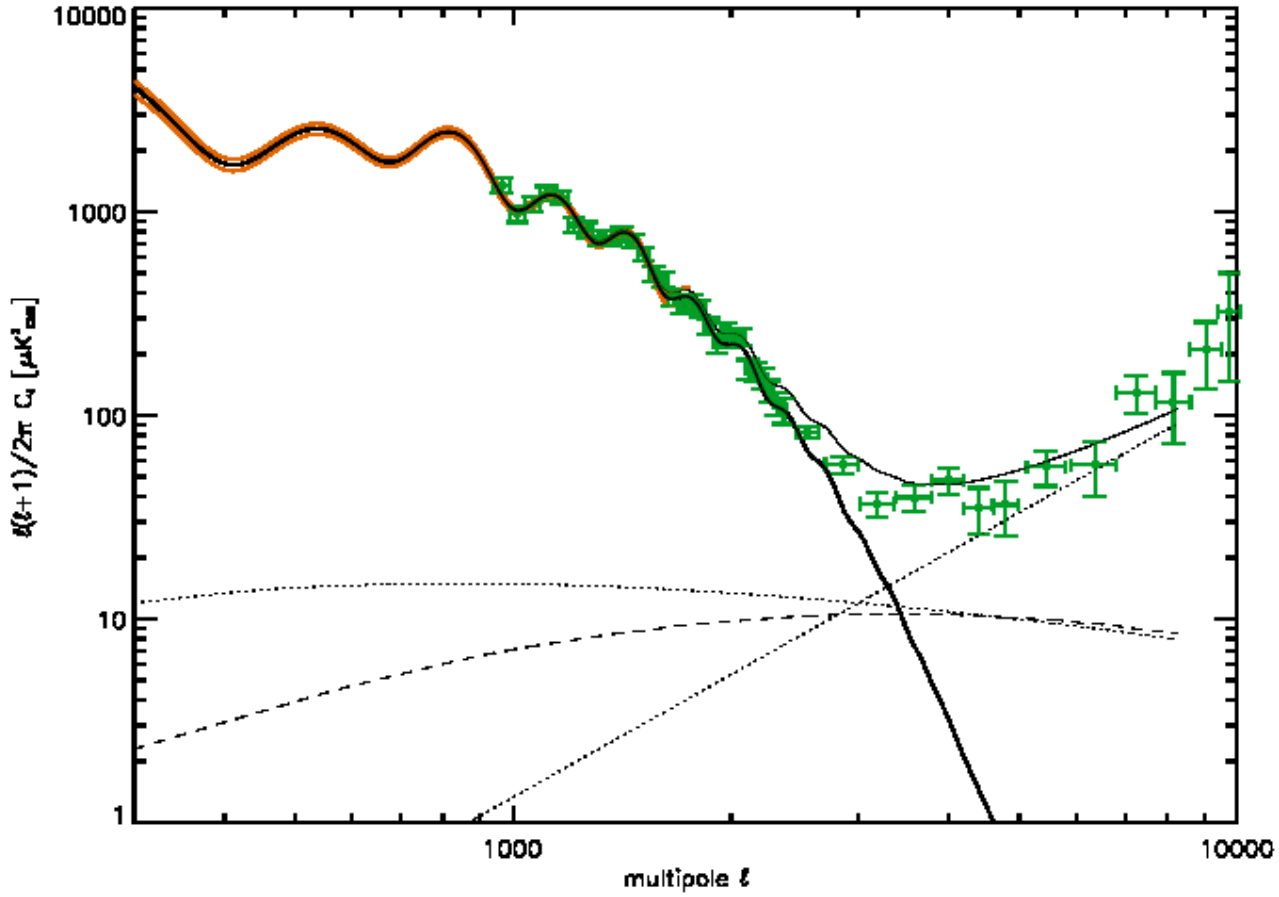
10000
1000
100
10
1
1000
10000
multipole ℓ

Planck: Cosmic Infrared Background

Raw data

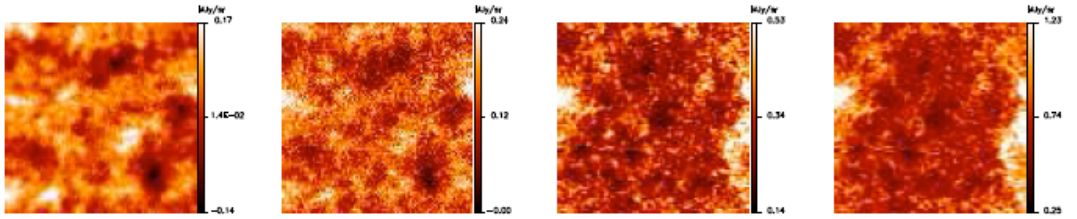

… minus the CMB and point sources

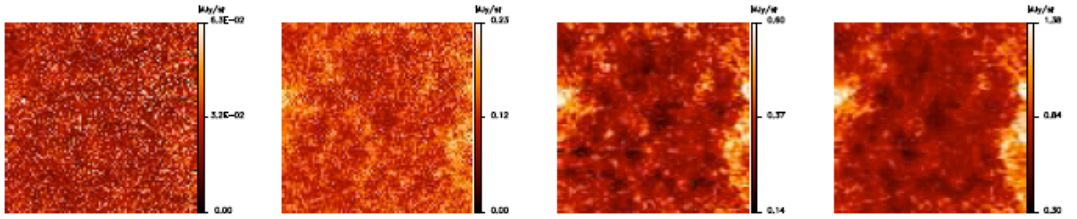

… minus (most) of the Galactic dust

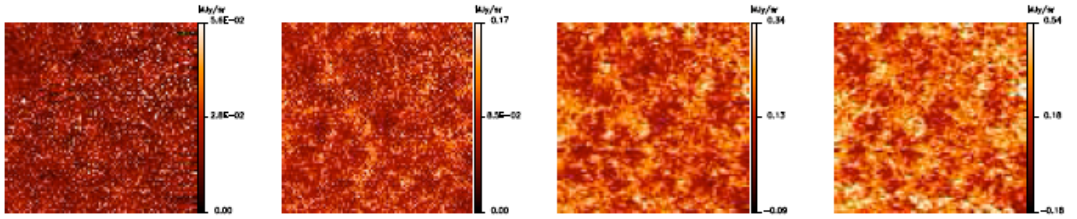

CIB fluctuations

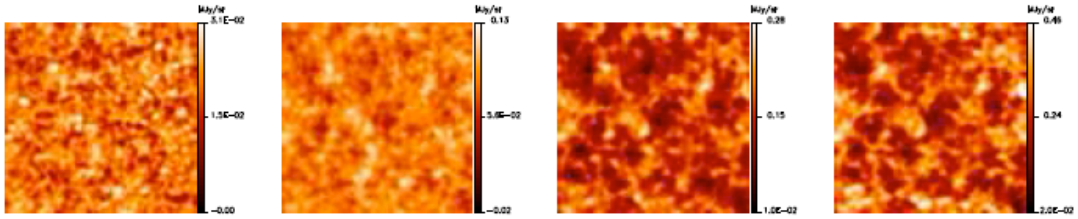

Planck: The (Early) SZ Catalog

- First all sky cluster survey since ROSAT (1992)
- Sensitive to massive clusters
- 189 SZ detected clusters (169 previously known, 20 new [11 confirmed])

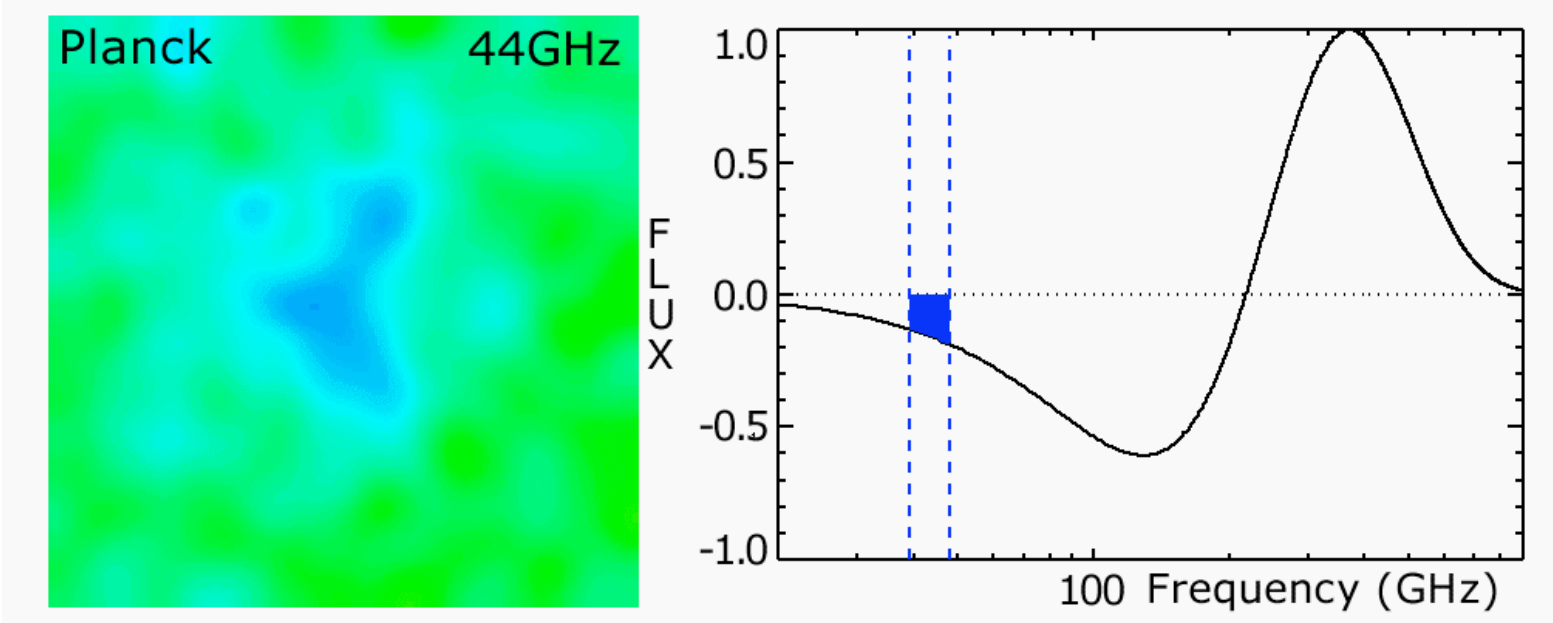

CMB Polarization

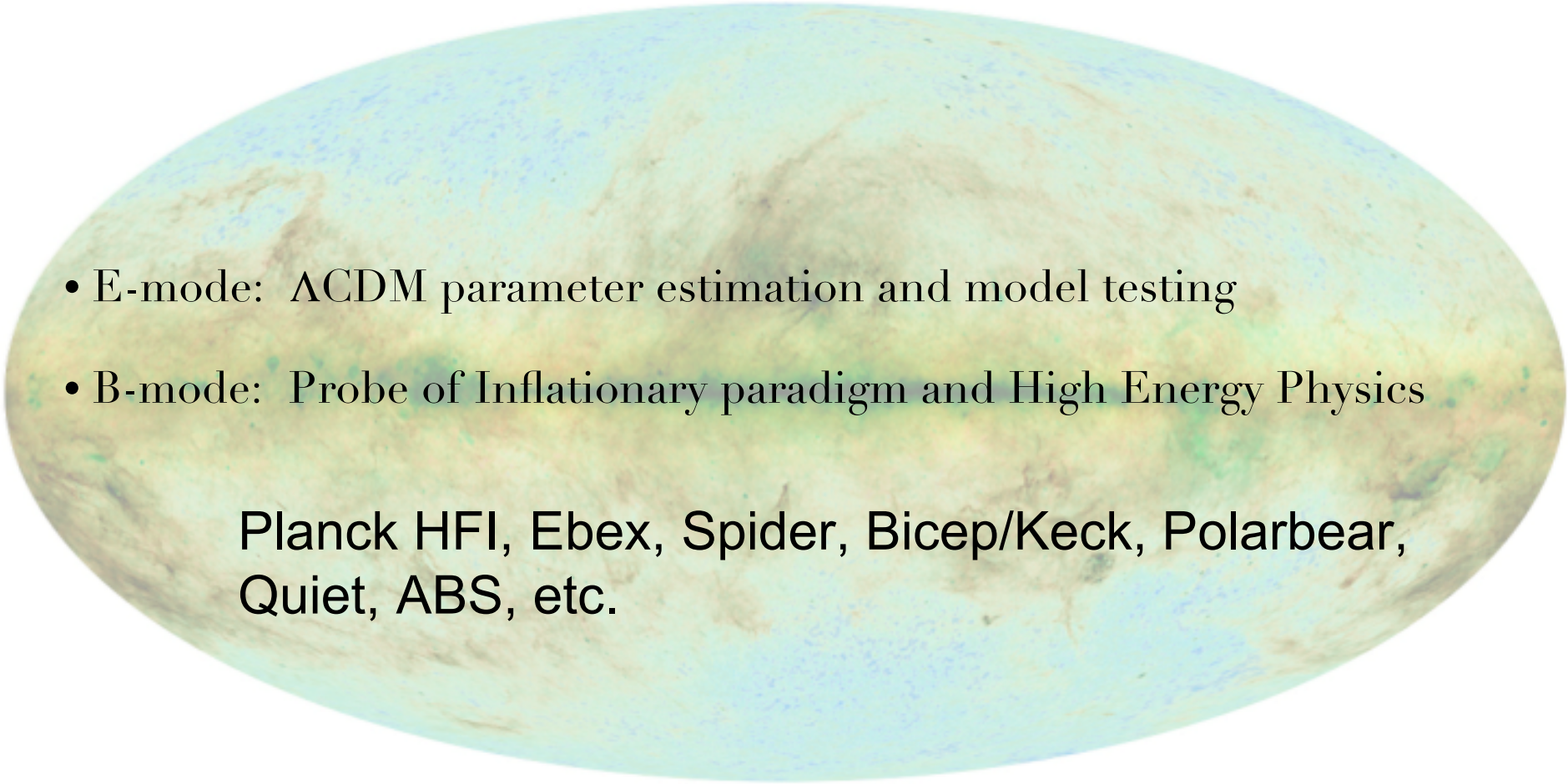

- E-mode: ΛCDM parameter estimation and model testing
- B-mode: Probe of Inflationary paradigm and High Energy Physics

Planck HFI, Ebex, Spider, Bicep/Keck, Polarbear, Quiet, ABS, etc.

CMB Polarization Power Spectra

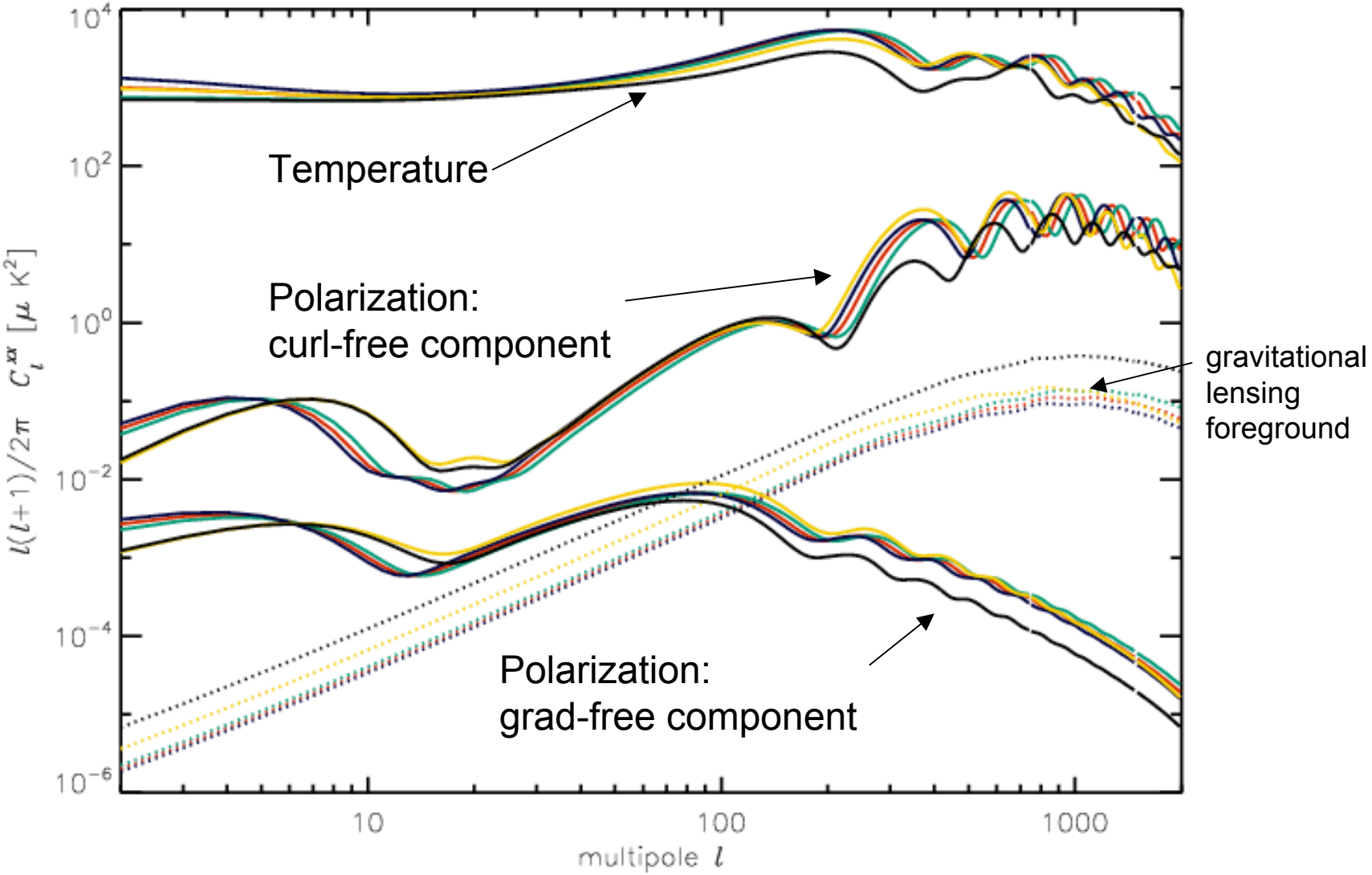

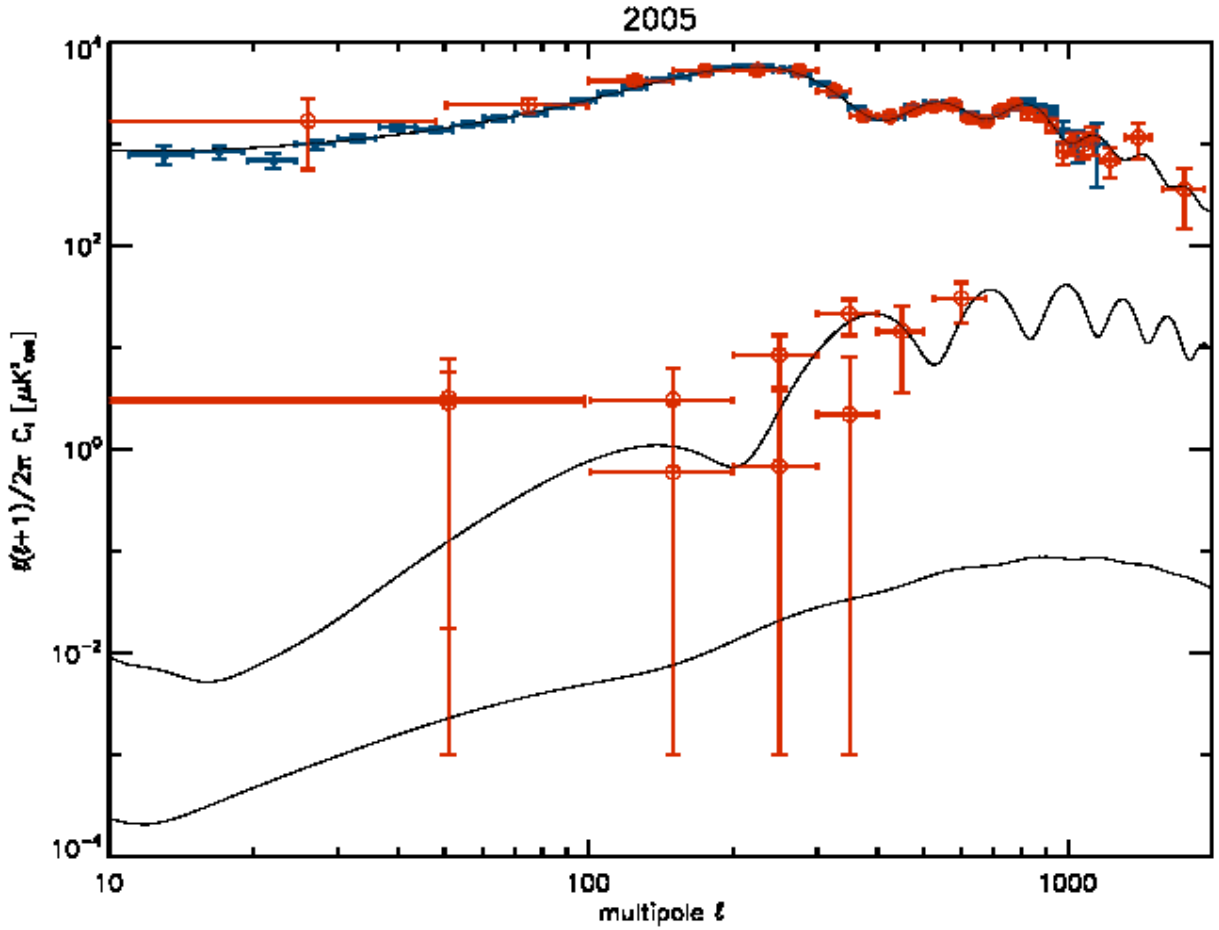

WMAP

Boomerang

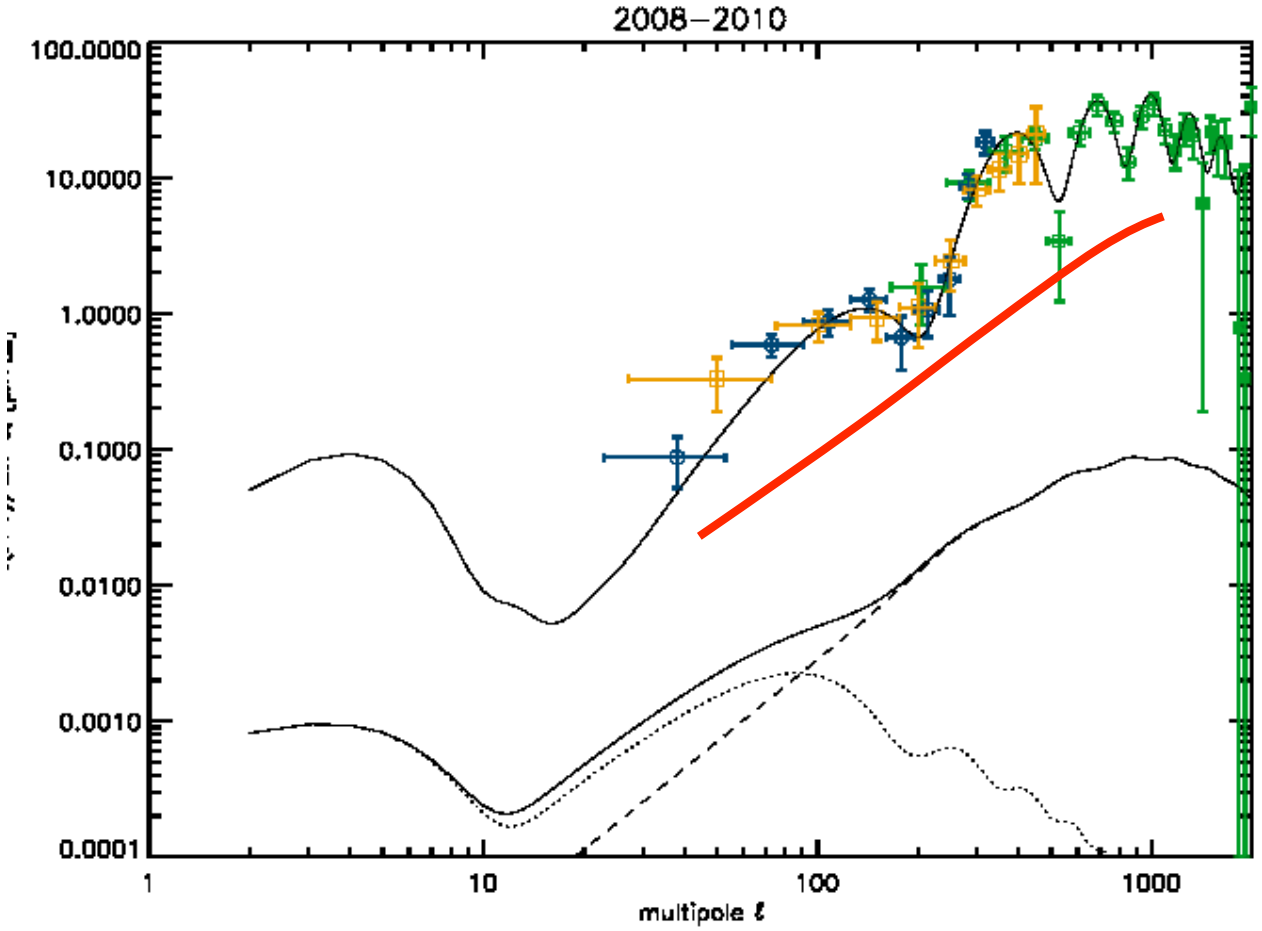

Bicep

Quiet

Quad

Achieving nano-Kelvin sensitivity: massively scaled bolometric arrays

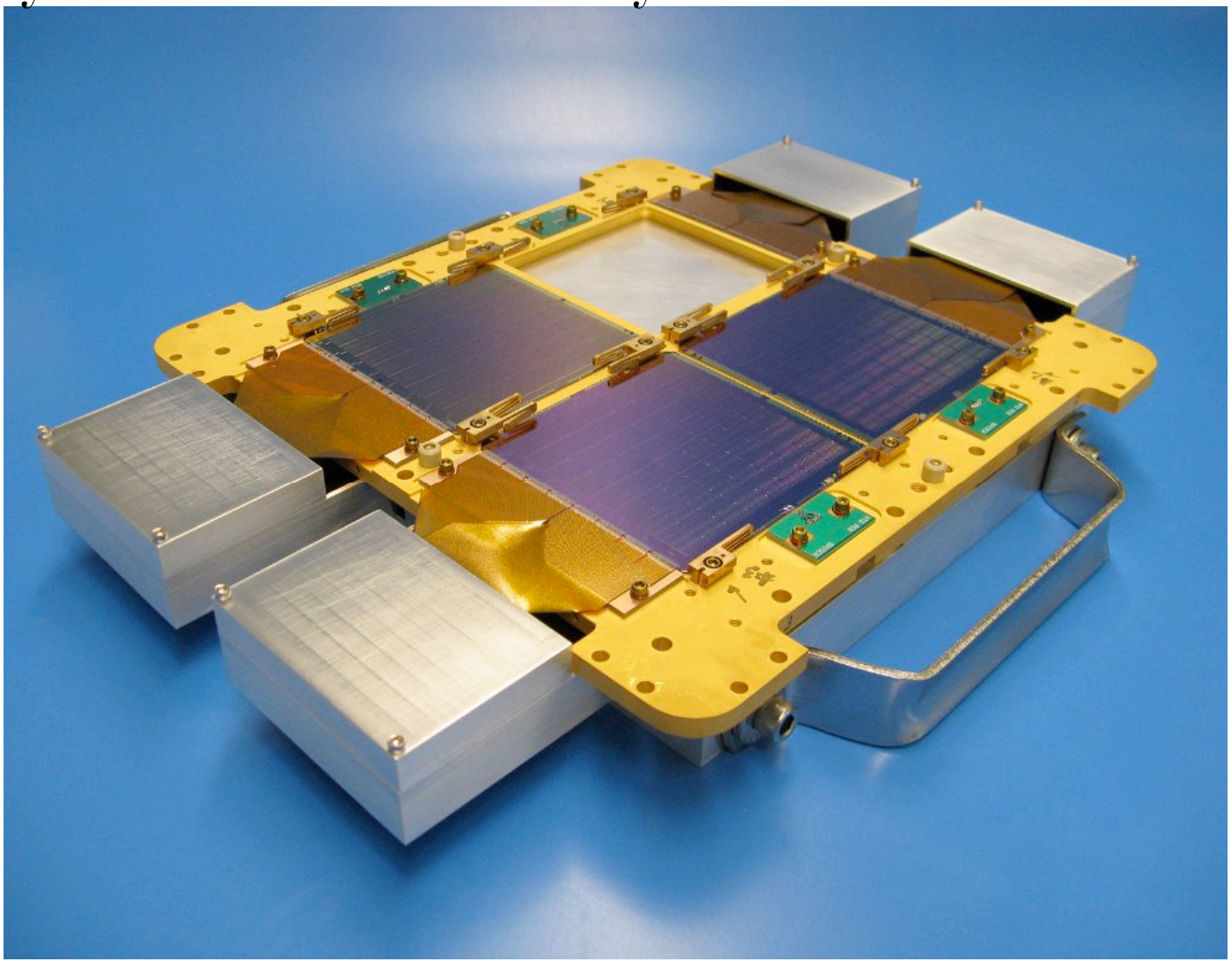

Achieving nano-Kelvin sensitivity: a massive data analysis problem.

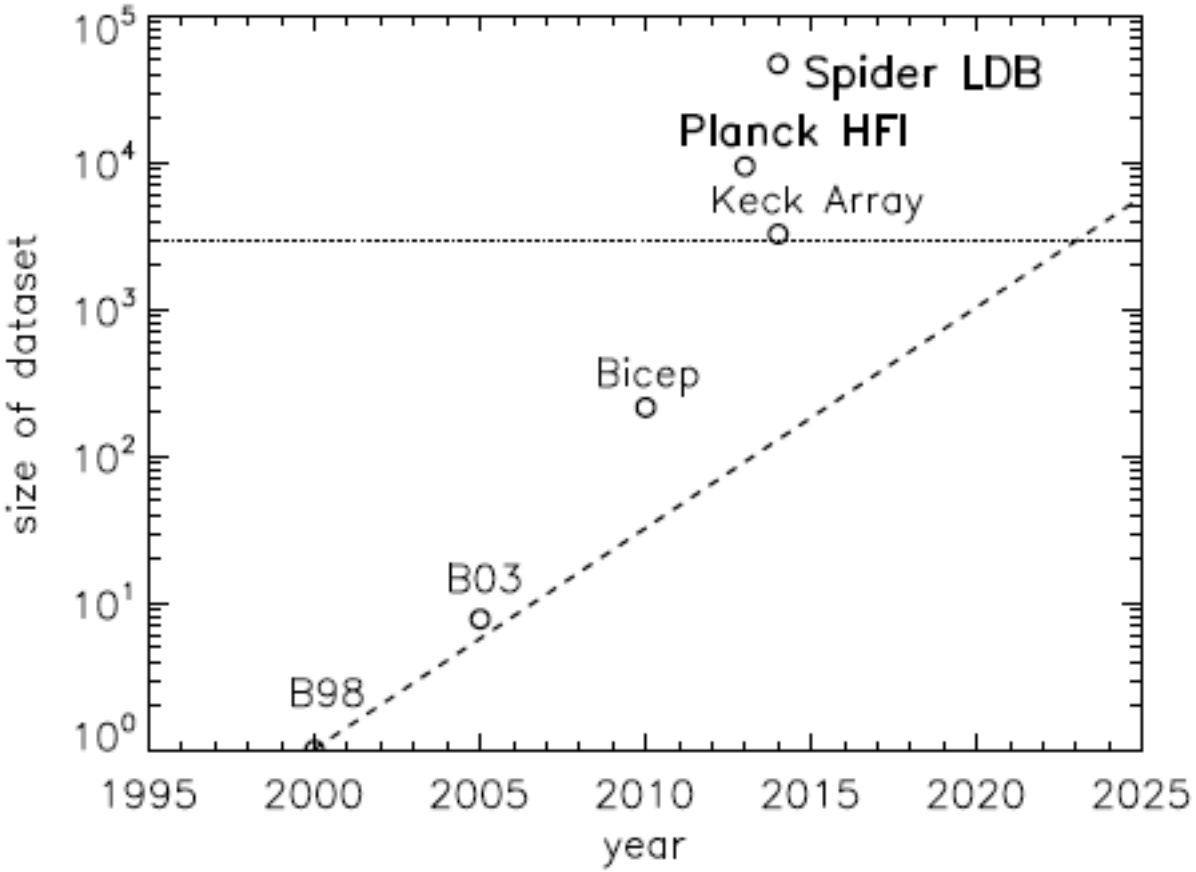

Spider: a Suborbital Probe of Inflation, Dust and the epoch of Reionization

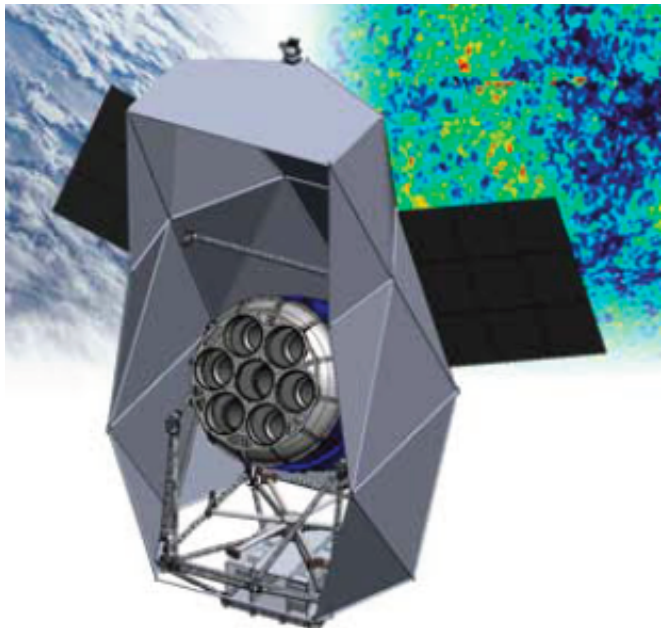

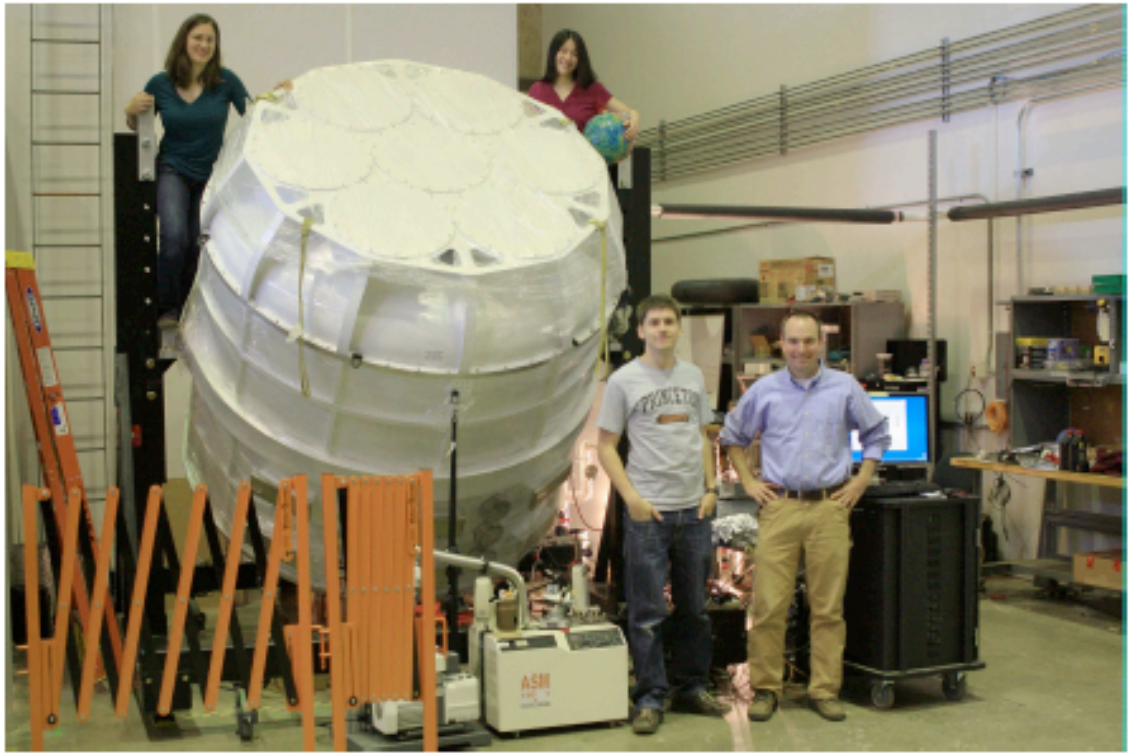

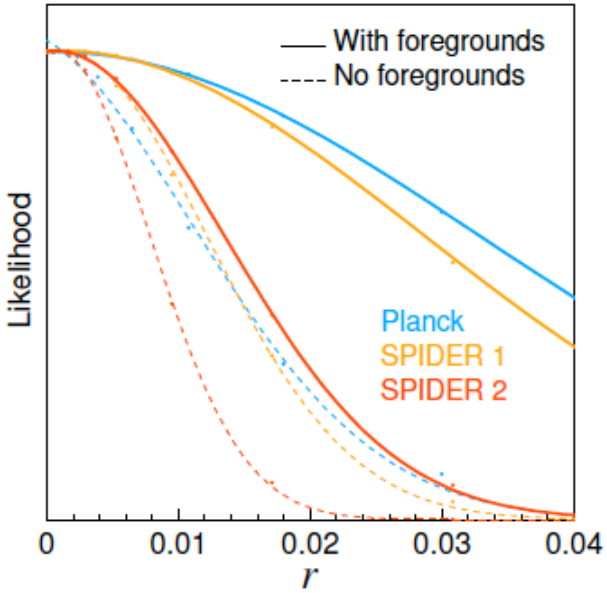

Major experimental challenges

- sensitivity (impact on cryogenics, optics, etc)
- atmosphere
- beams and sidelobes
- gain stability, calibration, pointing
- noise properties (instrumental & environmental)
- the Galaxy
- …everything else

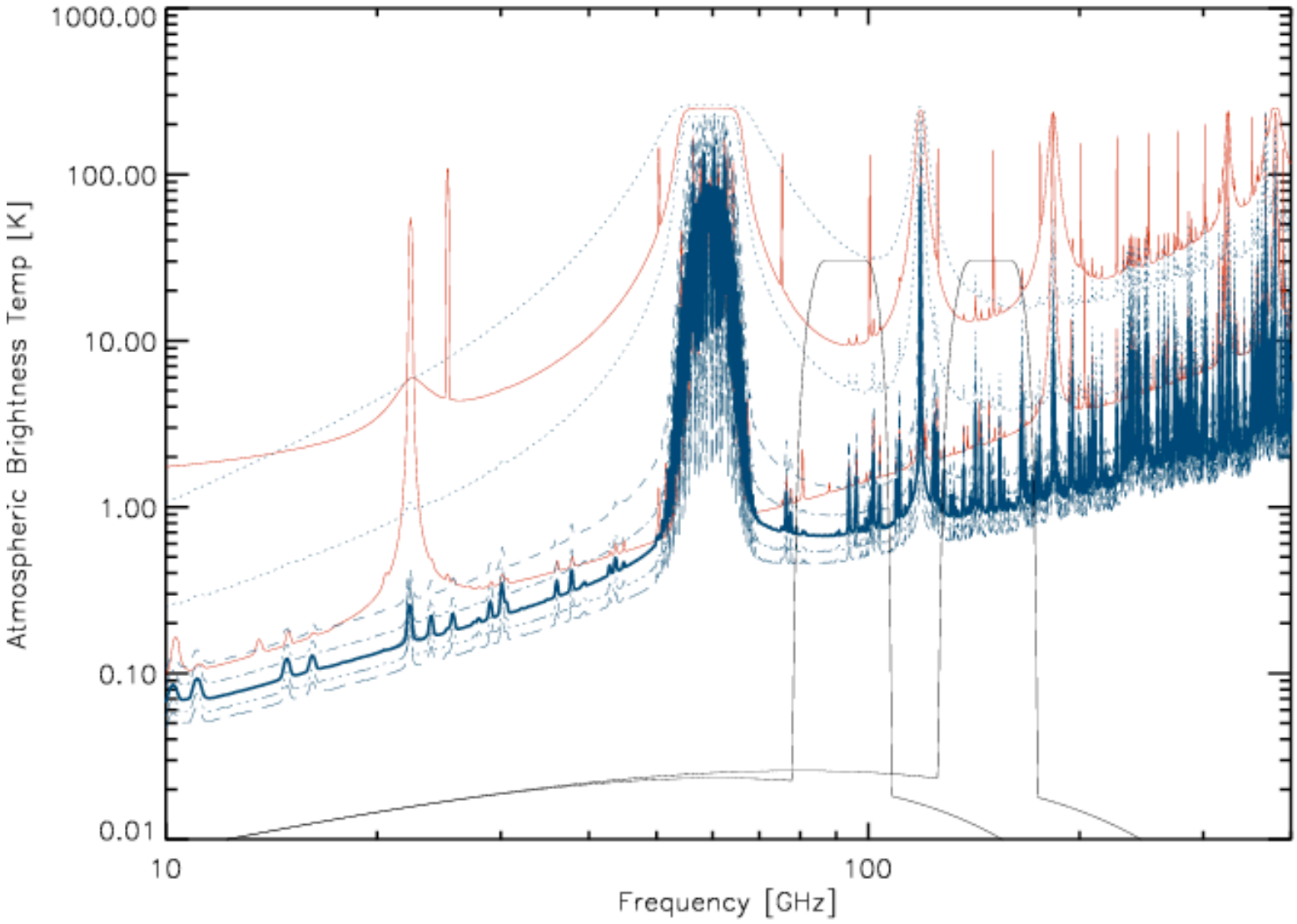
1000.00
100.00
10.00
1.00
0.10
0.01
Atmospheric Brightness Temp [K]
10
100
Frequency [GHz]

The millimeter-wave sky

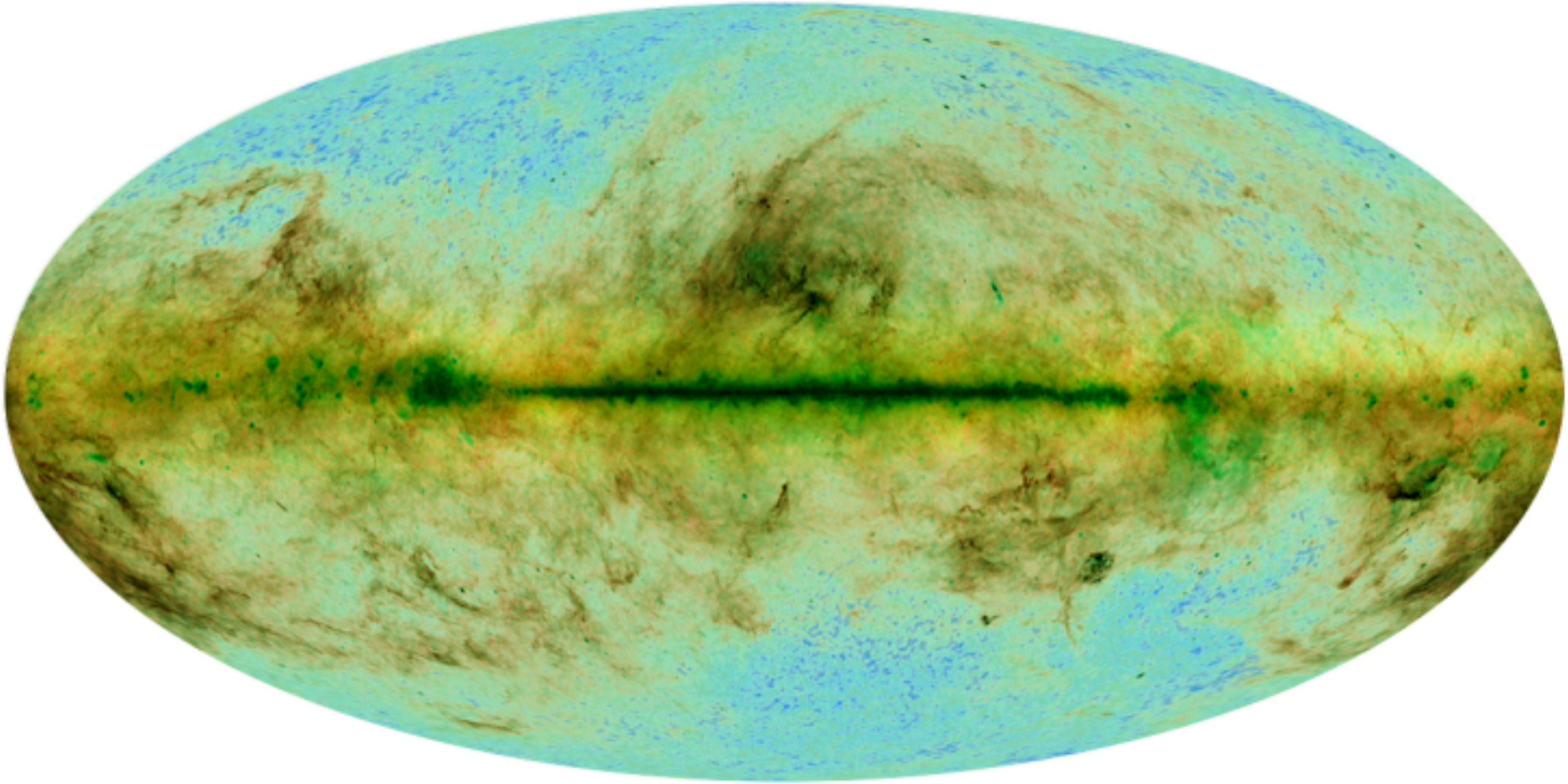

Planck all-sky foreground maps

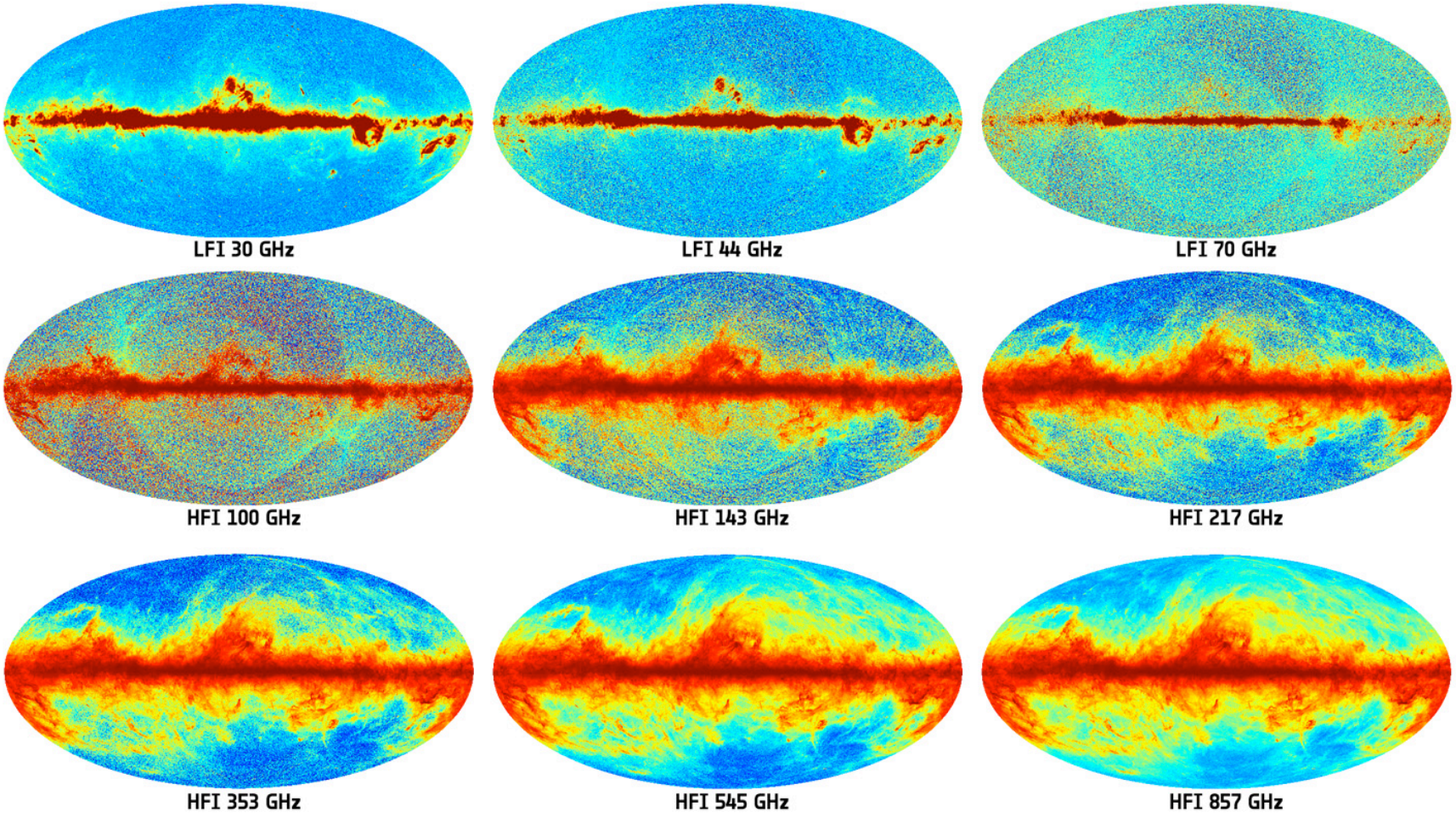

Fraisse et al.

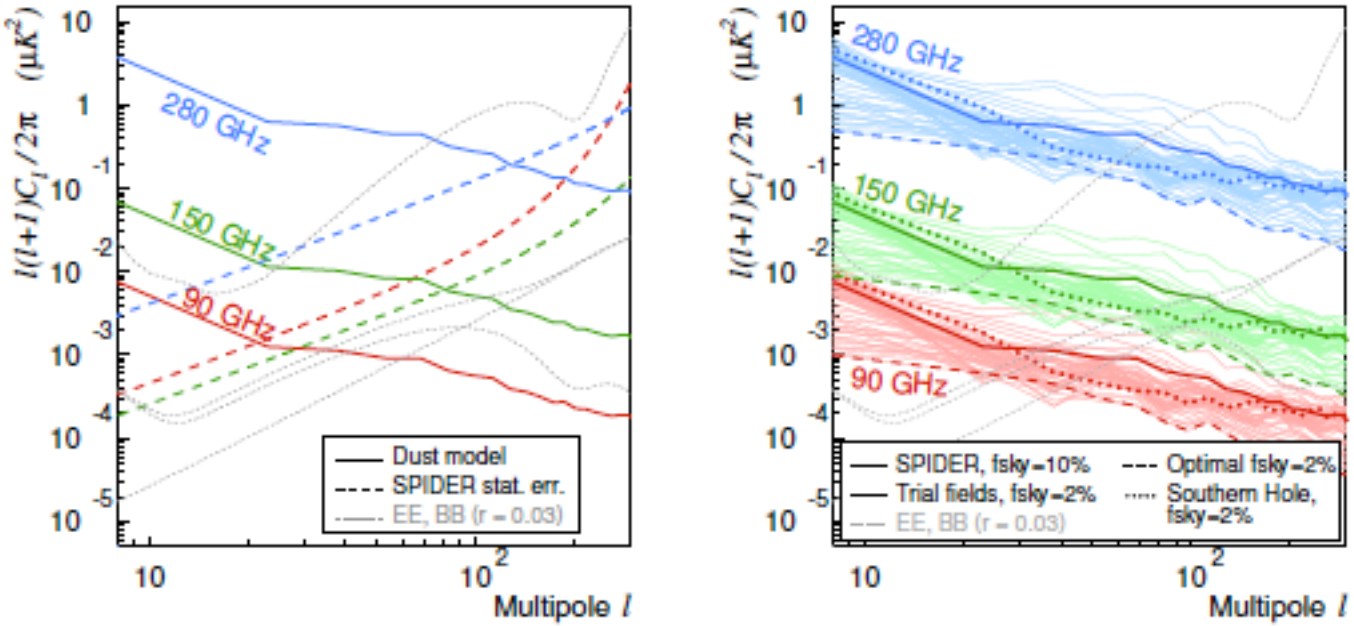

In case they ask…

Planck: Cosmology

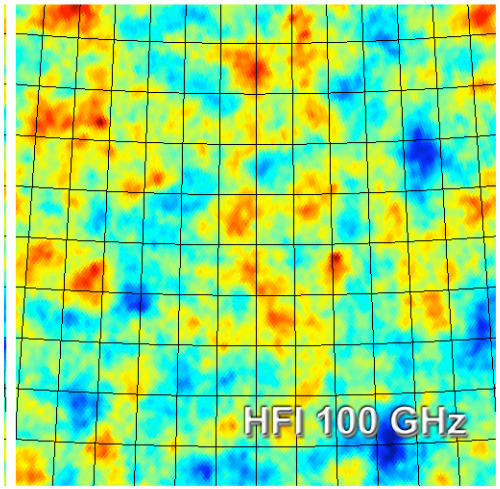

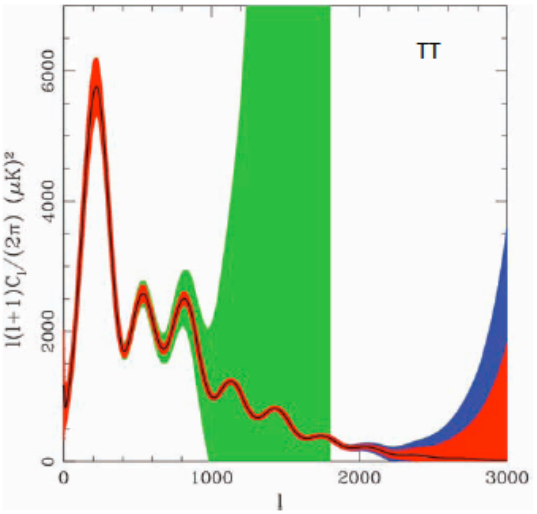

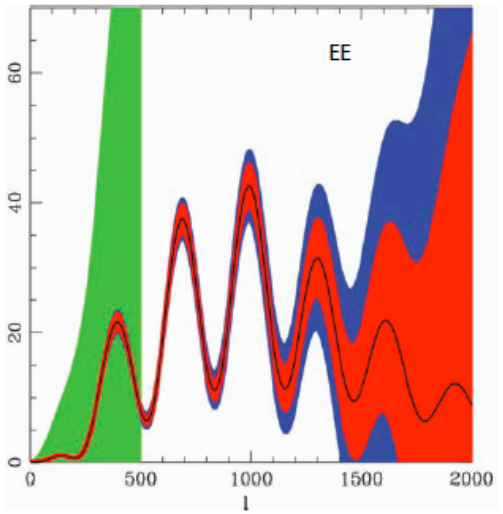

PARAMETER UNCERTAINTIES, STANDARD & EXTENDED MODELS

	STANDARD MODEL[a]			EXTENDED MODEL[b]		
Parameter	WMAP9	Planck15	Planck30	WMAP9	Planck15	Planck30
ω_b	5.2×10^{-4}	1.3×10^{-4}	1.1×10^{-4}	9.1×10^{-4}	2.2×10^{-4}	1.8×10^{-4}
ω_m	4.6×10^{-3}	1.2×10^{-3}	0.9×10^{-3}	24.3×10^{-3}	7.2×10^{-3}	6.0×10^{-3}
n_s	0.0130	0.0034	0.0028	0.0550	0.0084	0.0069
$\log(10^{10} A_s)$	0.0230	0.0076	0.0064	0.0360	0.0100	0.0092
Ω_Λ	0.0250	0.0068	0.0057	0.5000	0.3600	0.3400
τ	0.0110	0.0038	0.0033	0.0130	0.0049	0.0043
Ω_K				0.096	0.051	0.046
w				1.3	0.9	0.9
M_ν(eV)				2.1	0.66	0.56
Y_{He}				0.13	0.014	0.011
n_{run}				0.0360	0.0069	0.0060

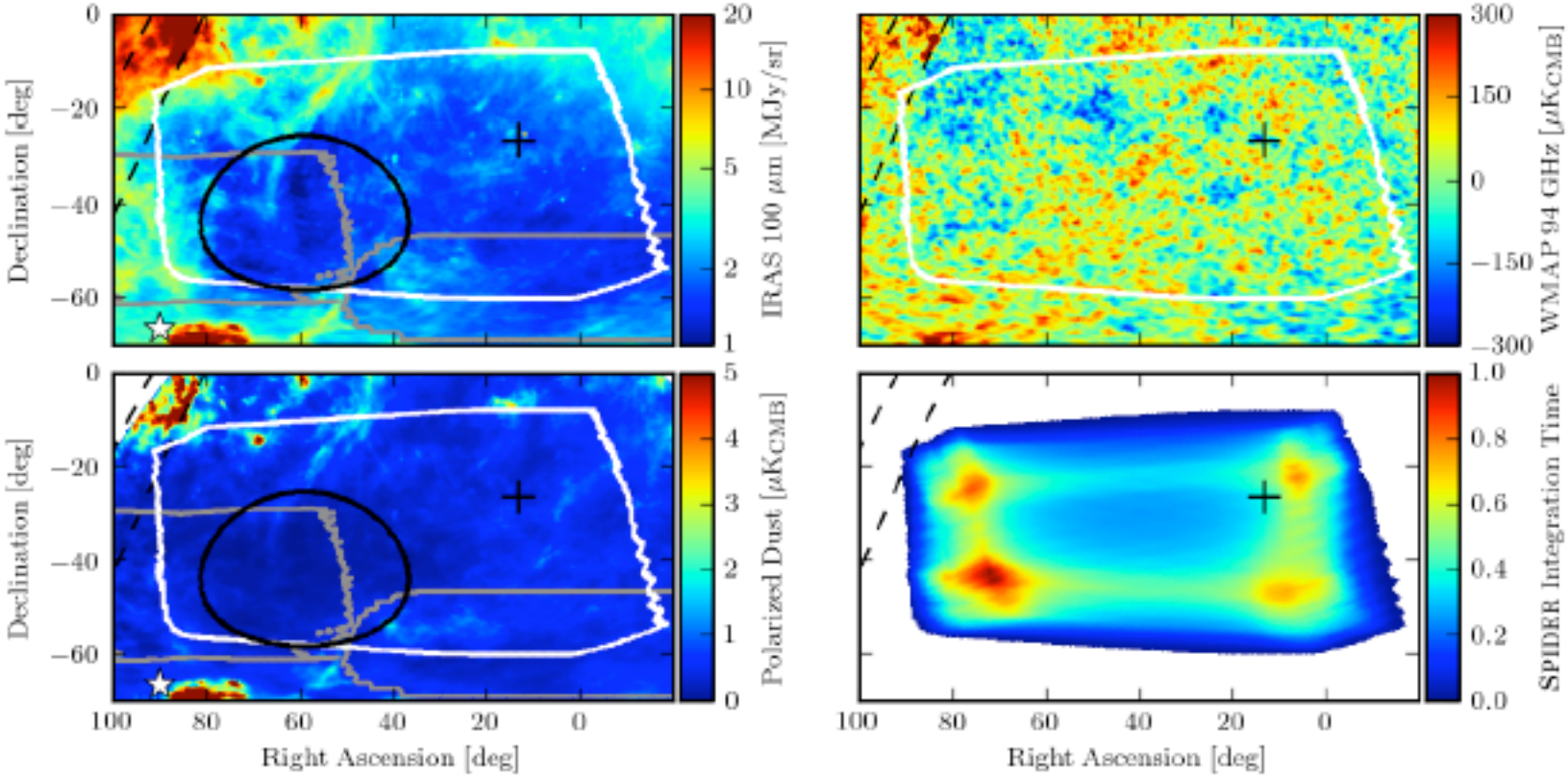

FIG. 4.— SPIDER observing region and scan profile. All four panels show the same portion of the sky, in equatorial coordinates, smoothed with a 30' beam. The southern Galactic pole (black +) is overplotted, along with the 10- and 20-degree Galactic latitude lines (dashed). *Top left:* IRAS 100 μm data showing dust morphology, the SPIDER observing region (white outline), and the south ecliptic pole (white $\star$). Also shown are the BOOMERANG and BICEP fields (left and right gray outlines, respectively), and the region of minimum foreground contamination in the SPIDER field (black outline). *Bottom left:* Polarized dust emission amplitude at 150 GHz, according to the model in Section 3.2. Clear differences in dust emission morphology are visible between this model and the IRAS data. *Top right: WMAP* 94 GHz *TT* data in the same area, showing relative absence of foreground contamination in the SPIDER observation region. *Bottom right:* Distribution of integration time, averaged over all detectors in a single 150 GHz focal plane, for the observing strategy in Section 4.1.

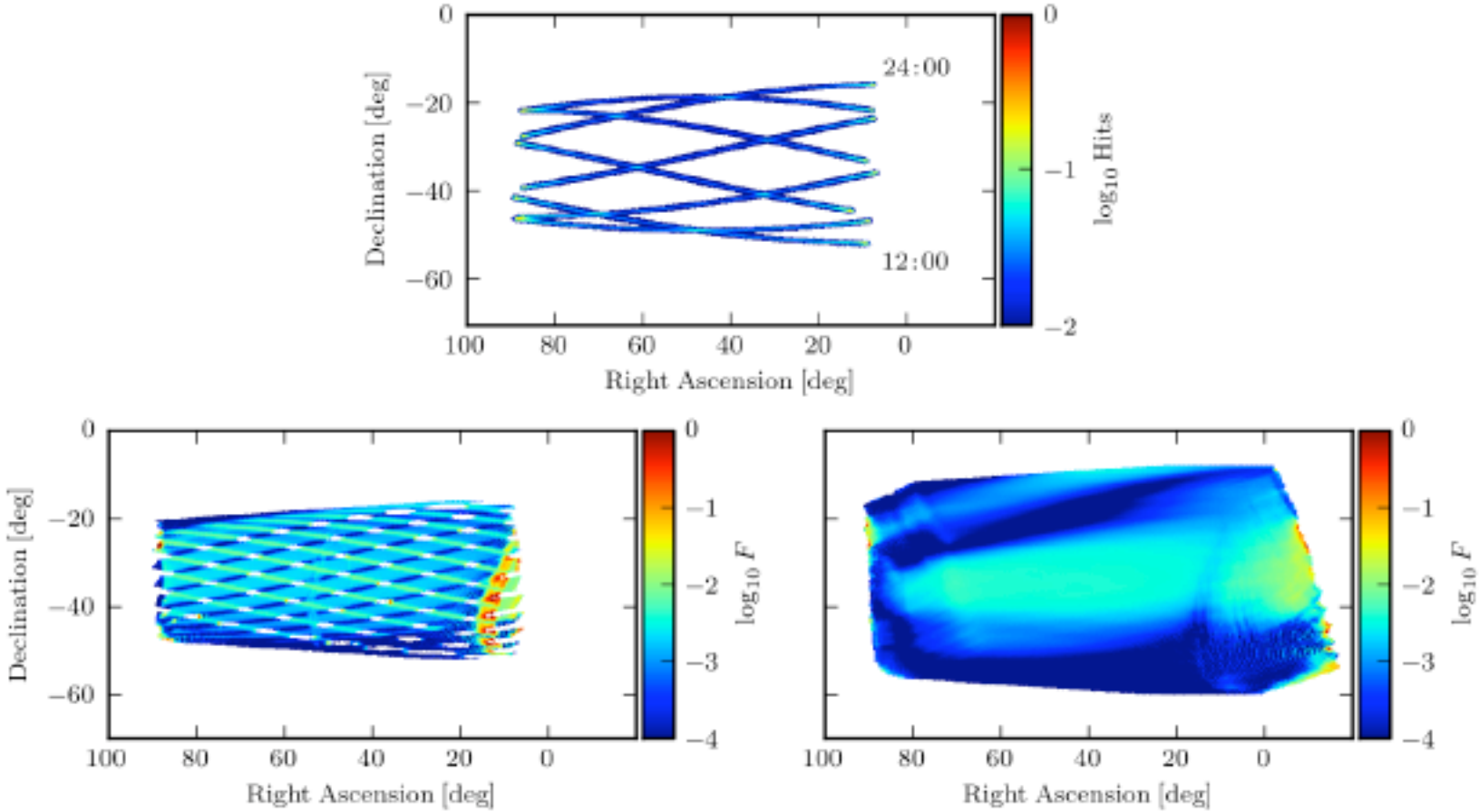

FIG. 5.— The SPIDER scan profile. All three panels show the same portion of the southern sky, in equatorial coordinates, smoothed with a 30' beam. *Top:* A 24-hour period for a single detector, illustrating the change in telescope orientation throughout the day. Five-minute periods every three hours are shown. Detector pairs in a single pixel are oriented 22.5 and 112.5 degrees relative to the scan direction. *Bottom left:* Fraction of excess variance (see definition in Section 4.1) due to anisotropic angular coverage in the Stokes Q and U maps for the above detector over a four-day period. *Bottom right:* Fraction of excess variance for a full focal plane of 512 bolometers, over a four-day period. This observing profile covers 9.5% of the sky, of which 96% is observed with near-isotropic coverage in crossing angles to reconstruct the Stokes Q and U parameters with $< 1\%$ excess variance.

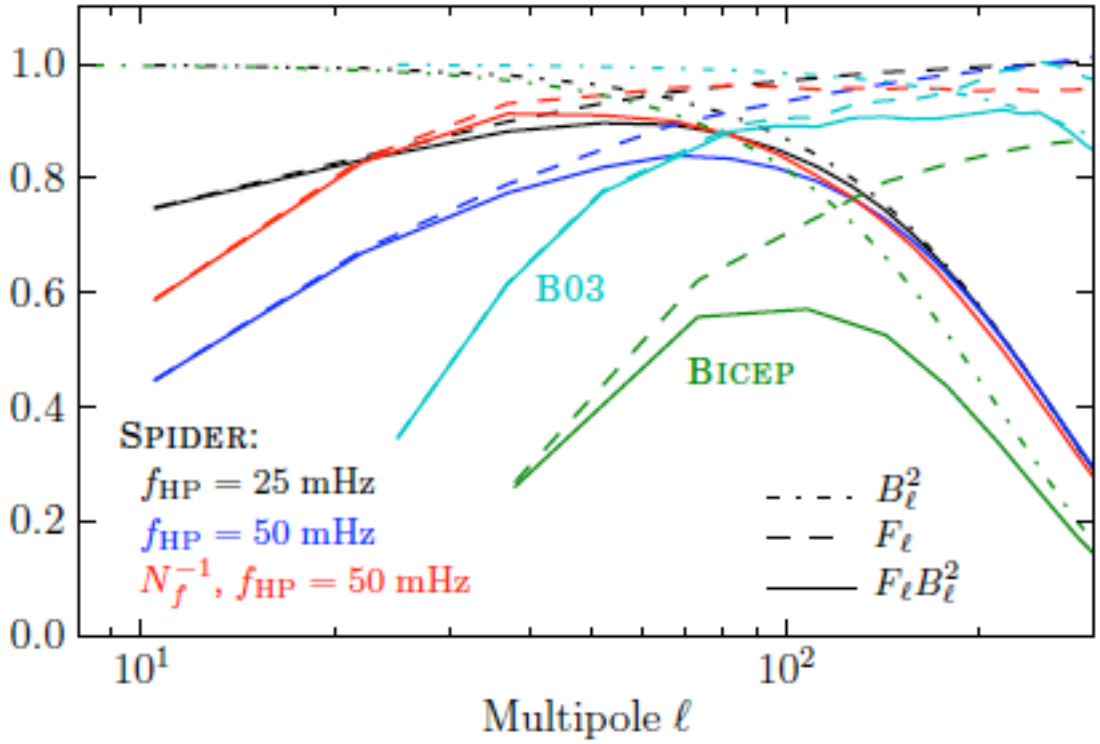
1.0
0.8
0.6
0.4
0.2
0.0
10^1
10^2
Multipole ℓ
B03
BICEP
SPIDER:
$f_{\rm HP} = 25$ mHz
$f_{\rm HP} = 50$ mHz
N_f^{-1}, $f_{\rm HP} = 50$ mHz
B_ℓ^2
F_ℓ
$F_\ell B_\ell^2$

Spider: Probing Inflation

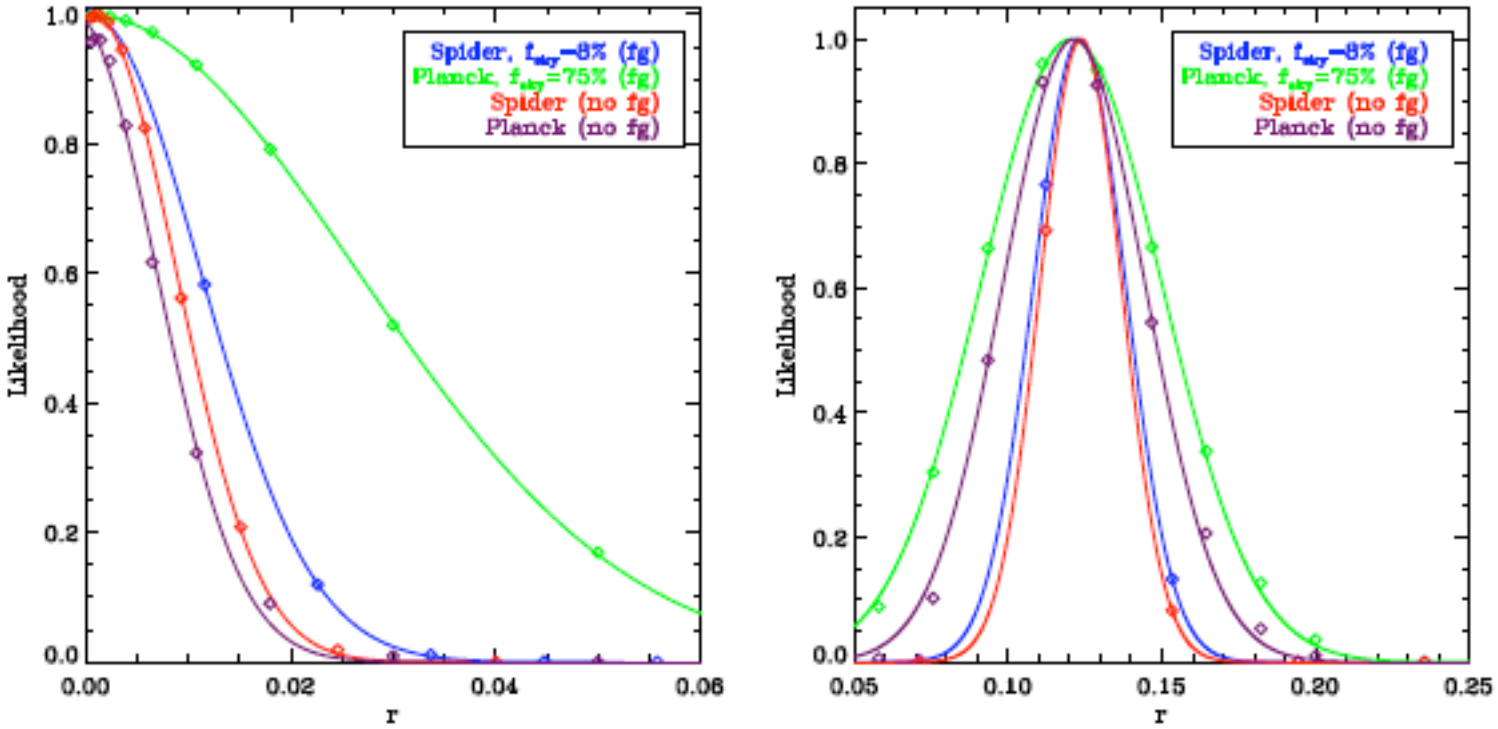

NASA CSA ASC C.S.B.F. PALESTINE, TEXAS NSERC CRSNG JPL CALIFORNIA INSTITUTE OF TECHNOLOGY UNIVERSITY OF TORONTO CASE WESTERN RESERVE UNIVERSITY EST. 1826 CARDIFF UNIVERSITY PRIFYSGOL CAERDYDD UBC NIST PRINCETON UNIVERSITY CITA ICAT Canadian Institute for Theoretical Astrophysics L'institut canadien d'astrophysique theorique Imperial College London

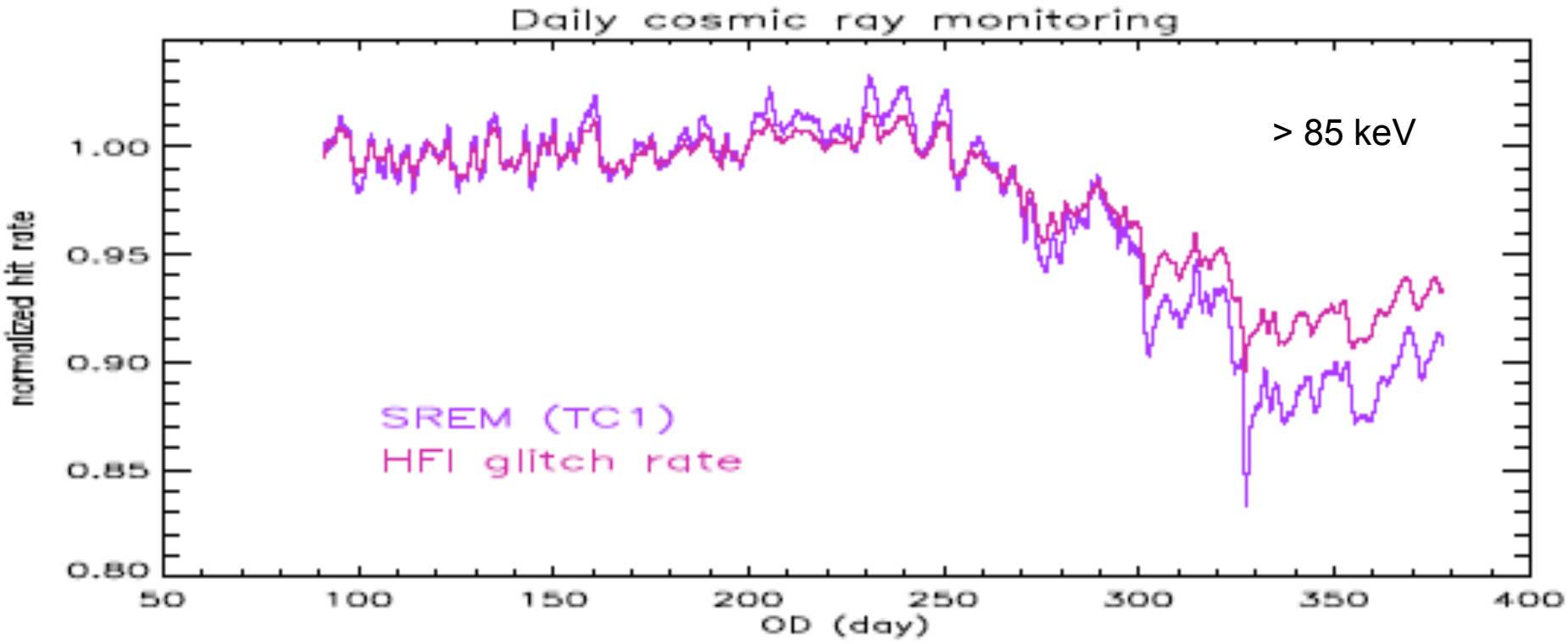

	100	143	217	353	545	857	Dark
N_b	8	11	12	12	3	3	2
%	13.4	15.4	15.8	15.8	9.4	9.2	14.7

Table 3. *Planck* performance parameters determined from flight data.

Channel	$N_{detectors}$[a]	ν_{center}[b] [GHz]	Mean Beam[c] FWHM	Mean Beam[c] Ellipticity	White-noise[d] Sensitivity [$\mu K_{RJ}\ s^{1/2}$]	White-noise[d] Sensitivity [$\mu K_{CMB}\ s^{1/2}$]	Calibration[e] Uncertainty [%]	Faintest Source[f] in ERCSC $\lvert b\rvert > 30^{\circ}$ [mJy]
30 GHz	4	28.5	32.65	1.38	143.4	146.8	1	480
44 GHz	6	44.1	27.92	1.26	164.7	173.1	1	585
70 GHz	12	70.3	13.01	1.27	134.7	152.6	1	481
100 GHz	8	100	9.37	1.18	17.3	22.6	2	344
143 GHz	11	143	7.04	1.03	8.6	14.5	2	206
217 GHz	12	217	4.68	1.14	6.8	20.6	2	183
353 GHz	12	353	4.43	1.09	5.5	77.3	2	198
545 GHz	3	545	3.80	1.25	4.9	. . .	7	381
857 GHz	3	857	3.67	1.03	2.1	. . .	7	655

Spider: Mapping the cleanest area of sky

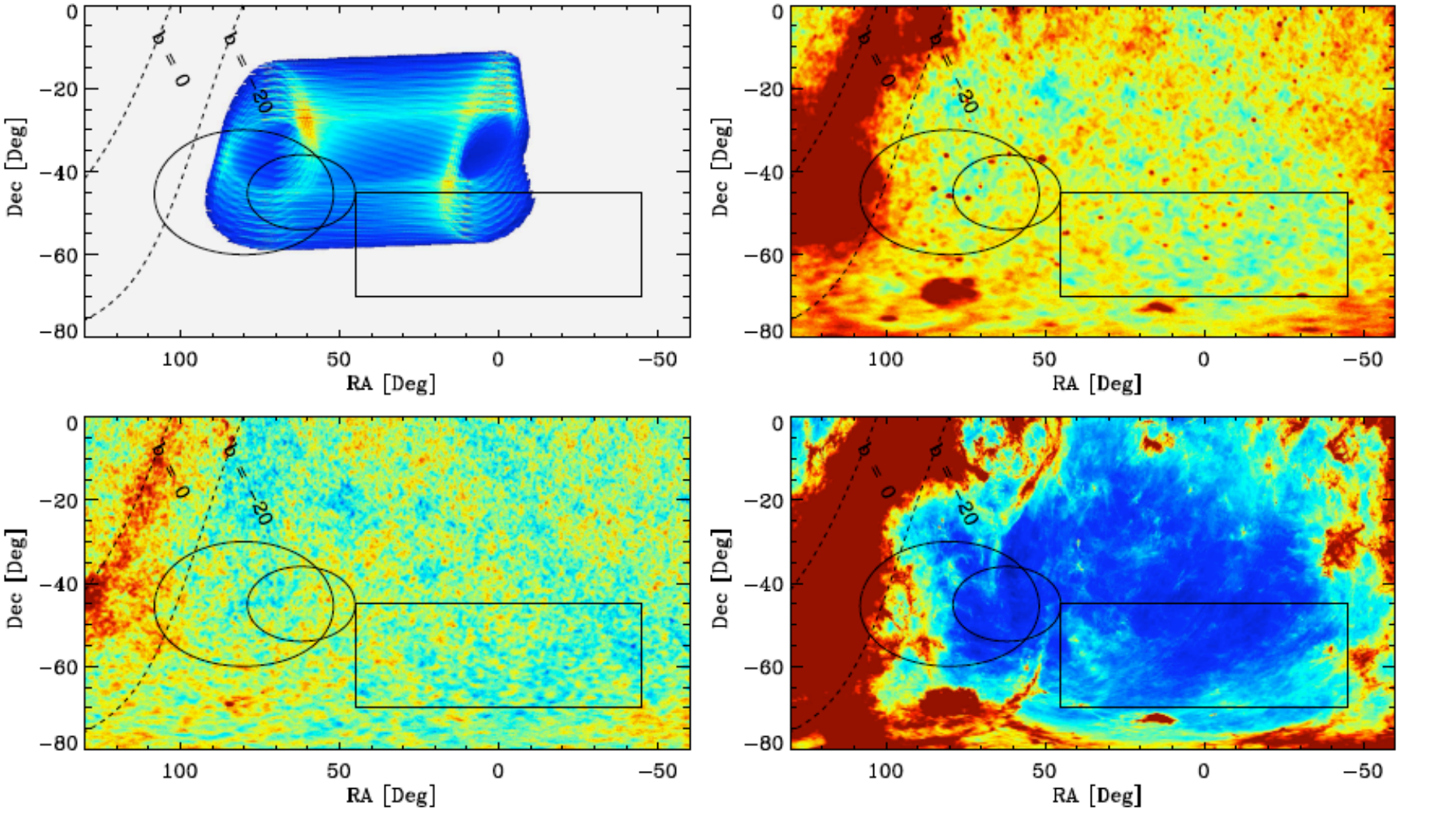

NASA CSA ASC C.S.B.F. PALESTINE, TEXAS NSERC CRSNG JPL California Institute of Technology University of Toronto Cardiff University Prifysgol Caerdydd UBC Case Western Reserve University est. 1826 NIST Princeton University CITA ICAT Canadian Institute for Theoretical Astrophysics L'institut canadien d'astrophysique theorique Imperial College London

Spider: Polarized Sensitivity

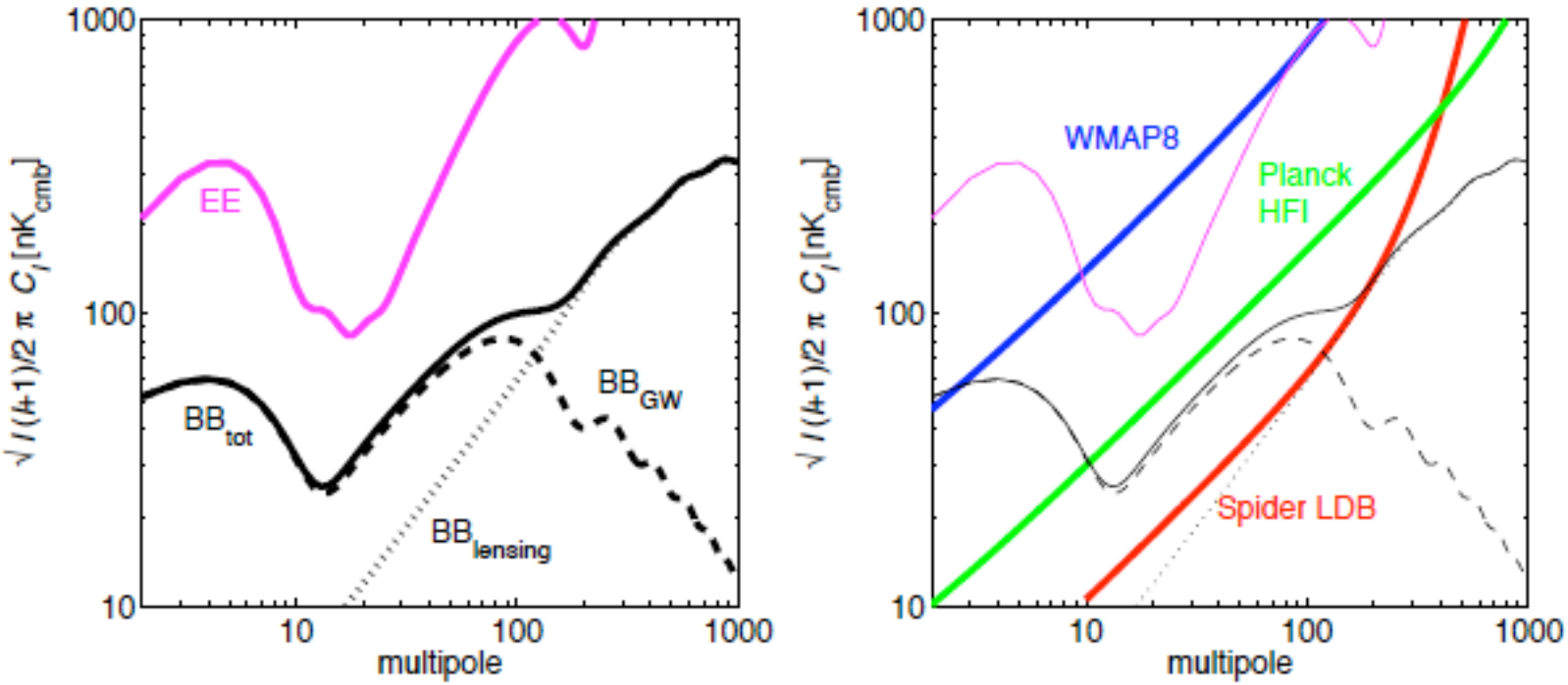

Gondola and Sunshields

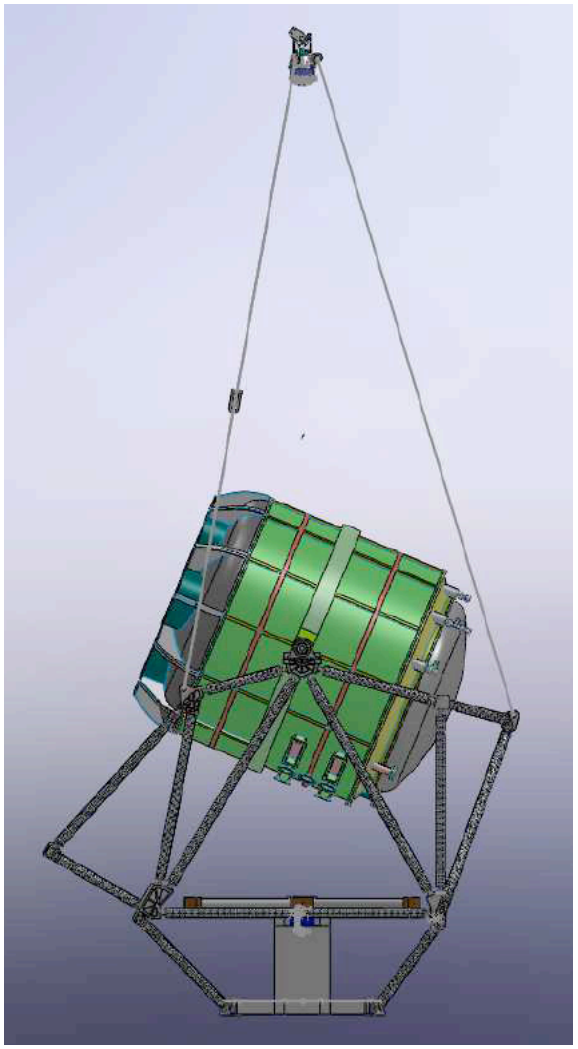

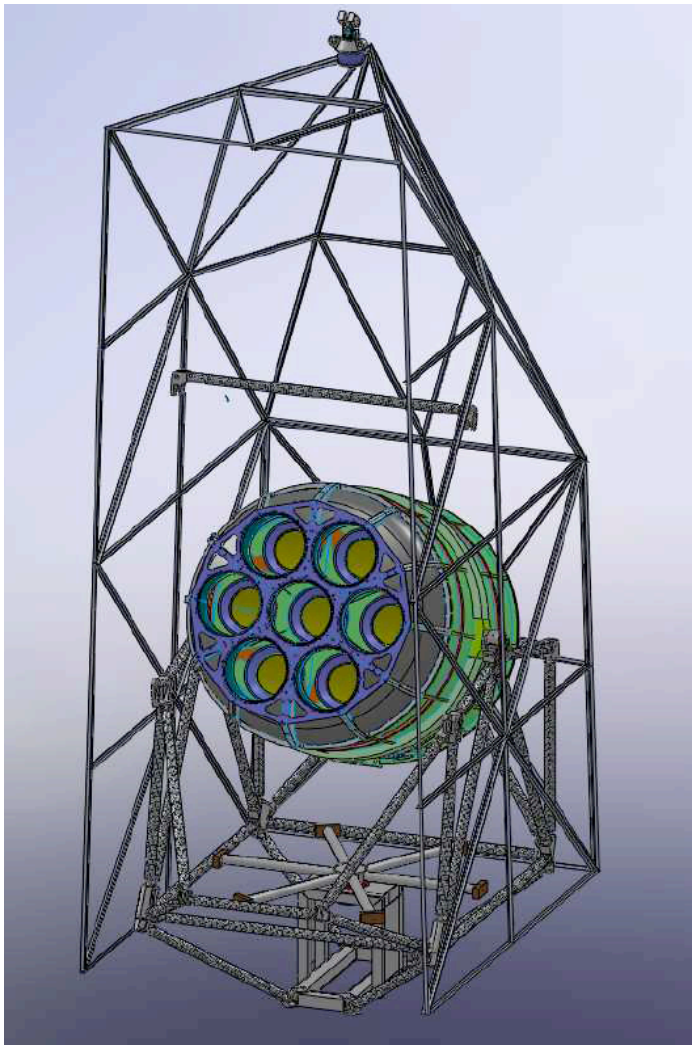

~4600 lb Science Mass

Spider Instrument Insert

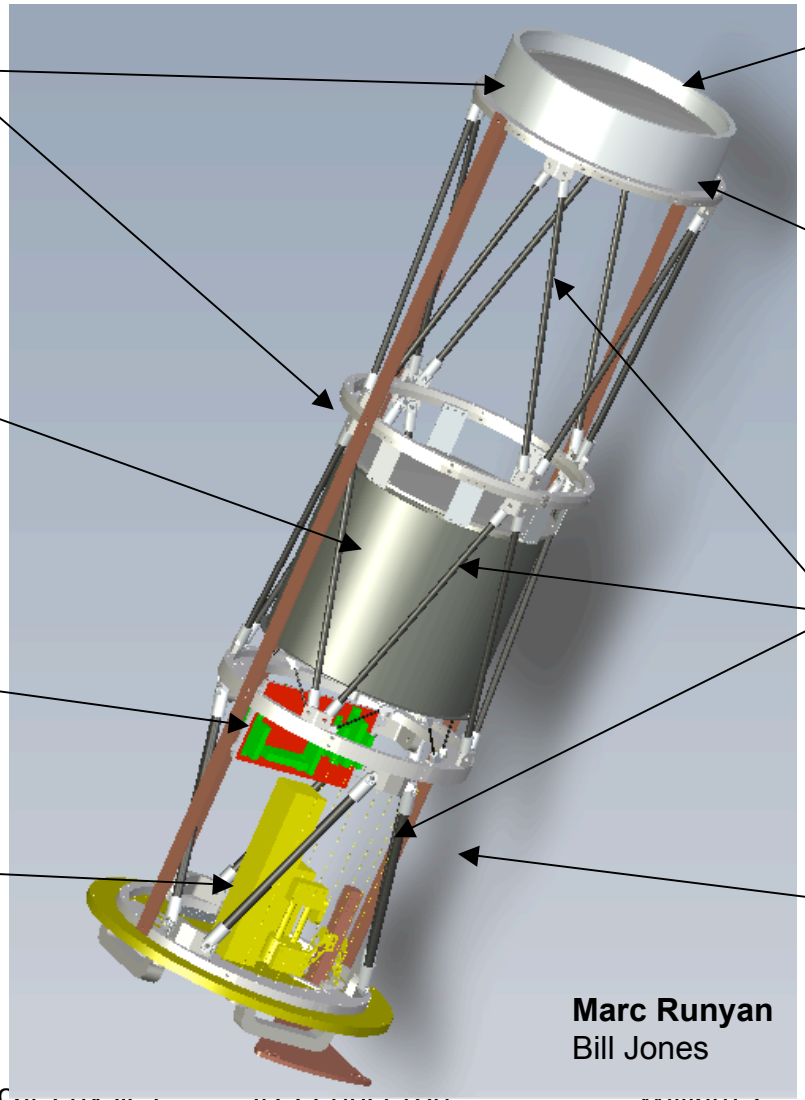

Spider Fabrication and Integration

lightweight / low cost mechanical and thermal truss structure

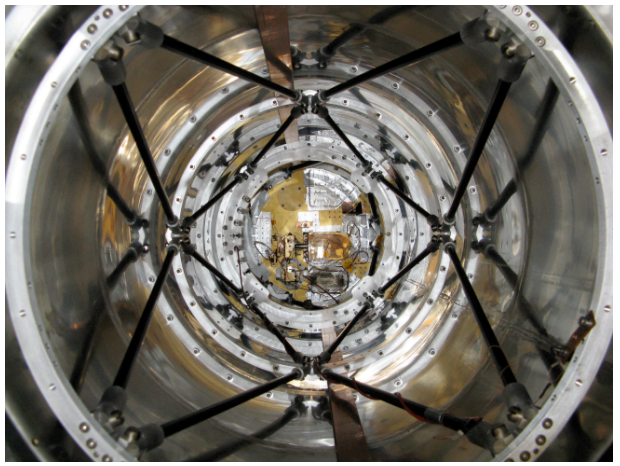

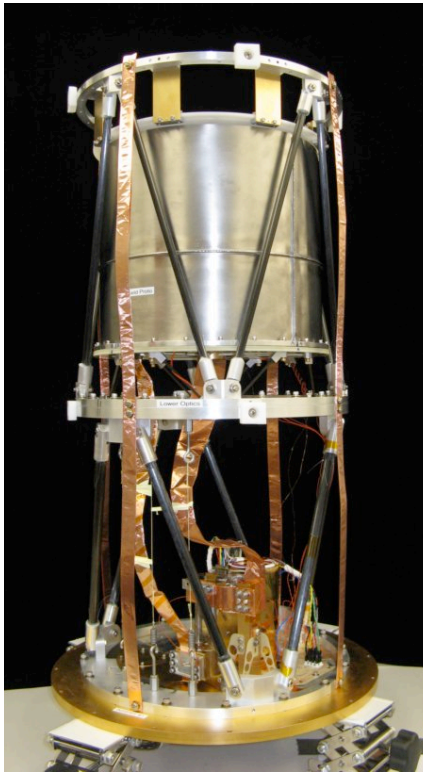

cryogenic half waveplate assembly (single plate sapphire)

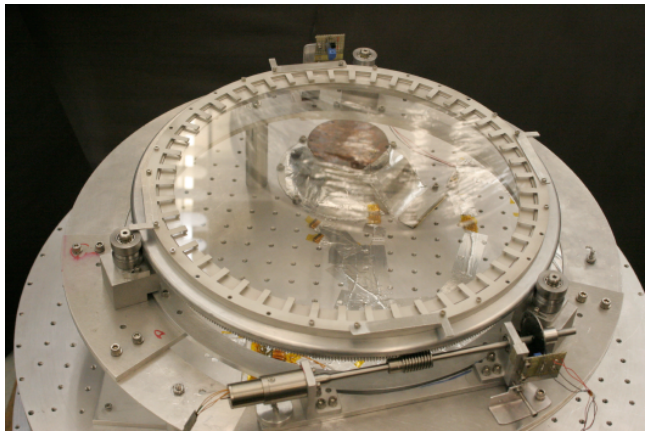

Spider Fabrication and Integration

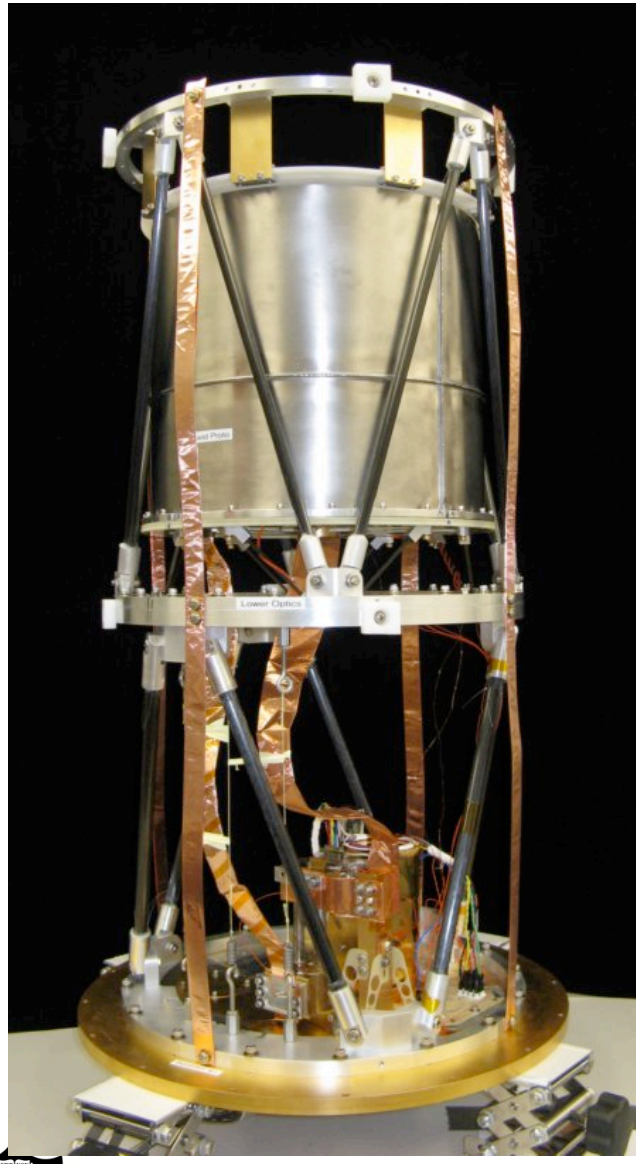

Sub-Kelvin Stage
- Graphite standoffs for rapid cooldown
- Passive thermal lowpass filter
- G-10 backed niobium shield

Focal Plane Assembly
- Niobium backshort/shield
- 300 mK array enclosure
- Copper thermalizing plate

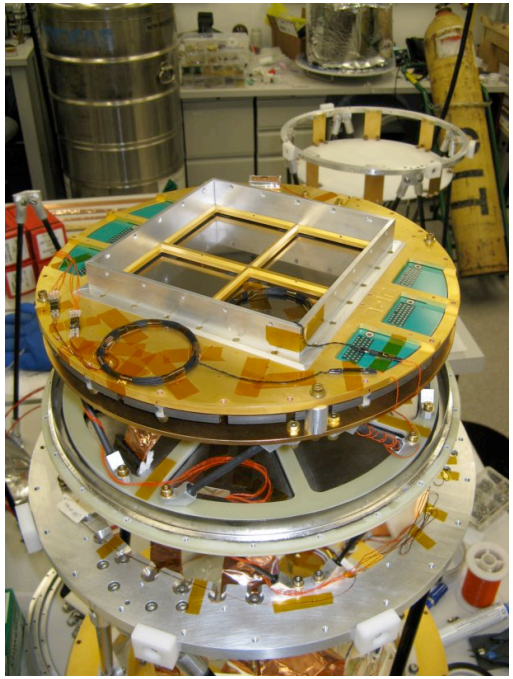

High efficiency sub-K cooler
- 10 STP Liters of 3He
- 556 J applied (~500J to 4K, 50J to 1.4K)
- Cooling capacity >3.8 J
- Cooling Power ~ 0.2 mK/μW @ 280 mK

Spider Fabrication and Integration

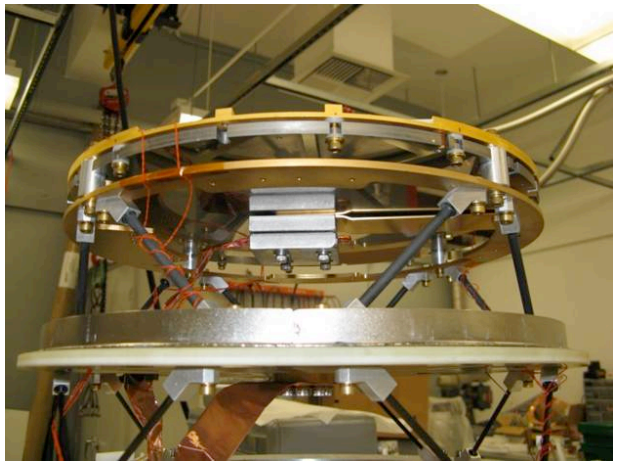

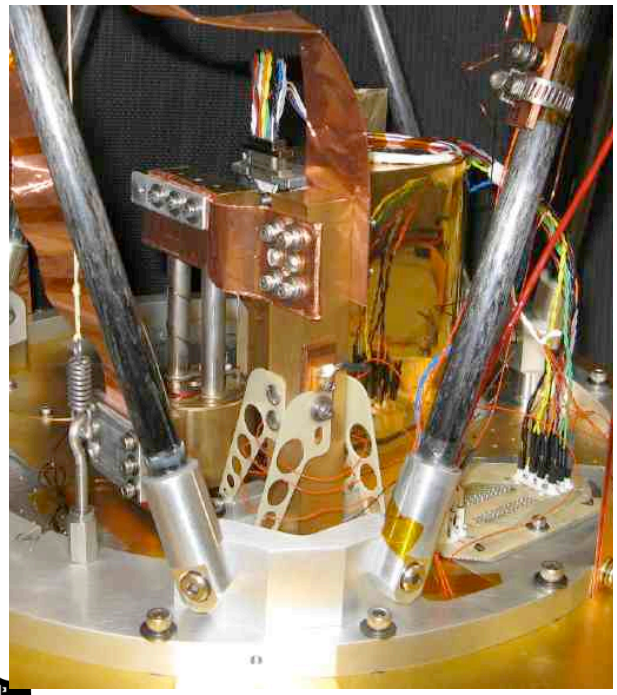

Sub-Kelvin Stage
- Graphite standoffs for rapid cooldown
- Passive thermal lowpass filter
- G-10 backed niobium shield

Focal Plane Assembly
- Niobium backshort/shield
- 300 mK array enclosure
- Copper thermalizing plate

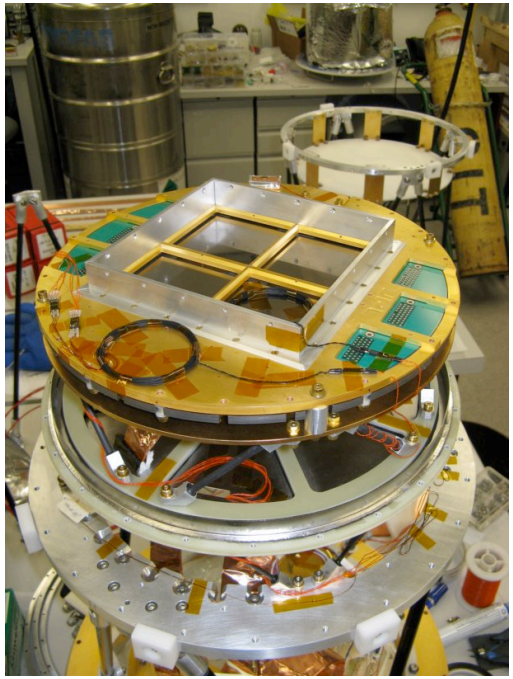

High efficiency sub-K cooler
- 10 STP Liters of 3He
- 556 J applied (~500J to 4K, 50J to 1.4K)
- Cooling capacity >3.8 J
- Cooling Power ~ 0.2 mK/μW @ 280 mK

$$d_i \simeq \frac{s}{2} \int \mathrm{d}\nu\, \lambda^2\, F_\nu \iint \mathrm{d}\Omega\, [I + \gamma \mathcal{P}\, (Q \cos 2\psi_i + U \sin 2\psi_i)]$$

$$\begin{pmatrix} d_i \\ d_i \gamma c_i \\ d_i \gamma s_i \end{pmatrix} = \begin{pmatrix} 1 & \gamma c_i & \gamma s_i \\ \gamma c_i & \gamma^2 c_i^2 & \gamma^2 s_i c_i \\ \gamma s_i & \gamma^2 c_i s_i & \gamma^2 s_i^2 \end{pmatrix} \begin{pmatrix} I \\ Q \\ U \end{pmatrix},$$

$$\hat{M}_p = \sum_j^{N_{\mathrm{ch}}} w_j \sum_{i \in p} \begin{pmatrix} 1 & \gamma_j c_i & \gamma_j s_i \\ - & \gamma_j^2 c_i^2 & \gamma_j^2 c_i s_i \\ - & - & \gamma_j^2 s_i^2 \end{pmatrix}.$$

Planck: Galactic Astrophysics

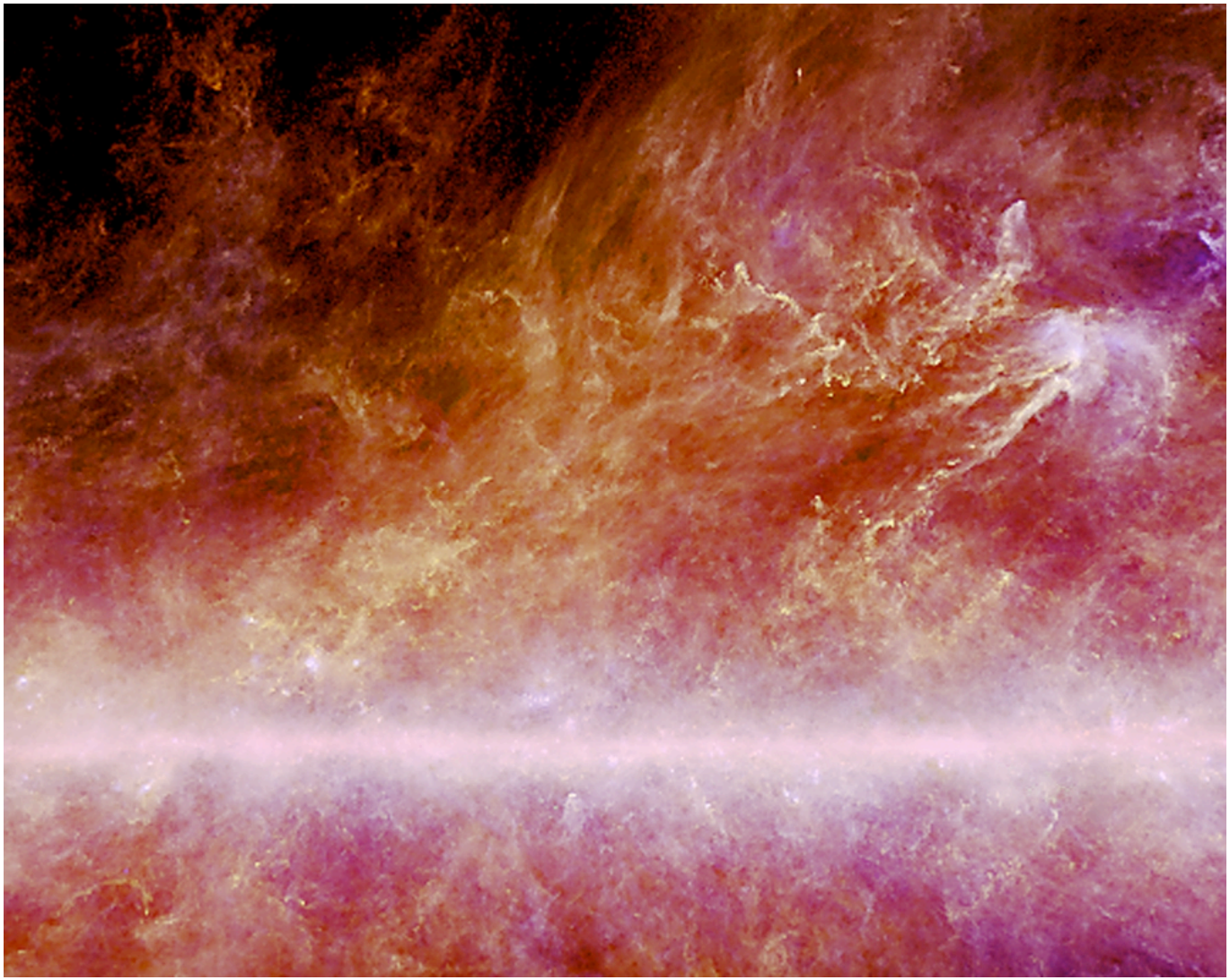


ACT Telescope